NOAA Technical Memorandum OAR PMEL-139

DEVELOPMENT OF THE FORECAST PROPAGATION DATABASE FOR NOAA's SHORT-TERM INUNDATION FORECAST FOR TSUNAMIS (SIFT)

Edison Gica[1,2]
Mick C. Spillane[1,2]
Vasily V. Titov[1,2]
Christopher D. Chamberlin[1,2]
Jean C. Newman[1,2]

[1]Joint Institute for the Study of the Atmosphere and Ocean (JISAO)
University of Washington, Seattle, WA

[2]Pacific Marine Environmental Laboratory
Seattle, WA

Pacific Marine Environmental Laboratory
Seattle, WA
March 2008

UNITED STATES DEPARTMENT OF COMMERCE

Carlos M. Gutierrez
Secretary

NATIONAL OCEANIC AND ATMOSPHERIC ADMINISTRATION

VADM Conrad C. Lautenbacher, Jr.
Under Secretary for Oceans and Atmosphere/Administrator

Office of Oceanic and Atmospheric Research

Richard W. Spinrad
Assistant Administrator

NOTICE from NOAA

Mention of a commercial company or product does not constitute an endorsement by NOAA/OAR. Use of information from this publication concerning proprietary products or the tests of such products for publicity or advertising purposes is not authorized. Any opinions, findings, and conclusions or recommendations expressed in this material are those of the authors and do not necessarily reflect the views of the National Oceanic and Atmospheric Administration.

Contribution No. 2937 from NOAA/Pacific Marine Environmental Laboratory

Also available from the National Technical Information Service (NTIS)
(`http://www.ntis.gov`)

Contents

List of Figures

List of Tables

Development of the forecast propagation database for NOAA's Short-term Inundation Forecast for Tsunamis (SIFT)

E. Gica[1,2], M.C. Spillane[1,2], V.V. Titov[1,2], C.D. Chamberlin[1,2], and J.C. Newman[1,2]

Abstract. The NOAA Center for Tsunami Research (NCTR) is developing an operational tool that provides quick and accurate tsunami forecasts known as Short-term Inundation Forecast for Tsunamis (SIFT). The SIFT system uses Deep-ocean Assessment and Reporting of Tsunamis (DART™), data inversion techniques, tsunami propagation estimates, and site specific inundation forecasts. SIFT is an efficient and accurate operational tool that can provide offshore forecasts of tsunami time series quickly at any specified site. Providing a quick tsunami forecast is possible with the aid of the forecast propagation database which is set up by pre-computing earthquake events using unit sources along the known and potential earthquake zones in the Pacific, Atlantic, and Indian oceans. Currently 1160 unit sources have been simulated to provide Pacific, Atlantic, and Indian ocean coverage. Tsunami generation and propagation is simulated using the MOST propagation code. Exploiting the linearity of the generation/propagation dynamics, the propagation database can simulate arbitrary earthquake scenarios using combination unit sources that can accurately reproduce tsunami time series as validated with ten real tsunami events since 2003.

1. Background and Motive

NOAA tsunami warning centers and officials at other agencies are in urgent need of an operational tool that can provide quick and accurate tsunami forecasts to guide their decisions for issuing tsunami warnings. Forecasting tsunami impacts for any coastal area right after a tsunamigenic event is a tremendous achievement and is very useful to the tsunami warning centers and hazard mitigation managers.

The NOAA Center for Tsunami Research (NCTR) is developing a tsunami forecast system known as Short-term Inundation Forecast for Tsunamis (SIFT) that uses data inversion technique and site-specific inundation forecasts (referred to as Standby Inundation Models or SIMs). Data inversion will combine real-time DART™ data (recordings from the NTHMP tsunameters: González *et al.*, 2005) with pre-computed scenarios (forecast propagation database) while SIMs will provide forecasts for coastal areas.

The forecast propagation database is set up by pre-computing earthquake events. Developing the offshore forecast database is possible because of the linearity of the generation/propagation dynamics whereby "base" scenarios can be combined linearly to relate the earthquake parameters to the generated tsunami's wave height, period, and directionality off the coast. The results of the propagation scenario also serve as input for the SIMs that numerically predict the tsunami wave height, current speeds, and inundation extent of a specific coastal area of interest.

Fast real-time forecast modeling of tsunami waves is complicated by the fact that current technology cannot provide all the earthquake parameters needed for simulation immediately after an earthquake event. NCTR's data

[1]NOAA, Pacific Marine Environmental Laboratory, Seattle, WA 98115-6349, USA
[2]Joint Institute for the Study of the Ocean and Atmosphere (JISAO), Box 354235, University of Washington, Seattle, WA 98115-4235, USA

inversion technique is a solution for this problem. Forecast is done using pre-defined typical earthquake parameters (i.e., dip and rake-angles, slip, depth of source), which are adjusted to the epicenter and moment magnitude, M_w, obtained after an event. Once the DART™ buoys pick up the tsunami waves, inversion is done to refine the tsunami source region. The propagation database has been validated with ten real tsunami events since 2003 and is thoroughly tested for accuracy, reasonableness of results, and error sensitivity.

It should be noted that the variability of an arbitrary tsunami generation mechanism is too large to store in a database. Doing so would require infinitely large storage. The solution is to select a limited number of scenarios that would represent all possible events with accountable accuracy. This can be done by sensitivity tests to determine which earthquake parameters provide the most variability for generated tsunami waves.

The methodologies, theories, and sensitivity tests used in the development of the pre-defined, pre-computed sources—validation with historical and real-time events, practical use, and sensitivity of the propagation database itself—are discussed in this report.

2. Methodology

SIFT uses a two-step process: (1) data inversion, which combines real-time seismic and tsunami data with the pre-computed scenarios (forecast propagation database); (2) the site-specific inundation forecast using SIMs. This section describes the theories and methodologies used in the development of the propagation database.

2.1 Tsunami Generation

The initial tsunami generation model follows a commonly used method whereby the initial sea surface displacement follows that of the final vertical displacement of the ocean bottom due to an earthquake. An elastic deformation (Okada, 1985) source model is applied to determine the shape of the earthquake's vertical displacement, which assumes the rupture of a single rectangular fault plane. The earthquake parameters required for the model are the fault's length, L, and width, W, location or epicenter, fault's orientation or strike angle, θ, dip angle, δ, rake angle, λ, average slip, u_o, and depth of source, h. Calculation of the earthquake's seismic moment uses the following equation:

$$M_o = \mu u_o L W \tag{1}$$

where the earth's rigidity, μ, is assumed to be 4.0×10^{11} dynes/cm^2, u_o, L and W in cm.

The moment magnitude, M_w, can then be computed by using the following formula:

$$M_w = \frac{2}{3}\log\left(M_o\right) - 10.7 \tag{2}$$

An earthquake source could contain multiple sub-faults with very complex slip distributions. Obtaining all details of an earthquake source could take months of analysis using high-quality data. Okada's (1985) source model is very simple; however, estimates of earthquake parameters (i.e., slip, depth of source, epicenter, and moment magnitude, M_w) are readily available after an earthquake event, making it very useful for tsunami mitigation. The earthquake parameters then serve as input to the MOST deformation code, which uses the Okada (1985) source model, to generate the earthquake source deformation, which will determine the initial tsunami's characteristics. This becomes one of the input files for the MOST propagation code.

2.2 Tsunami Propagation

After the initial tsunami wave is generated by an earthquake, the waves will radiate away from the source and propagate in the open ocean. Tsunami waves can propagate across entire ocean basins, and since it covers a very large area, the curvature of the earth is taken into account.

The MOST propagation code uses the non-linear shallow water equation in spherical coordinates with Coriolis force and a numerical dispersion scheme to take into account the different propagation wave speeds with different frequencies. The equations, shown below, are numerically solved using a splitting method (Titov, 1997):

$$h_t + \frac{(uh)_\lambda + (vh\cos\phi)}{R\cos\phi} = 0 \tag{3}$$

$$u_t + \frac{uu_\lambda}{R\cos\phi} + \frac{vu_\phi}{R} + \frac{gh_\lambda}{R\cos\phi} - \frac{uv\tan\varphi}{R} = \frac{gd_\lambda}{R\cos\phi} - \frac{C_f u\left|u\right|}{d} + fv \tag{4}$$

$$v_t + \frac{uv_\lambda}{R\cos\phi} + \frac{vv_\phi}{R} + \frac{gh_\phi}{R} + \frac{u^2\tan\varphi}{R} = \frac{gd_\phi}{R} - \frac{C_f v\left|u\right|}{d} - fu \tag{5}$$

where:

λ = longitude
ϕ = latitude
$h = h\left(\lambda,\phi,t\right) + d\left(\lambda,\phi,t\right)$
$h\left(\lambda,\phi,t\right)$ = amplitude
$d\left(\lambda,\phi,t\right)$ = undisturbed water depth
$u\left(\lambda,\phi,t\right)$ = depth-averaged velocity in longitude direction
$v\left(\lambda,\phi,t\right)$ = depth-averaged velocity in latitude direction
g = gravity
R = radius of the earth
$f = 2\omega\sin\phi$, Coriolis parameter
$C_f = gn^2/h^{1/3}$, n is Manning coefficient

The propagation database covers Pacific, Atlantic, and Indian oceans. The Pacific Ocean bathymetry for the numerical simulation is based on Smith and Sandwell (1994) 2 arc-minute data. The Atlantic Ocean bathymetry is derived from several sources. Higher resolution data are generally available near the coastal areas. Sources for the Atlantic are from Smith and Sandwell (1994) 2 arc-minute data, General Bathymetric Chart of the Oceans (GEBCO), National Ocean Service, National Tsunami Warning and Mitigation Program, National Geospatial-Intelligence Agency (NGA), Scripps Institution of Oceanography, University of Rhode Island, Woods Hole Oceanographic Institution, Lamont-Doherty Earth Observatory, U.S. Geological Survey, and Center for Coastal and Ocean Mapping/Joint Hydrographic Center (CCOM/JHC) of the University of New Hampshire, Instituto Nacional de Estadística Geografía e Informática (INEGI), NOAA's Office of Ocean Resources Conservation and Assessment, Strategic Environmental Assessments (SEA) Division, Joint Airborne LIDAR Bathymetry Technical Center of Expertise-JALBTCX (U.S. Army Corps of Engineers) and International surveys. The Indian Ocean bathymetry is also derived from several sources: data are from SRTM30, coastal and ridge multibeam (Scripps Institution of Oceanography, 2004), University of Southern California Tsunami Research Center (Greeninfo Network), and National Geospatial-Intelligence Agency (NGA). Although high-resolution bathymetry data is available for the Pacific, Atlantic, and Indian oceans, the bathymetry is re-gridded to 4 arc-minute, which is used in the simulation. The output data is reduced in size by saving a coarser grid of 16 arc-minutes resolution and 1 minute in time.

There are currently two Pacific grid domains. The regular Pacific grid covers 62°N to 50°S and 120°E to 292°E and the extended one covers 62°N to 74°S and 120°E to 292°E, which extends 24° further south as compared to the regular Pacific grid. The grid extent for the Atlantic is from 105°W to 20°E and 72°N to 72°S, while the Indian Ocean covers 0°E to 60°E and 32°N to 70°S. The time step used in the simulation depends on the grid that is being used since it has to follow the CFL condition. For the regular Pacific grid, the CFL condition requires a time step of 15 seconds, while the extended Pacific requires a time step of 12 seconds. The Atlantic Ocean uses a time step of 10 seconds, while the Indian Ocean uses 12 seconds as required by the CFL condition. Comparison of the two Pacific grid domains was conducted and is explained in section 5.2. Tests are currently being done to develop a global grid containing all the unit sources in the Pacific, Atlantic, and Indian oceans.

2.3 Pre-Defined Unit Sources

The main objective of the pre-computed tsunami database is to be able to provide offshore forecasts of tsunami amplitudes and other wave parameters quickly without having to run simulations right after a tsunamigenic event. The goal is to define an earthquake source region such that a finite combination of those could closely reproduce the tsunami time series

of the actual event. This is feasible because of the linearity of the generation/propagation dynamics. Each pre-defined earthquake source is referred to as a "unit source." Each unit source has a fault length of 100 km, fault width of 50 km, and a slip value of 1 m, generating an equivalent moment magnitude, M_w, of 7.5.

Two rows of unit sources are set up, one for the shallower region and one for the deeper region. Additional rows may be possible depending on the characteristics of the region. These unit sources are located along the known fault zones for the entire Pacific Basin, Caribbean for the Atlantic region and Indian Ocean. Figure A1 shows how the unit sources will be set up.

2.4 Tsunami Model Input Parameters and Input/Output Data

- Earthquake parameters: the generation of the initial tsunami wave requires the input of earthquake parameters: epicenter (longitude and latitude), fault length, fault width, dip , rake, and strike angles, slip value, and depth.
- Bathymetry data: A 4 arc-minute grid resolution (see section 2.2); land is specified as a negative value, water as positive.

Three output files are generated in netcdf format for the following variables:

- Simulated tsunami wave height, "ha"
- Simulated tsunami velocity in x-direction, "u"
- Simulated tsunami velocity in y-direction, "v"

3. MOST Propagation Model Validation and Sensitivity Tests

This section briefly discusses the validation of the MOST propagation code with a real tsunami event; other validations (i.e., lab experiments, etc.) are described in Titov (1997). Sensitivity tests of the tsunami time series to earthquake source parameters for far-field tsunamis are also investigated.

3.1 Model Validation

The first validation of the global propagation (i.e., MOST) code was done with the 10 June 1996 Andreanov tsunami (Titov and González, 1997). Several deep ocean Bottom Pressure Recorder (BPR) records of the event were compared with the simulation for the 10 June 1996 Andreanov tsunami. The estimated seismic moment, M_o, of 7.3×10^{20} N·m was obtained from the Harvard solution; aftershock distribution estimated the source region to be 140 km long and 70 km wide. Assuming a shear modulus, μ, of 4.5×10^{20}

N·m, the average slip, u_o, was estimated to be 2 m (using Equations 1 and 2). Using a single-fault mechanism for the source region, a comparison was made between the simulated tsunami wave time series with that of the data obtained by the BPRs from the actual event.

The location of the Andreanov earthquake source and the BPRs are shown in Fig. A2. The grid domain for the simulation covers the North Pacific region (15°N to 65°N and 180°W to 120°W) with 4 arc-minute bathymetry data from Smith and Sandwell (1994). Comparison was made at five BPR stations and the results showed that the MOST propagation code was able to reproduce with sufficient accuracy the dominant deep-ocean wave form for the Andreanov tsunami (Fig. A3).

3.2 Tsunami Sensitivity to Earthquake Source Parameters

A commonly used method to define the initial tsunami surface is to apply the same displacement as the vertical deformation of the ocean bottom due to the earthquake. This makes the initial sea surface displacement a function of the earthquake parameters, namely: fault length, fault width, dip, rake, and strike angles, epicenter, depth, and slip values. The question is, would the tsunami time series be sensitive to the details of the source?

Earthquake parameters available right after an earthquake are preliminary and could be inaccurate. Determining which earthquake source parameters would affect the far-field tsunami time series will show the sensitivity of the tsunami time series to seismic source details.

Sensitivity to the earthquake parameters was studied using the 10 June 1996 Andreanov Island tsunami event, since the MOST generation and propagation model showed favorable comparison with the deep-ocean data from the BPRs (Titov and González, 1997), as shown in Fig. A3. The sensitivity tests (Titov *et al.*, 1999) were conducted to determine if deviation of the earthquake source parameters would produce an unacceptable model-data comparison and is discussed here.

Certain earthquake parameters are geographically constrained. The focal depth was set to 5 km and the strike angle was aligned with the Aleutian trench, which tends to be characteristic of most large underthrust earthquakes in the Alaskan-Aleutian subduction zone (AASZ). The last important constraint was setting the seismic moment, M_o, to 7.3×10^{20} N·m, as estimated for the Andreanov earthquake for all the model sources.

With those constraints in place, earthquake source parameters such as epicenter, fault length, fault width, dip and rake angles, were then varied. The mean slip value, u_o, is determined from Equation 1. Reference values are listed in Table 1.

Numerical stations to compare the simulated tsunami time series are shown in Fig. A4. Numerical gage 1 is located near Hawai‘i at a depth of 4747 m, while gage 2 is between Hawai‘i and the AASZ at a depth of 5910 m. Both numerical gages 1 and 2 are deep enough to ensure linearity of the wave dynamics. Numerical gage 3 is located on Axial Seamount at

Table 1: 1996 Andreanov reference earthquake source parameters.

Earthquake Source Parameter*	Value
Epicenter (latitude, longitude)	51.2°N, 182.7°E
Fault Length (km)	140
Fault Width (km)	70
Dip angle (degrees)	20
Rake angle (degrees)	108

*Source: Titov and González (1997).

a depth of 1550 m. The bottom pressure recorder (BPRs) locations are marked as Nos. 4 to 7.

Using the reference earthquake source parameter (Table 1), variations for the earthquake's epicenter, fault area, and dip and rake angles are simulated and compared. Table 2 lists the epicenter variation, while Tables 3 and 4 list the variation for fault dimensions and dip- and rake angles, respectively.

It can be seen in Table 3 that the slip values change as the fault dimension is varied. This has been done to preserve the earthquake's magnitude. It should be noted that the rupture size of an earthquake right after the event is not immediately available. High-quality data with months or even years of analysis are required to get a reasonable estimate. Several empirical formulas that relate the fault's size and rupture extent to the earthquake magnitude are currently used for quick evaluation of real-time tsunami assessment.

3.2.1 Sensitivity to epicenter

The characteristics of the tsunami waves generated from an earthquake source vary according to where the source is located. Its sensitivity is tested by varying the epicenter at seven different locations (Table 2). The strike angle values are adjusted to align with the Aleutian trench. To have a better view of the comparison, the timescale has been shifted to match that of the Andreanov tsunami arrival time.

Comparison at Gage 1 of the simulated results showed that the leading tsunami wave height is similar for almost all source locations, with the exception of source G (see Fig. A5 and Table 2), which is about half that of the other sources. The leading tsunami wave height at Gage 2 drops as the source location moves eastward. Source A is 2.7 times more than source G at Gage 2. This trend is reversed at Gage 3. Source G is 5.5 times that at Source A, which had the smallest amplitude. Cylindrical spreading causes the tsunami waves to decrease in height as they move further away from the generating source. Also, tsunami energy tends to be directional. The majority of the tsunami energy is propagating out at a right angle from the source region. The directionality of the tsunami beam is shown in Fig. A6, representing sources A and G with contours of maximum computed amplitudes. It can be seen that as the tsunami wave propagates off-shore, the amplitude is much higher in the direction which is perpendicular to the trench or the fault. The further away a coastal area is from the main beam the smaller

Table 2: Epicenter variation for sensitivity analysis*.

Sources	Lon °N	Lat °E	Length (km)	Width (km)	Strike (deg)	Dip (deg)	Rake (deg)	Depth (km)	Slip (m)
A	51.2	182.7	140	70	260	20	108	5	2
B	51.2	185.0	140	70	253	20	108	5	2
C	51.2	187.0	140	70	253	20	108	5	2
D	52.0	190.0	140	70	253	20	108	5	2
E	53.3	195.0	140	70	245	20	108	5	2
F	54.1	200.0	140	70	238	20	108	5	2
G	56.5	208.0	140	70	230	20	108	5	2

*Source: Titov *et al.* (1999).

Table 3: Fault dimension variation for sensitivity analysis*.

Sources	Lon °N	Lat °E	Length (km)	Width (km)	Strike (deg)	Dip (deg)	Rake (deg)	Depth (km)	Slip (m)
H	51.2	182.7	140	70	260	20	108	5	2
I	51.2	182.7	140	105	260	20	108	5	1.3
J	51.2	182.7	200	70	260	20	108	5	1.4
K	51.2	182.7	105	70	260	20	108	5	2.7
L	51.2	182.7	140	35	260	20	108	5	4
M	51.2	182.7	70	70	260	20	108	5	4

*Source: Titov *et al.* (1999).

Table 4: Dip and rake angle variations for sensitivity analysis*.

Sources	Lon °N	Lat °E	Length (km)	Width (km)	Strike (deg)	Dip (deg)	Rake (deg)	Depth (km)	Slip (m)
N	51.2	182.7	140	70	260	20	108	5	2
O	51.2	182.7	140	70	260	15	108	5	2
P	51.2	182.7	140	70	260	10	108	5	2
Q	51.2	182.7	140	70	260	20	90	5	2
R	51.2	182.7	140	70	260	20	100	5	2
S	51.2	182.7	140	70	260	20	120	5	2
T	51.2	182.7	140	70	260	20	135	5	2

*Source: Titov *et al.* (1999).

the tsunami amplitude will be. This is one factor in why the tsunami wave amplitude at Gage 1 for source G is much smaller than the other sources (see Fig. A6). Another factor is the bathymetry profile around the area of source G. The Gulf of Alaska has a series of seamounts that can affect the tsunami propagation characteristics, unlike other sources that are not affected by similar bathymetric features.

3.2.2 Sensitivity to fault dimensions

Sensitivity to fault dimensions was tested by varying the fault area as listed in Table 3. Comparison was made by maintaining the earthquake seismic moment ($M_o = 7.3 \times 10^{20}$ N·m); thus the slip values were adjusted according

to Equations 1 and 2. Results showed that even with a three-fold increase in the slip value (sources L and M in Table 3, with the corresponding fault dimensions) the leading tsunami wave height was within 25% of the maximum at Gages 1 and 2 (Fig. A7). The gages near the continental coast (Gages 3 and 4) showed more difference for the leading tsunami waves, but are within 50% of the maximum at these gages.

3.2.3 Sensitivity to dip and rake angles

A small variation of the dip and rake angles was tested for sensitivity of the tsunami wave heights. The epicenter of the source region is based on the Andreanov earthquake as shown in Table 5.

The dip angle was tested between 10° and 20° with a 5° increment. A 10° to 20° range is typical of the subduction earthquakes in the AASZ. Simulated results show that the leading tsunami waves (comparison at gages 1 and 2) increased by 30%, but the wave period and profile of the first wave were very similar for all the dip values (Fig. A8).

The variation of the rake angle ranges from a pure dip-slip mechanism (rake = 90°) to a 50% strike-slip mechanism with a rake value of 135°. Comparing the simulated results at Gages 1 and 2, the tsunami wave height did not show a significant variation (Fig. A9). The leading tsunami wave height for a strike-slip component is 20% less that a pure dip-slip one.

The earthquake source parameters that are available after an earthquake event are preliminary. Real-time data inversion of the tsunami signal obtained by the Deep-ocean Assessment and Reporting of Tsunamis (DART™) buoys will refine the tsunami source. However, the results of the sensitivity tests establish the fact that the far-field tsunami time series is only sensitive to the earthquake's epicenter and magnitude, which can be obtained with considerable accuracy. Variations of the other source parameters tested (i.e., fault dimensions, dip and rake angles) do not change the tsunami signal significantly.

4. The Forecast Propagation Database

This section describes how the unit source was defined, the regions it is applied to, and its validation with two real tsunami events.

4.1 Defining Unit Sources

The earthquake source region selected for the propagation database is based on a typical subduction mechanism with a moment magnitude (M_w) of 7.5. This is referred to as a unit source. These unit sources are arranged side-by-side along the subduction zones (trench axis) or earthquake source regions forming a continuous line of faults, and are referred to as B unit sources. A second set of unit sources is placed in parallel with the B unit sources, referred to as the A unit sources, which are located on the deeper part

Table 5: Number of unit sources for Pacific, Atlantic, and Indian Basins.

Location	No. of unit sources
Aleutian-Alaska-Canada-Cascadia Subduction Zone	130
Central America Subduction Zone	72
Columbia-Ecuador Subduction Zone	36
South America Subduction Zone	98
South Chile Subduction Zone[a]	30
New Zealand-Kermadec-Tonga Subduction Zone	78
New Britain-Solomons-Vanuatu Subduction Zone	74
Manus Ocean Convergence Boundary	34
North New Guinea Subduction Zone	30
East Philippines Subduction Zone	38
Ryukyu-Kyushu-Nankai Subduction Zone	44
Yap-Marianas-Izu Bonin Subduction Zone	78
Kamchatka-Kuril-Japan Trench Subduction Zone	62
South New Zealand Subduction Zone	14
Sub-total (Pacific Basin)	818
Atlantic Subduction Zone	184
Indian Ocean Subduction Zone	138
Makran Subduction Zone	20
Total	1160

[a]Overlap of 2 unit sources with South America

of the fault. Figure A10 shows the locations of the A and B unit sources in the Pacific, Atlantic, and Indian oceans. Table 5 lists the number of unit sources with the corresponding region name for the entire propagation database. The fault plane between the A and B unit sources is continuous, since the shallower edge of the A unit source is connected to the deeper edge of the B unit source (Fig. A11). Depending on the characteristics of the region, additional rows of unit sources might be added in the near future.

Based on the Aleutian Alaska Subduction Zone (AASZ) asperities (Johnson, 1998), the dimension of the unit source fault plane is selected at 100×50 km^2. The fault length is 100 km while the fault width is 50 km. This unit source earthquake fault dimension is used for the entire Pacific Basin. The strike angle for each unit source is set to align with the orientation of the subduction zone locally. Each pair (both A and B) of unit sources will have the same strike angle. The rake angle is set at 90°, since this is the most effective value for tsunami generation. The slip value for each unit source is set at 1 m.

The dip angle and depth values are based on a study by Kirby *et al.* (personal communication, 2005). In the absence of a depth value, the B unit source uses a value of 5 km, since it is believed that shallow faulting of large subduction zones are most effective in the generation of tsunamis. The depth value of the A unit source is easily calculated using simple trigonometry (see Fig. A11):

$$A_d = B_d + 50(\sin \delta) \tag{6}$$

where:

$$A_d = \text{depth of } A \text{ unit source}$$
$$B_d = \text{depth of } B \text{ unit source}$$
$$\delta = \text{dip angle of } B \text{ unit source}$$

If new data are available for depth value, those B unit sources that have a depth value of 5 km will then be updated, together with the A unit sources, and re-simulated.

The propagation runs do not include inundation and a vertical wall is placed at 20 m water depth. Simulation runs are done on a 4 arc-minute resolution but saved on a 16 arc-minute resolution to minimize file size. The simulation time step is 15 seconds for the regular Pacific grid (120°E to 292°E and 62°N to 50°S), 12 seconds for the extended Pacific grid (120°E to 292°E and 62°N to 74°S), 10 seconds for the Atlantic grid (105°W to 20°E and 72°N to 72°S) and 12 seconds for the Indian ocean grid (0°E to 60°E and 32°N to 70°S). The time steps are based on CFL stability criteria. Time step resolution for the output file is 1 minute. The total simulation time is 24 hours, with the exception of the East Philippines and North New Guinea sources, which were simulated for 30 hours. Discussions on the two different Pacific grids and the two simulation run times used in the simulations are in Section 5.2.

4.2 Forecast Propagation Database Validation

The main idea of the unit sources was that a finite combination would reproduce as close as possible to the actual tsunami time series. Preliminary forecast of the ocean wide tsunami time series are quickly produced by combining unit sources once the initial earthquake parameters (epicenter and magnitude) are obtained from the Tsunami Warning Center (TWC). Once the DART™ buoy(s) receives the actual tsunami wave, inversion is then performed to adjust the slip distribution of the selected unit sources or add unit sources as needed. This methodology was verified with ten real tsunami events since 2003 and a few are presented in this report, namely: the 4 October 1994 Kuril Island (Yeh *et al.*, 1995), the 17 November 2003 Rat Island (Titov *et al.*, 2005), and 15 November 2006 Kuril tsunamis.

For the 4 October 1994 Kuril Island tsunami, inversion was done from five DART™ buoy records and the forecast showed good comparison as seen in Fig. A12. When the closest DART™ buoy (Sta. 46401-D171) recorded the actual tsunami waves of the 17 November 2003 Rat Island tsunami, adjustments were made and the forecast even had an excellent comparison with the tsunami records at other locations (Fig. A13). In fact, the forecast gave a better estimate of the earthquake magnitude (M_w = 7.7–7.8) as confirmed later by USGS seismic analysis (M_w = 7.8) (NEIC, 2003), where the initial earthquake magnitude was M_s = 7.5 as provided by West Coast/Alaska TWC. It took only 1 hour 20 minutes after the earthquake to provide an accurate forecast.

Combining the propagation database and real-time DART™ data from the tsunameters, tsunami waves were predicted well before the actual waves

hit the coastlines. This again was demonstrated for the 15 November 2006 Kuril tsunamis. Figure A14 shows the good comparison between the DART™ time series and that based on inversion.

Although not part of the TWC operation, the validations of the propagation database with real events show that sets of pre-computed unit sources can be combined to produce tsunami scenarios that would closely match the recorded data from the tsunameters from real tsunamigenic events. The methodology is not only accurate but also very efficient, considering that an accurate forecast is provided a few hours after a tsunamigenic event.

5. Propagation Database Issues

With the unit source defined, simulation was done for the entire Pacific, Atlantic, and Indian oceans and stored in a database. Validation with ten real tsunami events since 2003 demonstrated that the forecast propagation database methodology can reproduce the tsunami signal of the actual event. This section investigates several non-critical issues, proposed solutions, and aspects of using the database itself for forecasts.

5.1 Initial Forecast Using M_w

Each unit source has been simulated and the tsunami wave height, ha, and u and v, velocity components stored in a database. Tsunami scenarios can then be constructed from a combination of unit sources by exploiting the linearity of the generation/propagation dynamics to match closely the actual tsunami wave amplitude recorded by the DART™ buoys. Initial forecasts will require the input of an earthquake magnitude and location. Once the tsunami wave has been detected by the DART™ buoys, then the initial model predictions from the propagation database will be adjusted to provide a more accurate prediction.

The unit sources are based on an earthquake magnitude, M_w, of 7.5. Using the linearity dynamics of generation and propagation, the tsunami amplitudes for an $M_w > 7.5$ are quickly estimated by multiplying numerical values in the database. These numerical values are obtained using Equations 1 and 2. For example, if we consider one unit source with an $M_w = 8.5$, with only u_o as the unknown, using Equations 1 and 2 would yield an average slip value, u_o, of 31.55 m. The value of 31.55 m will be the multiplying factor for the unit source database.

However, an average slip value of 26.6 m to 37.4 m can still produce an $M_w = 8.5$ when using Equations 1 and 2. Unit source B11 in the East Philippines was chosen arbitrarily to investigate by how much the tsunami amplitude would differ. Figure A15 shows the comparison at three deep ocean regions: near the source, Hawai‘i, and South America regions. An average slip of 31.55 m yields a tsunami wave time series that is ±20% from the two extremes (i.e., 26.6 m and 37.4 m), as seen in Fig. A16.

The ±20% variation in the forecasted tsunami wave time series is not an error range produced by the MOST propagation code. This variation is inherent in the equations for calculating the M_w (Equation 2) due to rounding off. Data inversion will provide a more accurate forecast with the adjusted tsunami source. Care must be taken when only seismic data is used to obtain the tsunami propagation forecast.

5.2 Extent of Pacific Grid Domain and Total Run Time

As the number of unit sources expand in the database, the need for possibly extending the previous Pacific grid (which covers 120°E to 292°E and 62°N to 50°S) became apparent, especially for the unit sources south of the South America region, and due to the presence of the great circle routes of tsunami propagation in the Antarctic. Using the propagation database, unit source A37 in the South America Subduction Zone was selected to determine the difference of the tsunami time series between using the regular Pacific grid and the extended Pacific grid (which covers 120°E to 292°E and 62°N to 70°S) at a station south of Australia (130°E, 40°S; see Fig. A17).

As the propagating tsunami moves toward Australia, it clearly show the difference between the Pacific grid that stops at 50°S from that at 74°S (Fig. A17). The open boundary at 50°S prevents the tsunami waves from traveling the great circle in that region, however; the additional 24° to the south puts this into the path of the propagating tsunami waves. The leading tsunami wave on the extended Pacific grid does not exist on the regular Pacific grid at time step 791 (Fig. A17). A plot of the tsunami time series for the regular Pacific grid shows that the entire tsunami time series of the previous grid is one order of magnitude smaller than the first wave alone using the extended grid (Fig. A18). A plot of the maximum wave height distribution (Fig. A19) shows that much higher maximum wave heights cover the entire northern coast and almost the entire eastern coast of New Zealand when using the extended Pacific grid as compared with the regular Pacific grid.

Another aspect investigated was the total number of hours required for each unit source simulation in the propagation database. The majority of the unit sources cover 24 hours of tsunami time series; a few (North New Guinea and East Philippines) cover 30 hours, since the leading tsunami wave would barely reach central South America. Using the same unit source (A37 in the South America Subduction Zone), the time series was checked near Japan (130°E, 30°N, Fig. A17). Figure A19 shows that the first wave was not completely simulated at this location, indicating that 24 hours or 30 hours of tsunami time series might not be enough to be able to capture the maximum tsunami wave.

Recognizing these two issues is crucial, although not critical, for the propagation database, especially since it is an offshore forecast tool, it should be noted that the 22 May 1960 Chile tsunami did reach Japan. These issues will be resolved by determining the maximum grid extent to be used for the Pacific Ocean, as well as the total run time, by conducting tests. Once

it has been determined, the propagation database will then be updated. It should be noted that the current issues do not affect the current propagation database, because there are sufficient tsunami time series for the Alaskan-Aleutian, U.S. West coast, and Hawai'i regions from all the unit sources.

6. Propagation Database Forecast

The output of the propagation database not only serves as input for the SIMs, but in itself can be used for offshore tsunami forecasts. As previously shown (see Section 4.2), a combination of unit sources can reproduce tsunami scenarios quickly, showing the offshore tsunami wave characteristics for the Pacific, Atlantic, or Indian ocean domains and offshore forecast for specific locations. Obtaining the arrival time, distribution of the first tsunami wave height, maximum wave height, and tsunami beam quickly are invaluable information needed for hazard mitigation.

A sample snapshot (Fig. A20) shows the first wave and maximum wave forecast in webSIFT using a single unit source located at the Aleutians with an earthquake M_w of 7.5. Plotting the forecast tsunami first wave height at selected offshore points in Pacific coasts can also be provided (Fig. A21). Information obtained can immediately provide assessments on which areas will primarily be affected by the simulated tsunami waves. It is also possible to include arrival time. This can serve as a guideline for prioritizing the inundation forecast of coastal areas using the SIMs.

The propagation database can also be used to determine the tsunami risk to a specific coastal area and which source region would provide the most threat. For illustrative purposes, using only one unit source, several earthquake scenarios with M_w values of 7.5, 8.0, 8.5, and 9.0 were generated and the tsunami's first wave height was determined for Hilo Bay, Hawai'i. A snapshot for sources from Ryukyus-Nankai, East Philippines, and North New Guinea subduction zones are shown in Fig. A22. Comparing the three subduction zones, the East Philippines source especially, the mid-section shows more of a threat for Hilo as compared with Ryukyus-Nankai and North New Guinea sources. It can also be seen that although the tsunami waves arrive close to 11 hours after the generation, the first wave from East Philippines unit source B11 is the highest compared to Ryukyus-Nankai and North New Guinea sources, which arrived at a much earlier time.

The forecast capability of the propagation database provides invaluable information to the TWC personnel. The propagation database forecast results can provide guidelines on prioritizing which specific coastal site needs immediate attention during a real tsunami event.

7. Conclusions

The operational tool that will provide quick and accurate tsunami forecasts, developed by the NCTR, has been tested to be efficient and accurate. The method referred to as Short-term Inundation Forecast for Tsunamis (SIFT) uses data inversion technique and SIMs. One of the key components of this system is the pre-computed earthquake scenarios (forecast propagation database). The pre-computed tsunami scenarios are simulated from a unit source with an earthquake moment magnitude, M_w, of 7.5. Unit sources have been established in the known and potential earthquake regions with a total of 1160 sources for the Pacific, Atlantic, and Indian oceans, (including Makran sources, not shown in Fig. A10). Exploiting the linearity of the generation/propagation, a combination of these unit sources can simulate tsunami scenarios. Tests conducted with real-time tsunami events show that, with data inversion, it can closely match the actual tsunami time series. Other than its accuracy, prediction of the tsunami wave signal took just 1.5 hours after the 17 November 2003 Rat Island earthquake event several hours before the actual waves hit the coastlines of Hawai'i, Alaska, and the U.S. West Coast. Accuracy of the source parameters might come into question; however, sensitivity tests conducted show that only the earthquake's epicenter and magnitude would cause a significant variation in the far-field tsunami time series using the MOST code. Also, data inversion of the tsunami signals obtained from the DART™ buoys will refine the tsunami source.

A few non-critical issues on the use of the propagation database for preliminary forecasts were investigated. Several values of slip can produce the same earthquake seismic magnitude, M_w, when using Equations 1 and 2, due to a one-decimal-place rounding. However, if slip value is to be obtained directly from Equations 1 and 2 with known fault dimensions and earth's rigidity, μ, the resulting slip value is roughly 1.4% below the average of the lowest and highest possible slip values producing the same M_w. This value is used as a multiplying factor for the propagation database for $M_w > 7.5$. Tests conducted show that the tsunami time series of the forecast propagation database is $\pm 20\%$ that of the lowest and highest possible slip values under the same M_w. This will not be an issue when data inversion is used, but should be kept in mind if a real-time tsunami signal is not available.

The other non-critical issues were the extent of the Pacific domain and the total simulation hours in the propagation database. Test results show that the presence of the great circle in the Antarctic could potentially pose a tsunami threat to South Australia as opposed to no threat, especially from sources in South America when the simulation domain does not include the great circle. Total simulation time was either 24 hours or 30 hours, since the tsunami signal for some sources (e.g., East Philippines and North New Guinea) would barely reach certain areas on the other side of the Pacific. The

reason for limiting simulation to 30 hours is that the tsunami signal would reach most of the regions on the other side of the Pacific basin, and would also generate a smaller output file size. However, it has been recognized that the non-critical issues of the extent of the Pacific domain and total simulation hours in the propagation database might pose a problem in the future. These issues are currently being resolved by conducting tests on what the maximum extent of the Pacific domain should be, including the total simulation hours, so as to obtain sufficient tsunami time series on either side of the Pacific basin.

The output of the forecast propagation database not only serves as input for the SIMs that numerically predict the tsunami wave height, current speeds, and inundation extent of a specific coastal area of interest, but can be used to forecast offshore tsunami wave heights at any specified location in the Pacific, Atlantic, and Indian oceans. Regional and site-specific first and maximum wave height and arrival time can be plotted quickly. It is also possible to plot the offshore wave height distribution for the entire Pacific, Atlantic, and Indian ocean coasts. This will graphically show the coastal areas that have a higher risk of tsunami threat during an actual event.

8. Acknowledgments

This publication is contribution 2937 from NOAA/Pacific Marine Environmental Laboratory and funded by the Joint Institute for the Study of the Atmosphere and Ocean (JISAO) at the University of Washington under NOAA Cooperative Agreement No. NA17RJ1232, JISAO contribution 1452. The authors would also like to thank R.L. Whitney for comments and edits, and Christopher Moore for providing the images for Figure A10.

9. References

González, F.I., E.N. Bernard, C. Meinig, M. Eble, H.O. Mofjeld, and S. Stalin (2005): The NTHMP tsunameter network. *Nat. Hazards*, *35*(1), Special Issue, U.S. National Tsunami Hazard Mitigation Program, 25–39.

Johnson, J. (1998): Heterogeneous coupling along the Alaskan-Aleutians as inferred from tsunami, seismic, and geodetic inversions. *Adv. Geophys.*, *39*, 1–116, (R. Dmowska, ed.), Academic Press.

Kirby, S., E. Geist, W.H.K. Lee, D. Scholl, and R. Blakely (2005): Tsunami source characterization for Western Pacific subduction zone: A preliminary report. USGS Tsunami Subduction Zone Working Group (personal communication).

NEIC (2003): Poster of the Rat Islands, Alaska earthquake of 17 November 2003—Magnitude 7.8. `http://neic.usgs.gov/neis/poster/2003/20031171.html`.

Okada, Y. (1985): Surface deformation due to shear and tensile faults in a half-space. *Bull. Seismol. Soc. Am.*, *75*, 1135–1154.

Scripps Institution of Oceanography (2004): Satellite geodesy. `http://topex.ucsd.edu/WWW_html/srtm30_plus.html`.

Smith, W.H.F., and D.T. Sandwell (1994): Bathymetric prediction from dense satellite altimetry and sparse shipboard bathymetry. *J. Geophys. Res.*, *99*, 21,803–21,824.

Titov, V.V. (1997): Numerical modeling of long wave run-up. Ph.D. thesis, University of Southern California, Los Angeles, California, 141 pp.

Titov, V.V., and F.I. González (1997): Implementation and testing of the Method of Splitting Tsunami (MOST) model. NOAA Tech. Memo. ERL PMEL-112 (PB98-122773), NOAA/Pacific Marine Environmental Laboratory, Seattle, WA, 11 pp.

Titov, V.V., F.I. González, E.N. Bernard, M. Eble, H.O. Mofjeld, J. Newman, and A.J. Venturato (2005): Real-time tsunami forecasting: Challenges and solutions. *Nat. Hazards*, *35*, 41–58.

Titov, V.V., H.O. Mofjeld, F.I. González, and J.C. Newman (1999): Offshore forecasting of Alaska-Aleutian Subduction Zone tsunamis in Hawaii. NOAA Tech. Memo. ERL PMEL-114, (NTIS PB2002-101567), NOAA/Pacific Marine Environmental Laboratory, Seattle, WA, 22 pp.

Yeh, H., V.V. Titov, V. Gusiakov, E. Pelinovsky, V. Khramushin, and V. Kaistrenko (1995): The 1994 Shikotan earthquake tsunami. *Pure Appl. Geophys.*, *144*(3/4), 569–593.

Appendix A. Figures

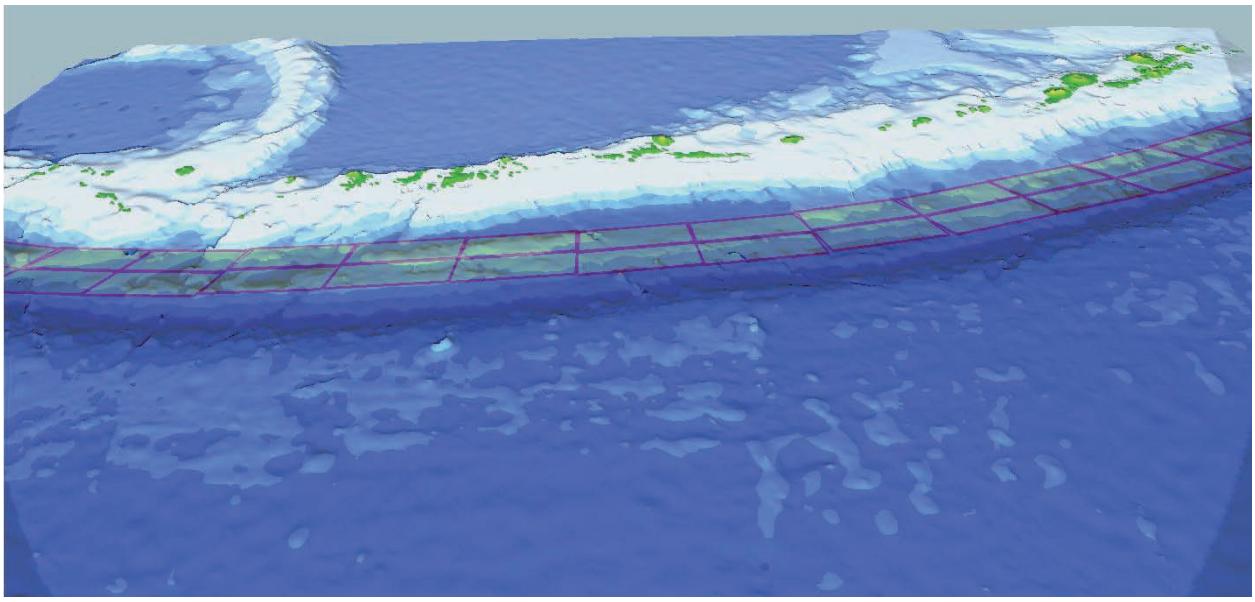

(a) aerial view

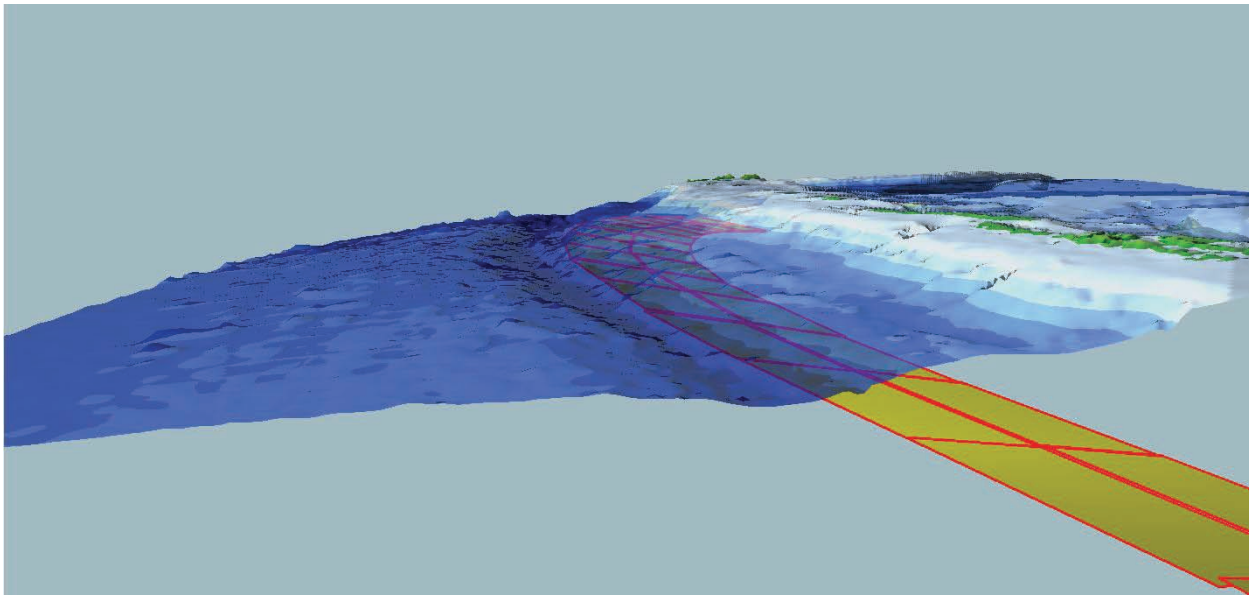

(b) side aerial view

Figure A1: Unit sources along the Aleutian Islands.

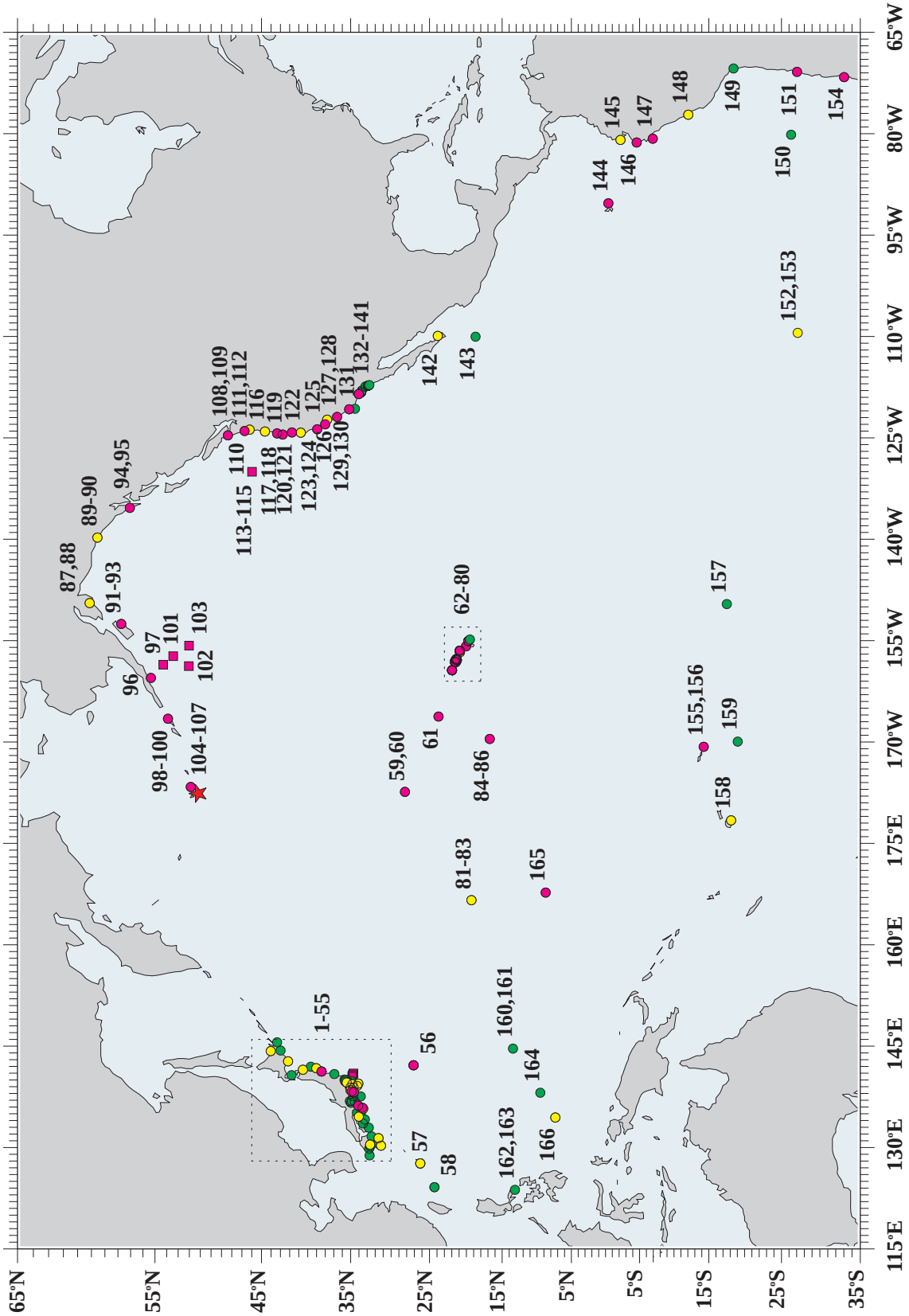

Figure A2: Pacific map with the 1996 Andreanov epicenter (star) and tsunami stations. Deep ocean BPR data (stations 97, 101–103 and 113–115) compared with MOST propagation model output. Source: Titov and González (1997).

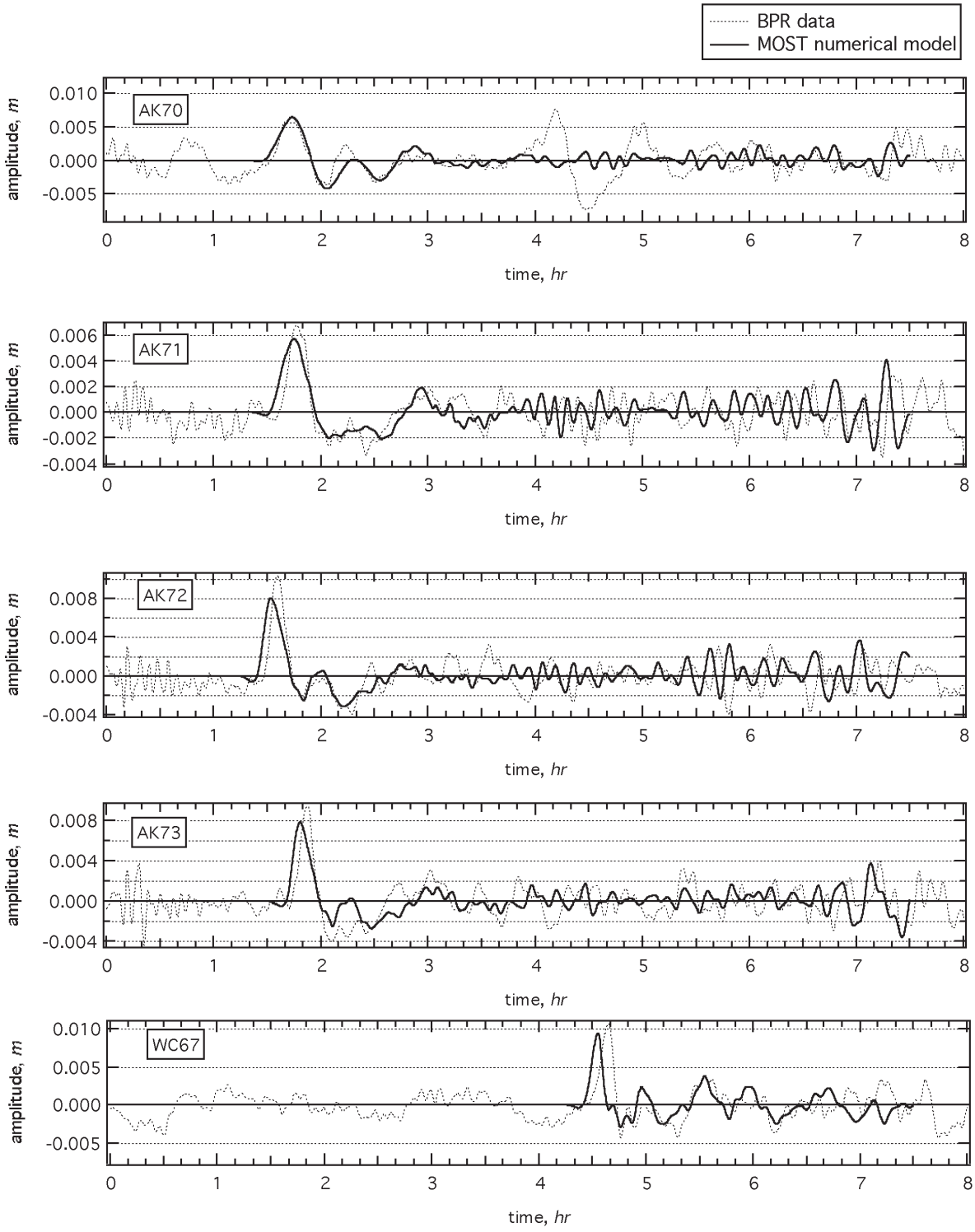

Figure A3: Comparison of simulated tsunami wave with BPR's for the 1996 Andreanov tsunami. Source: Titov and González (1997).

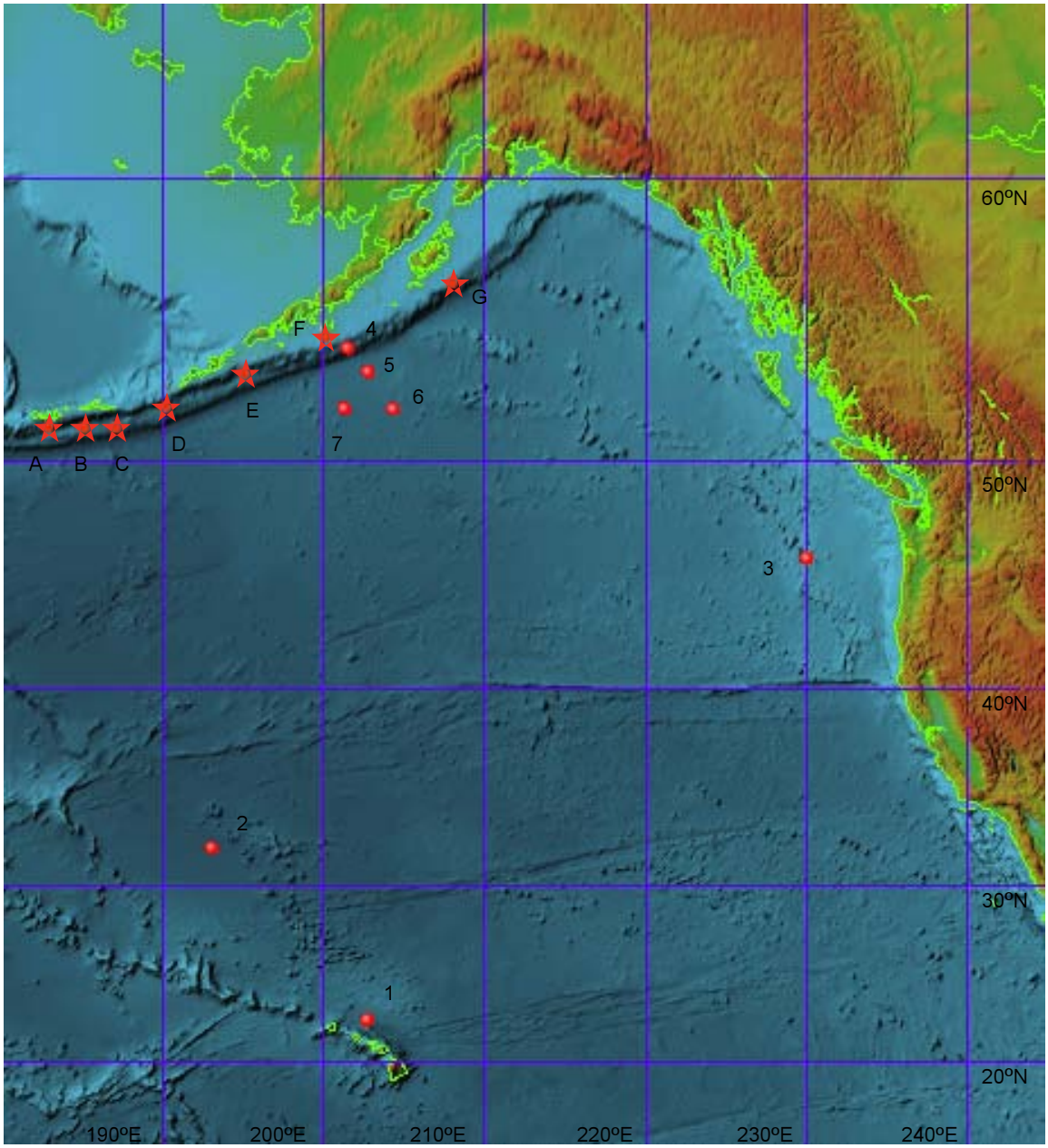

Figure A4: Bathymetry of the computational area, location of wave gages (red dots) and earthquake epicenters (red stars) for the sensitivity tests. Source: Titov *et al.* (1999).

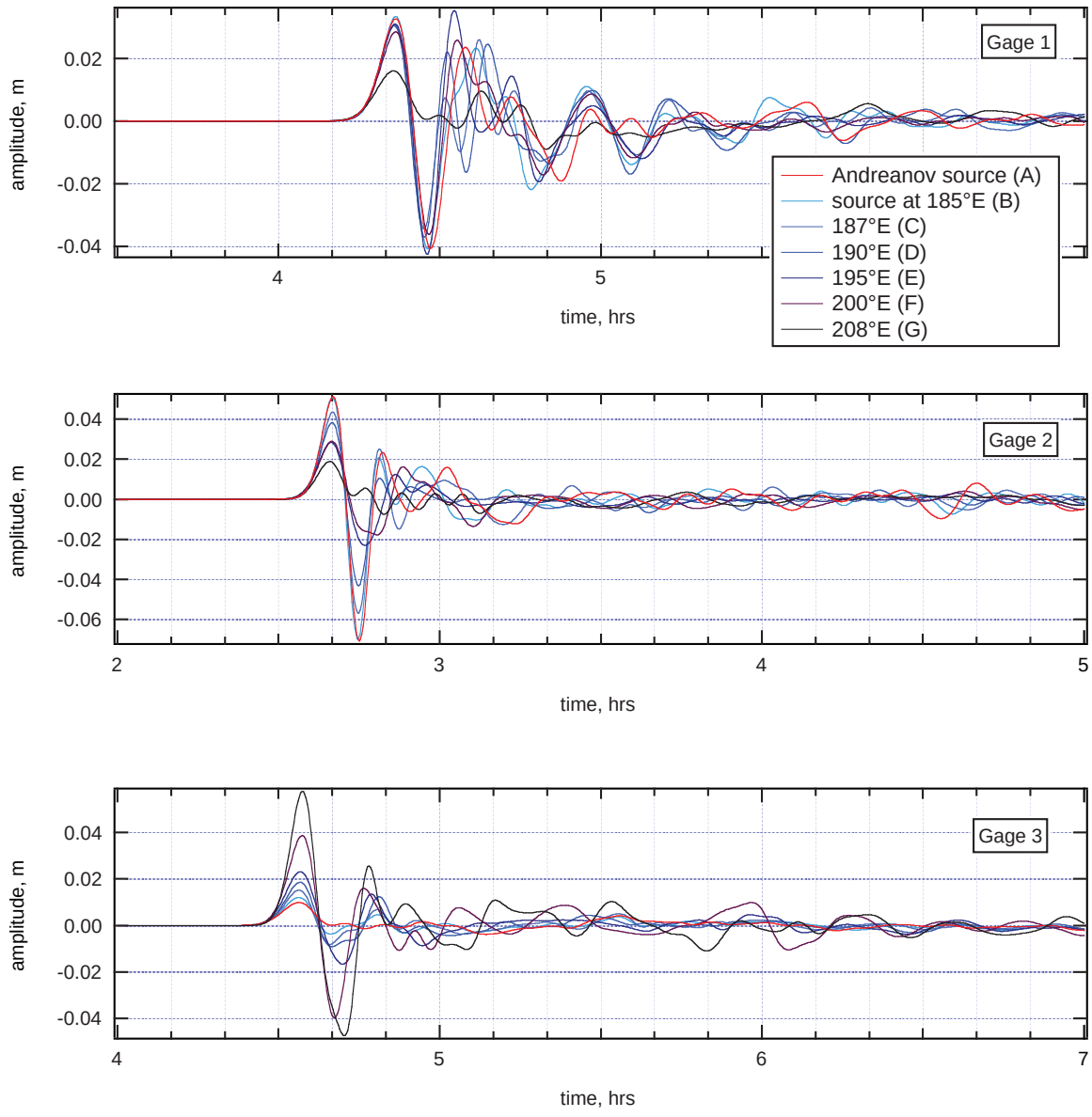

Figure A5: Tsunami time series from different source locations. Time scale shifted to match that of the 1996 Andreanov tsunami for comparison. Source: Titov *et al.* (1999).

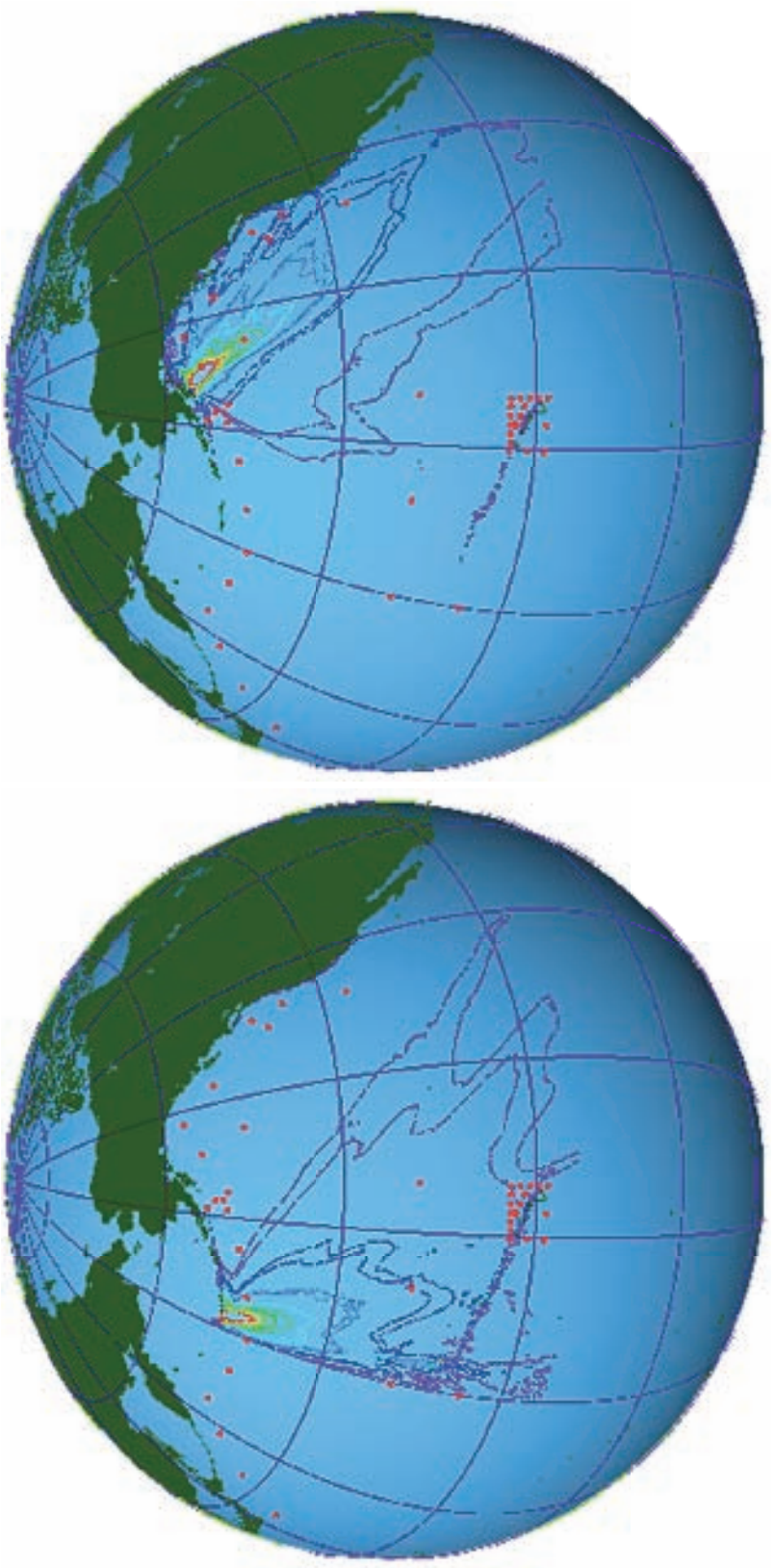

(a) (b)

Figure A6: Directionality of generated tsunami. Source: Titov *et al.* (1999).

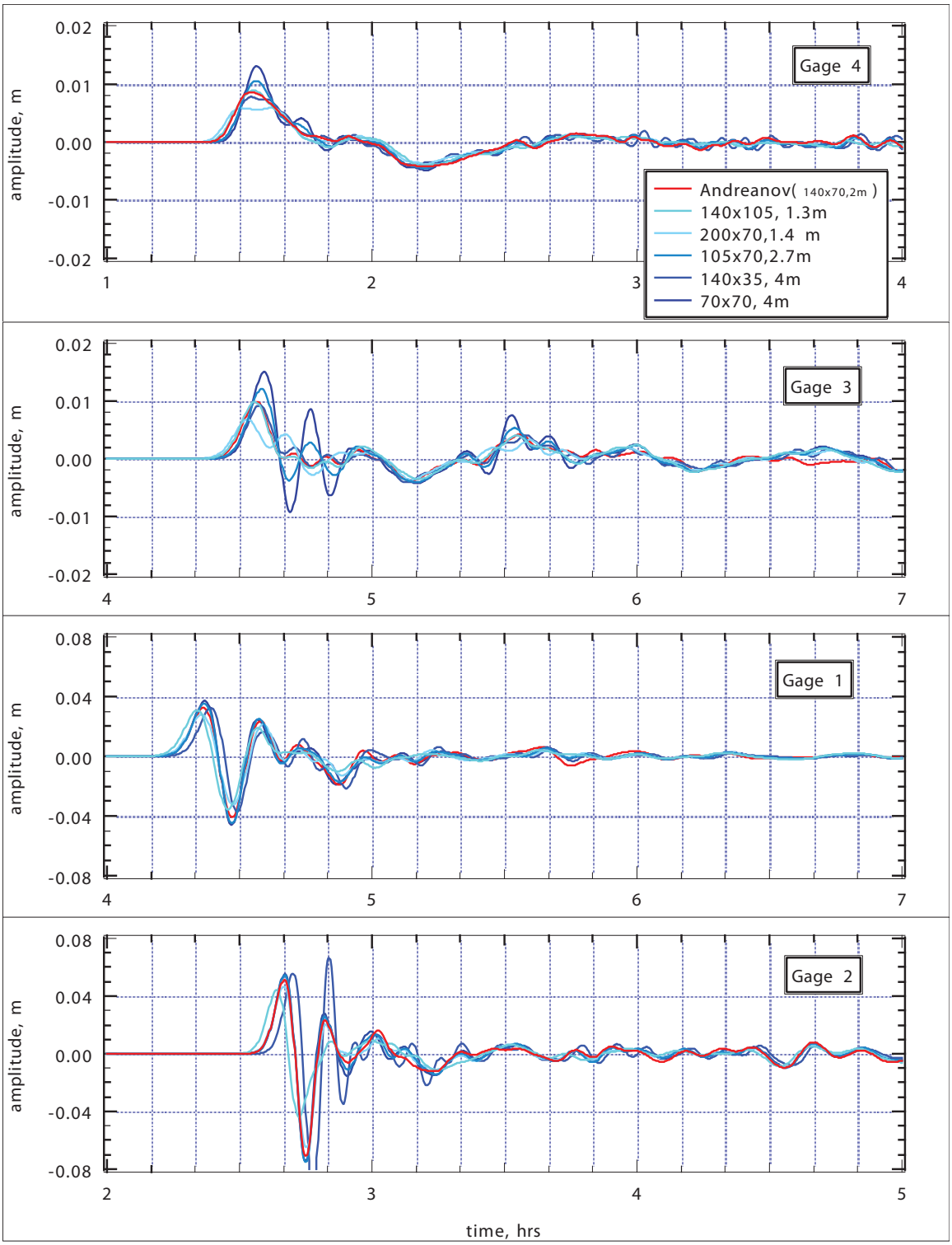

Figure A7: Tsunami time series comparison due to fault sensitivity. Source: Titov *et al.* (1999).

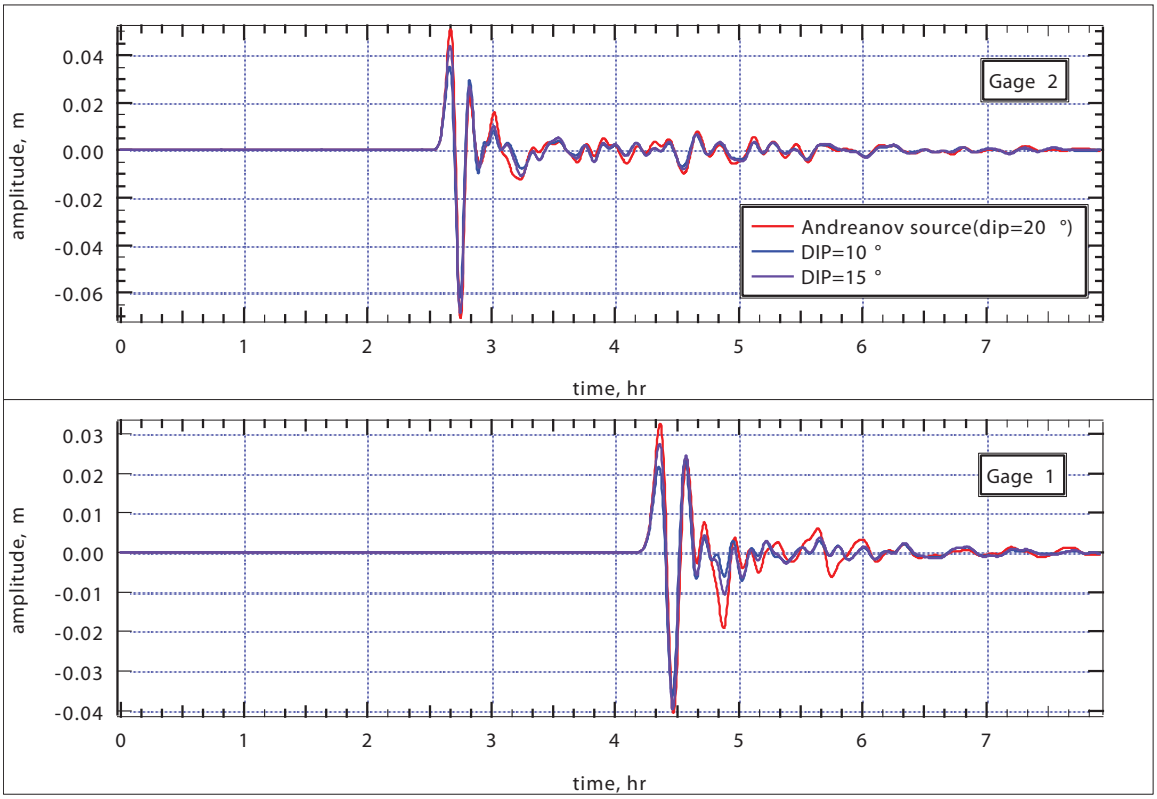

Figure A8: Tsunami time series comparison due to dip angle sensitivity. Source: Titov *et al.* (1999).) .

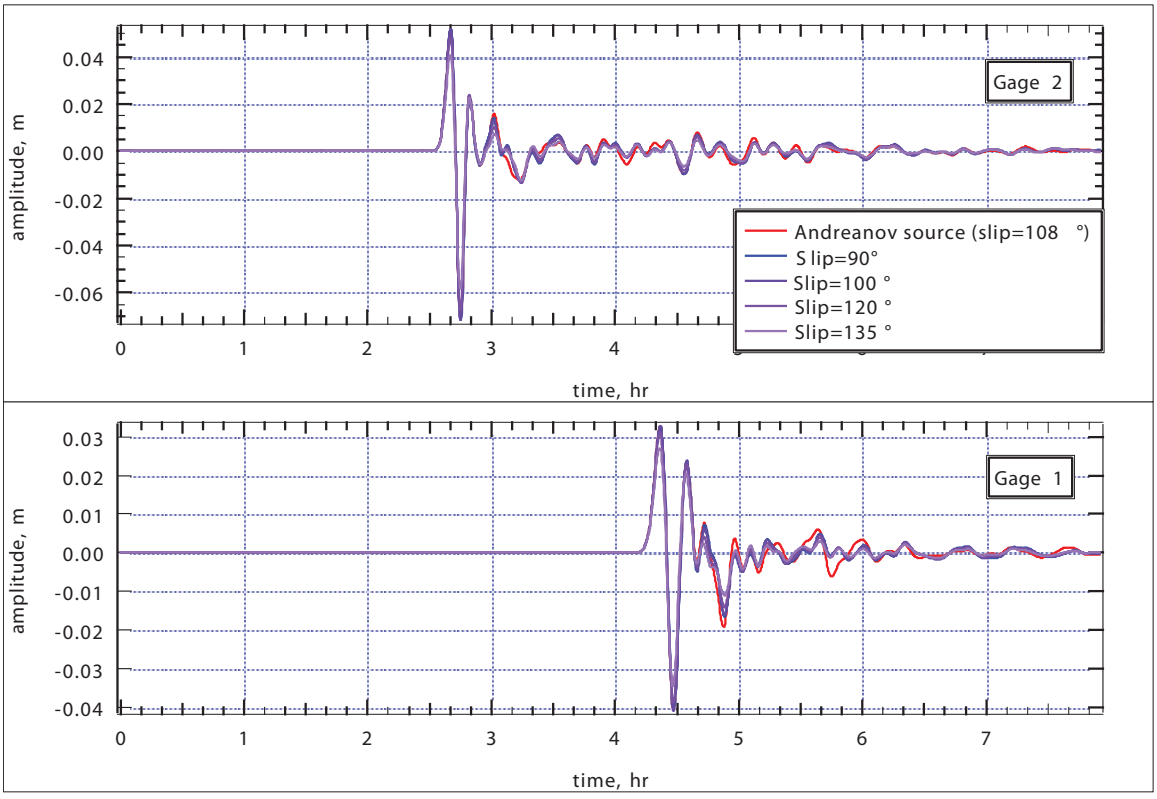

Figure A9: Tsunami time series comparison due to slip angle sensitivity. Source: Titov *et al.* (1999).

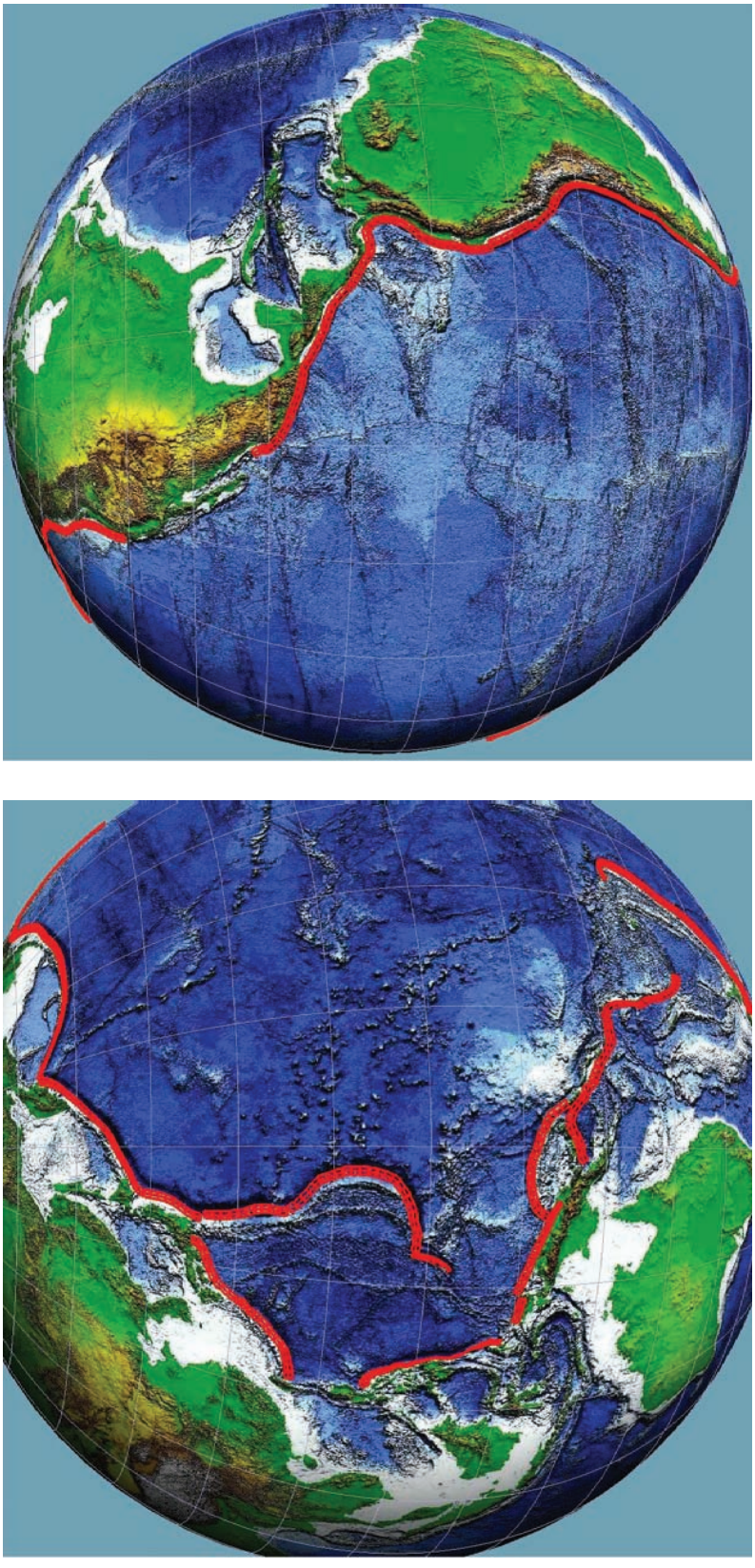

(a) West Pacific (b) East Pacific

Figure A10a,b: 818 unit sources for the Pacific Ocean.

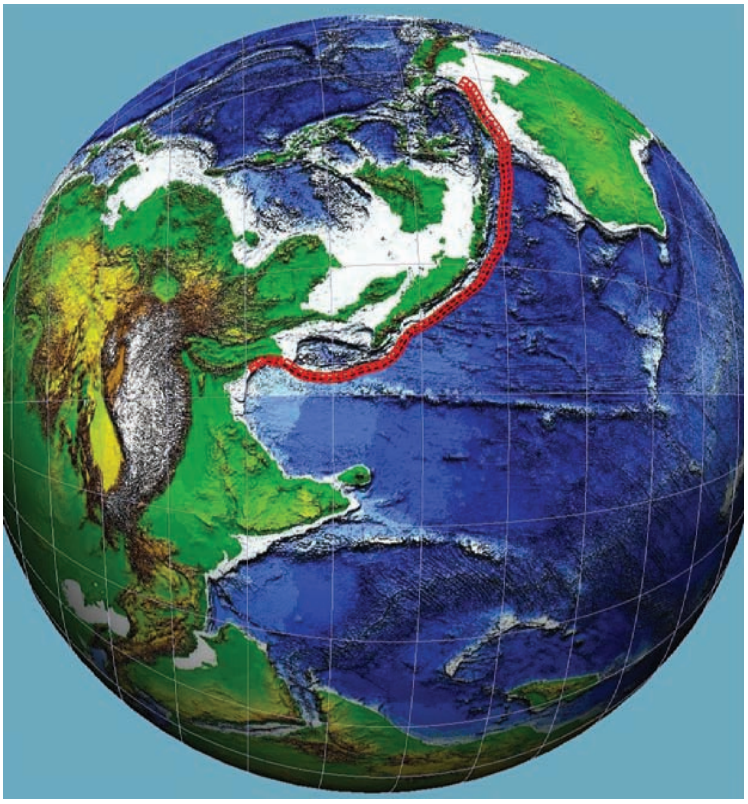

(d) Indian

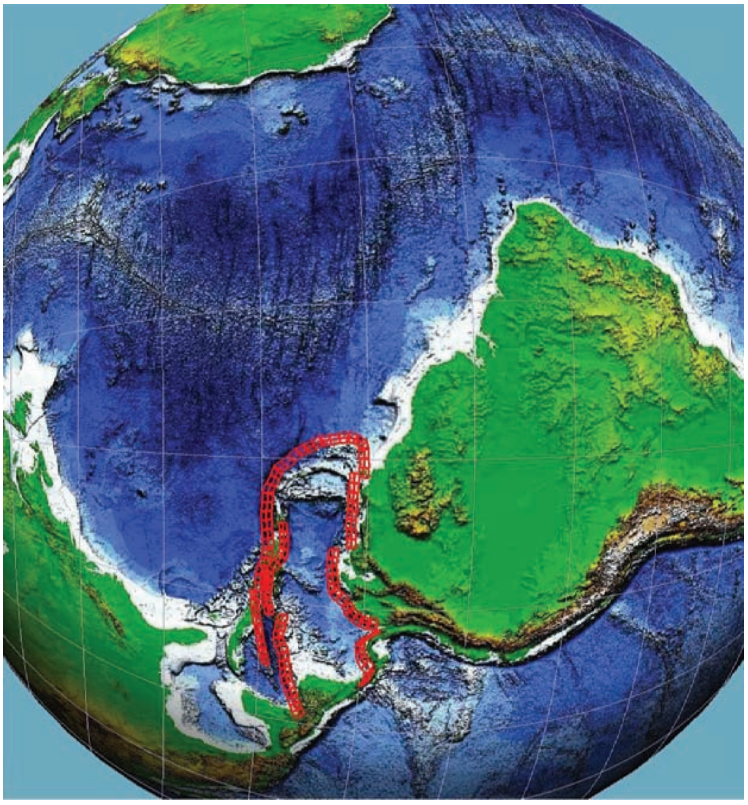

(c) Atlantic

Figure A10c,d: 184 unit sources for the Atlantic Ocean and 158 unit sources for the Indian Ocean (Makran sources not shown).

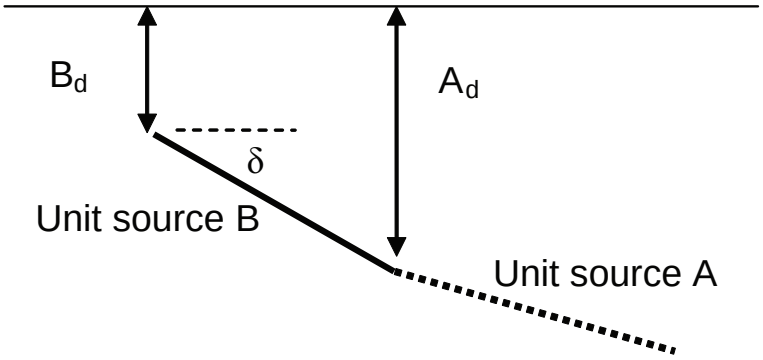

Figure A11: Sectional sketch of unit sources A and B.

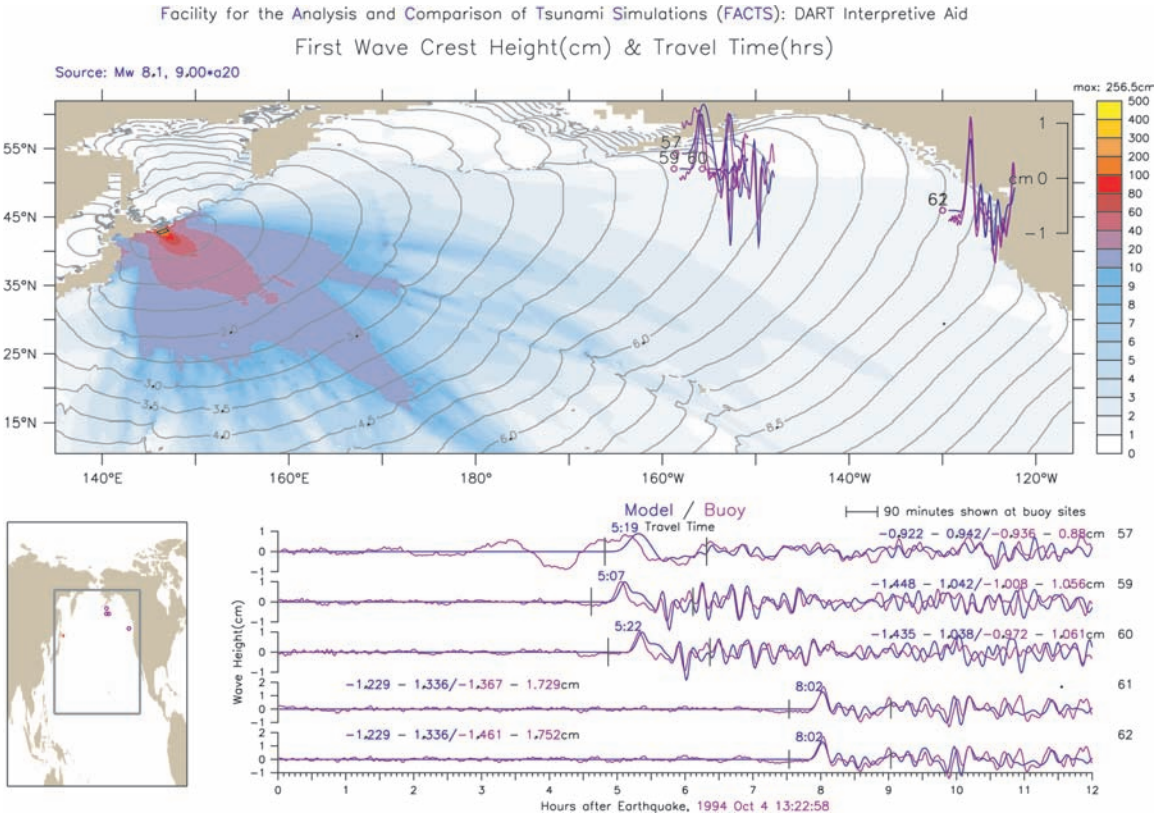

Figure A12: Propagation database forecast comparison with BPR records for the 1994 Kuril Island tsunami.

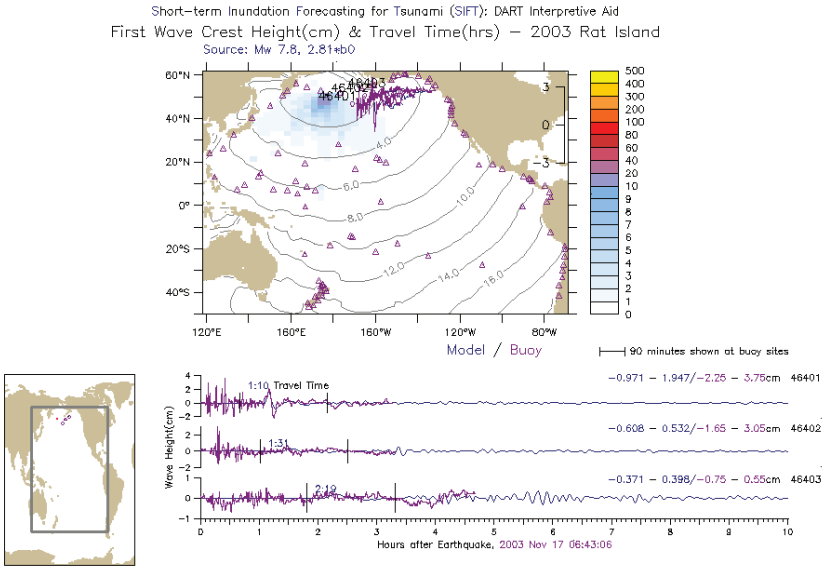

Figure A13: Propagation database forecast comparison with DART™ records for the 2003 Rat Island tsunami (blue line = model, purple line = buoy data).

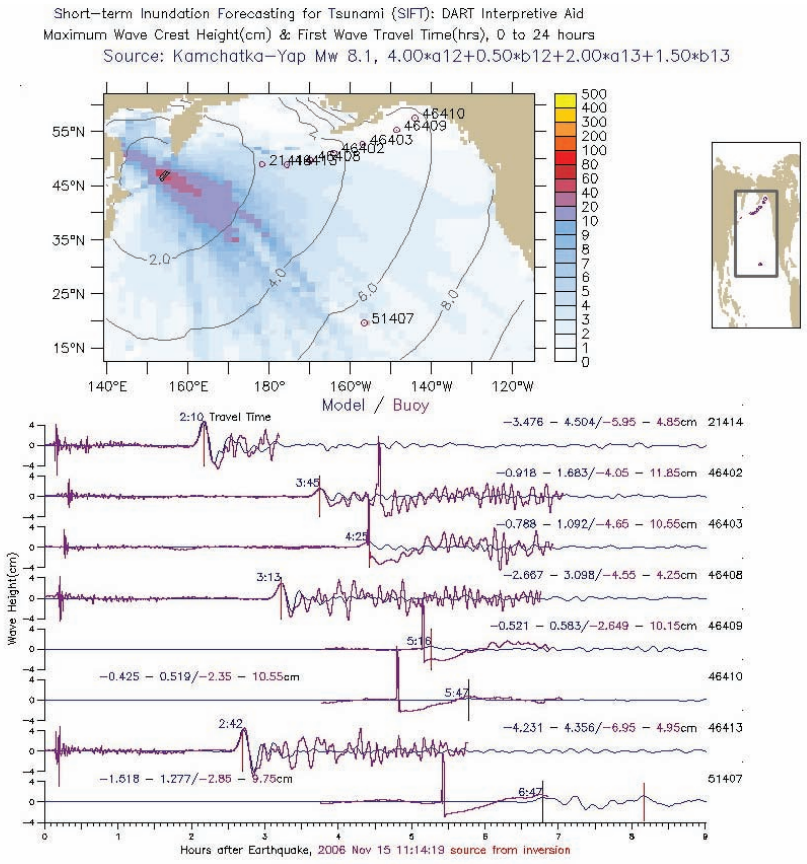

Figure A14: Propagation database forecast comparison with DART™ records for the 15 November 2006 Kuril tsunami (blue line = model, purple line = buoy data).

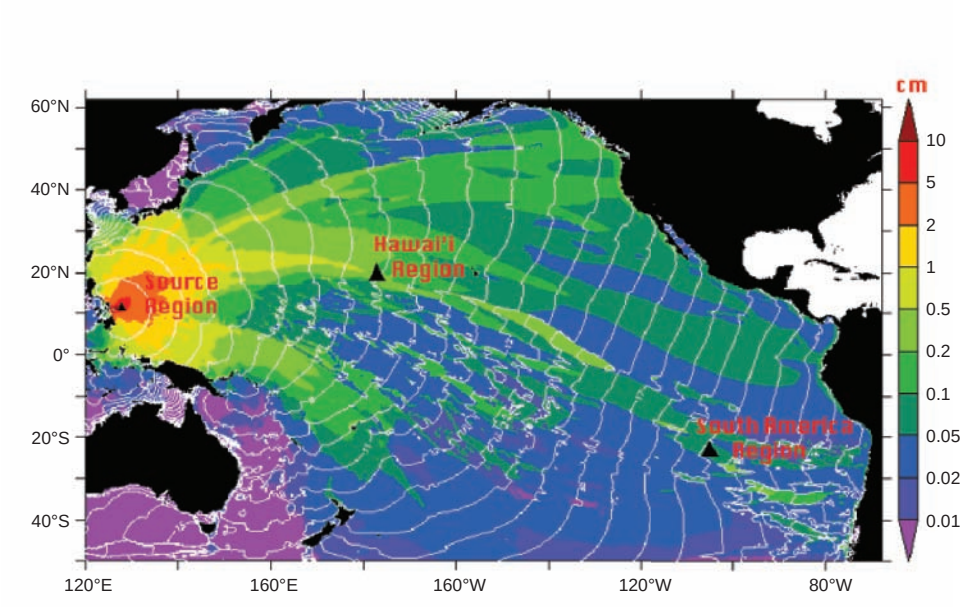

Figure A15: Location of offshore gages for comparison between MOST and SIFT results. Color shade is the distribution of the tsunami's first wave and the white lines are time of arrival (hourly). Source is East Philippines unit B11.

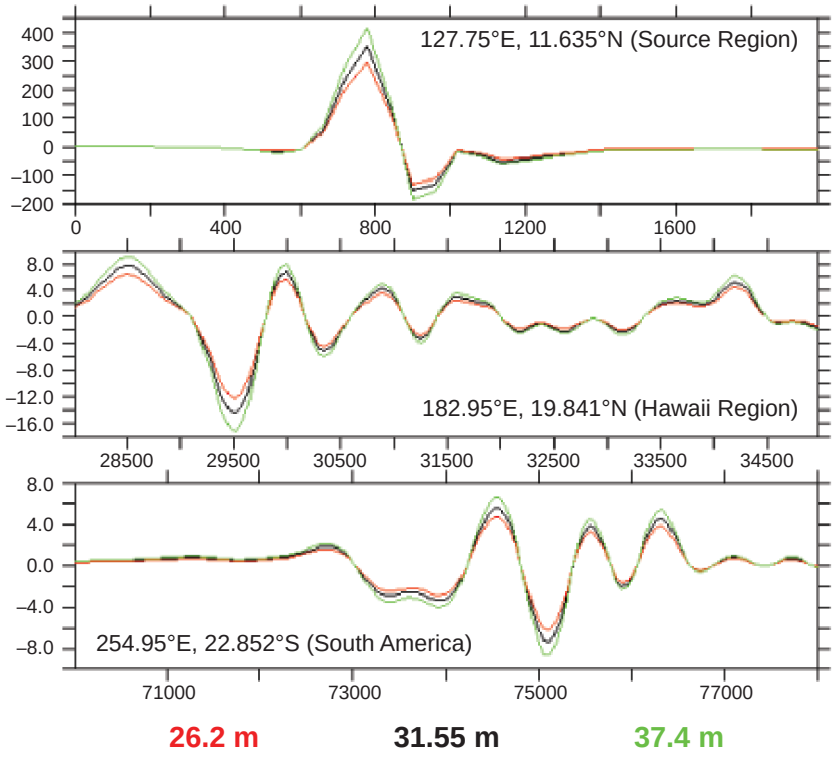

Figure A16: Tsunami time series comparison between MOST and SIFT for different slip values (26.2 m, 31.55 m and 37.4 m) with the same $M_w = 8.5$.

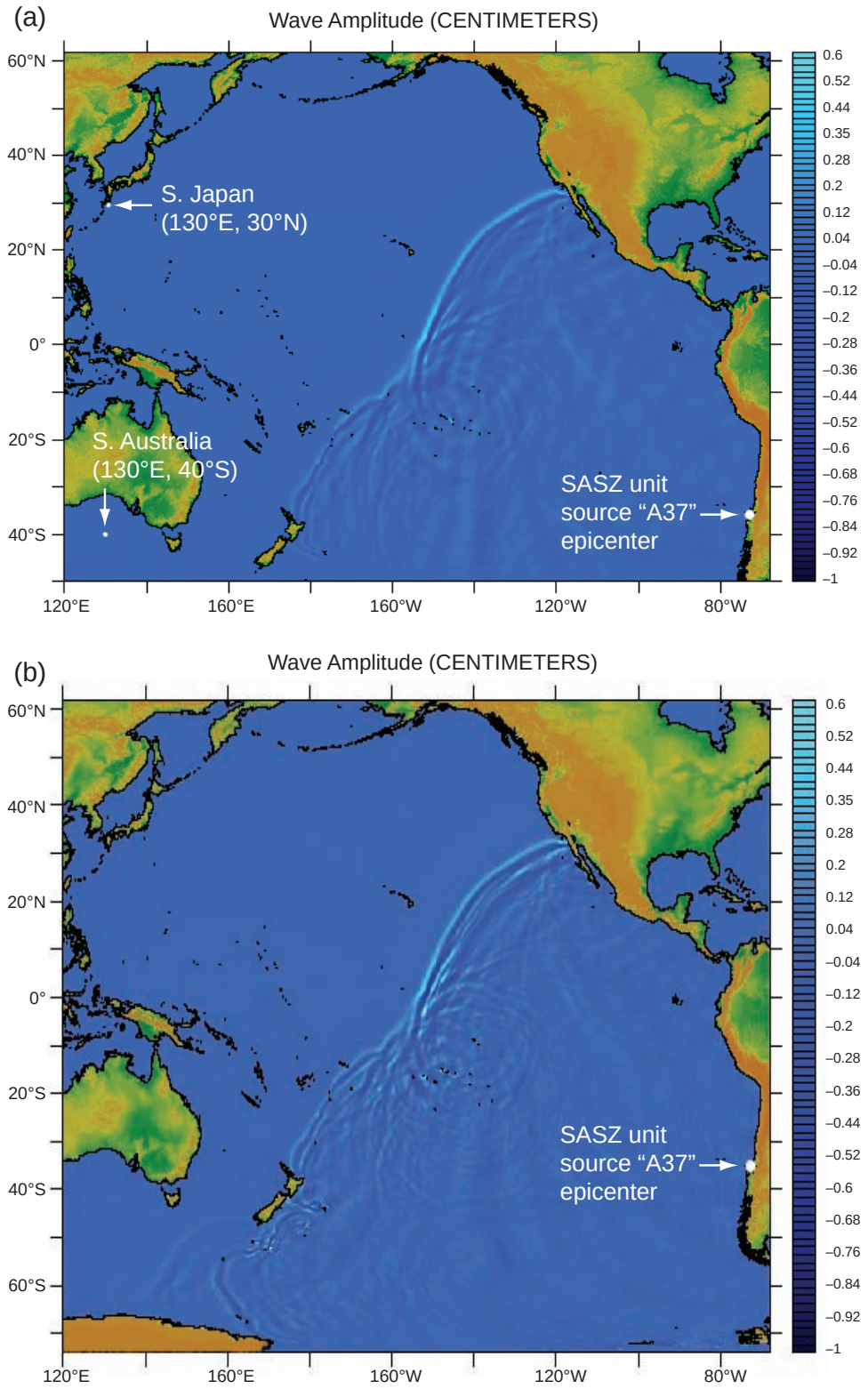

Figure A17: Propagating tsunami wave front comparison between two Pacific grids: (a) tsunami wave front using regular Pacific grid, time step 791, (b) tsunami wave front using extended Pacific grid, time step 791.

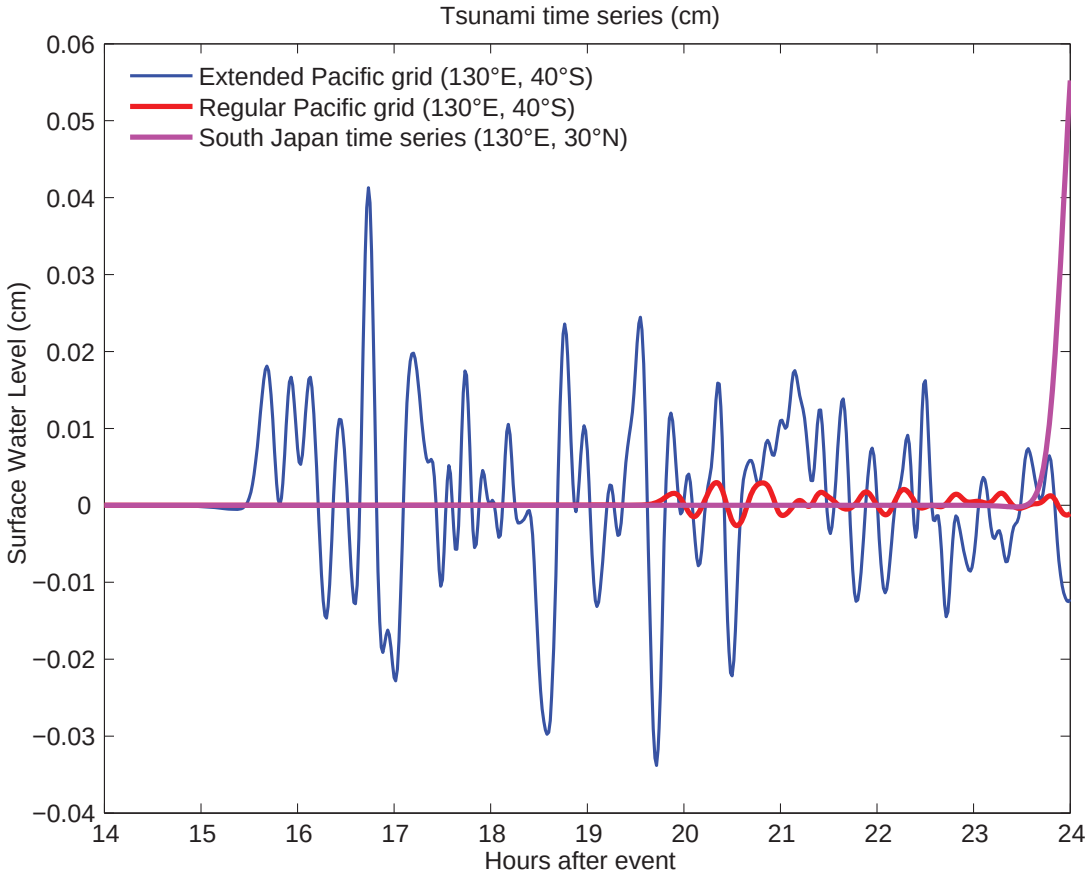

Figure A18: Tsunami time series. Red and blue lines are comparison at south Australia using different domain size, pink line is located at south Japan for a 24-hour simulation. Location of points are indicated in Fig. A17.

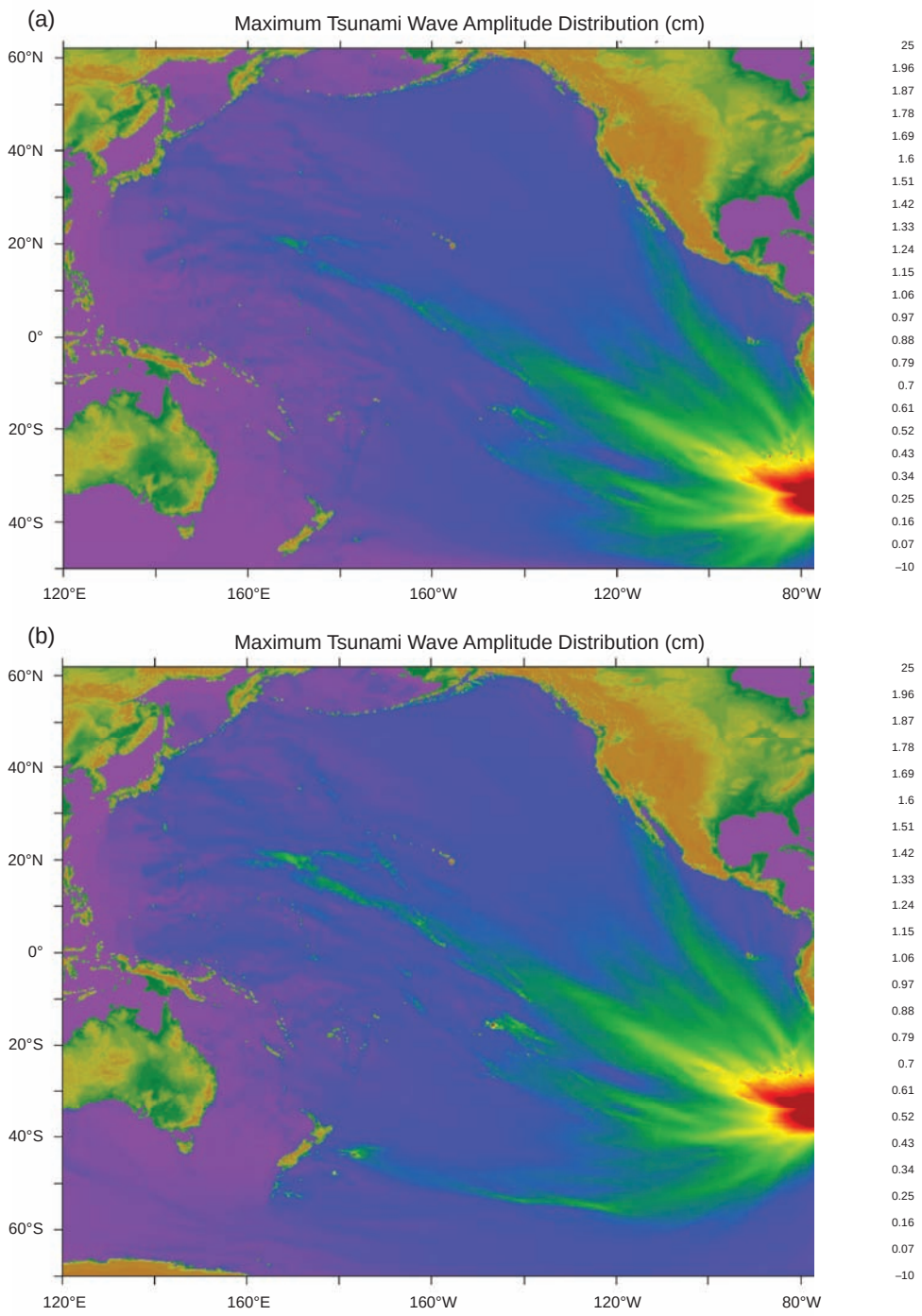

Figure A19: Comparison of maximum tsunami wave amplitude distribution between two Pacific grids; (a) regular Pacific grid, (b) extended Pacific grid.

(a)

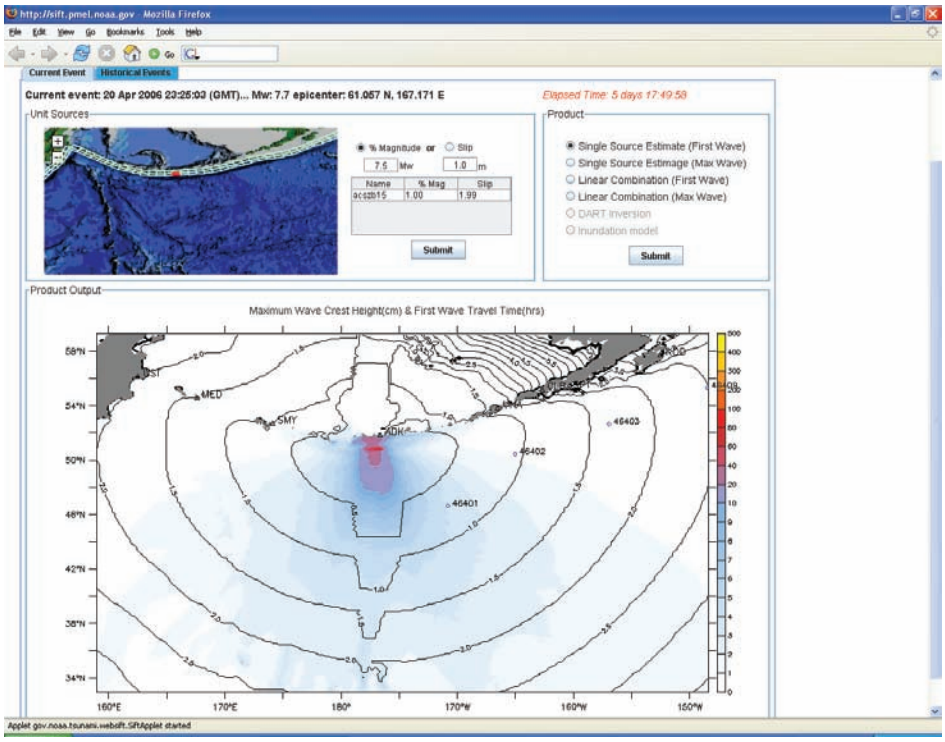

(b)

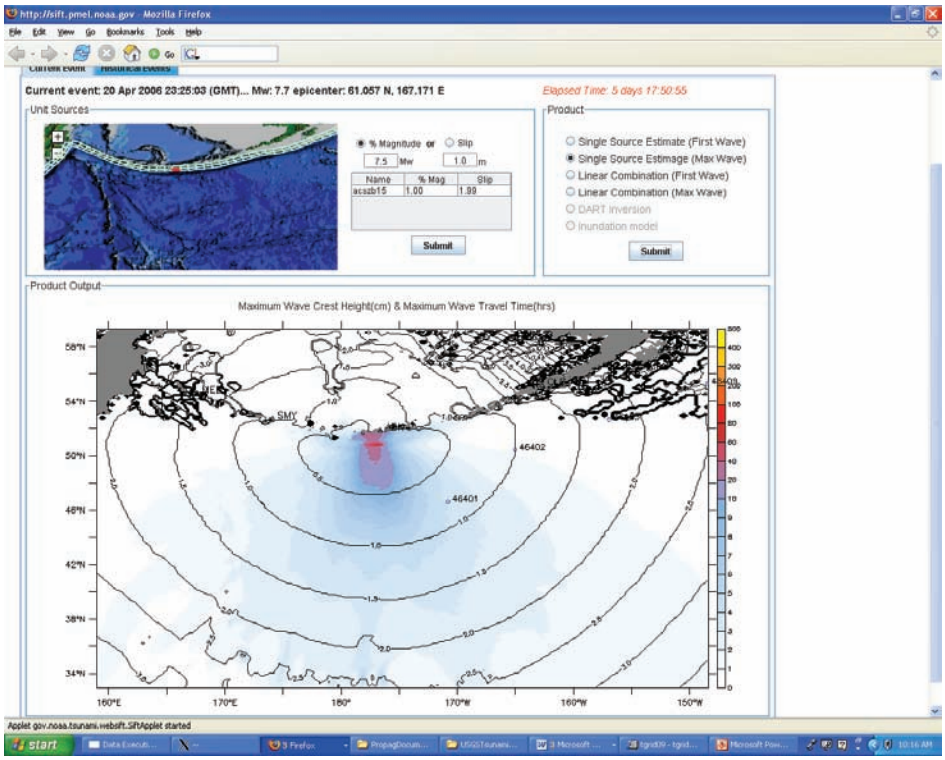

Figure A20: Snapshot of tsunami forecast using webSIFT; (a) first wave forecast, (b) maximum wave forecast.

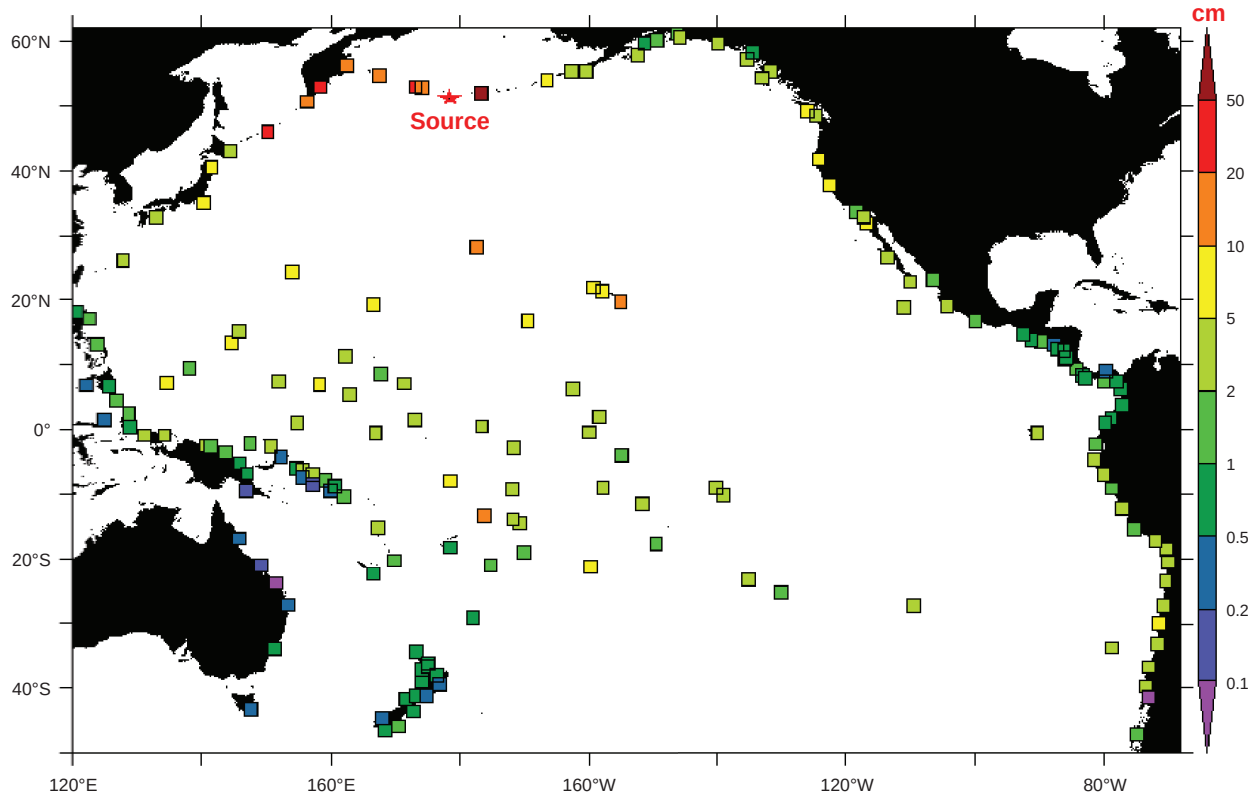

Figure A21: Forecasted tsunami first wave height at selected offshore locations based on an M_w = 7.5 in the Aleutian Islands.

Figure A22: Snapshot of forecasted first tsunami wave and arrival time for Hilo Bay, Hawai'i for sources from Ryukyus-Nankai, East Philippines and North New Guinea unit sources.

Appendix B. Propagation Database Unit Source Information

This section provides the earthquake parameters used for each base unit source. The strike angle for each base unit source is tangential to the subduction zone at that specific location. The slip angle used for all base unit sources is 90°.

The data is presented in a worksheet format with a figure showing the configuration of the unit source. The first column of the worksheet labeled "Locator" will correspond to the figure with the same name. Figure will come first then followed by the corresponding worksheet data.

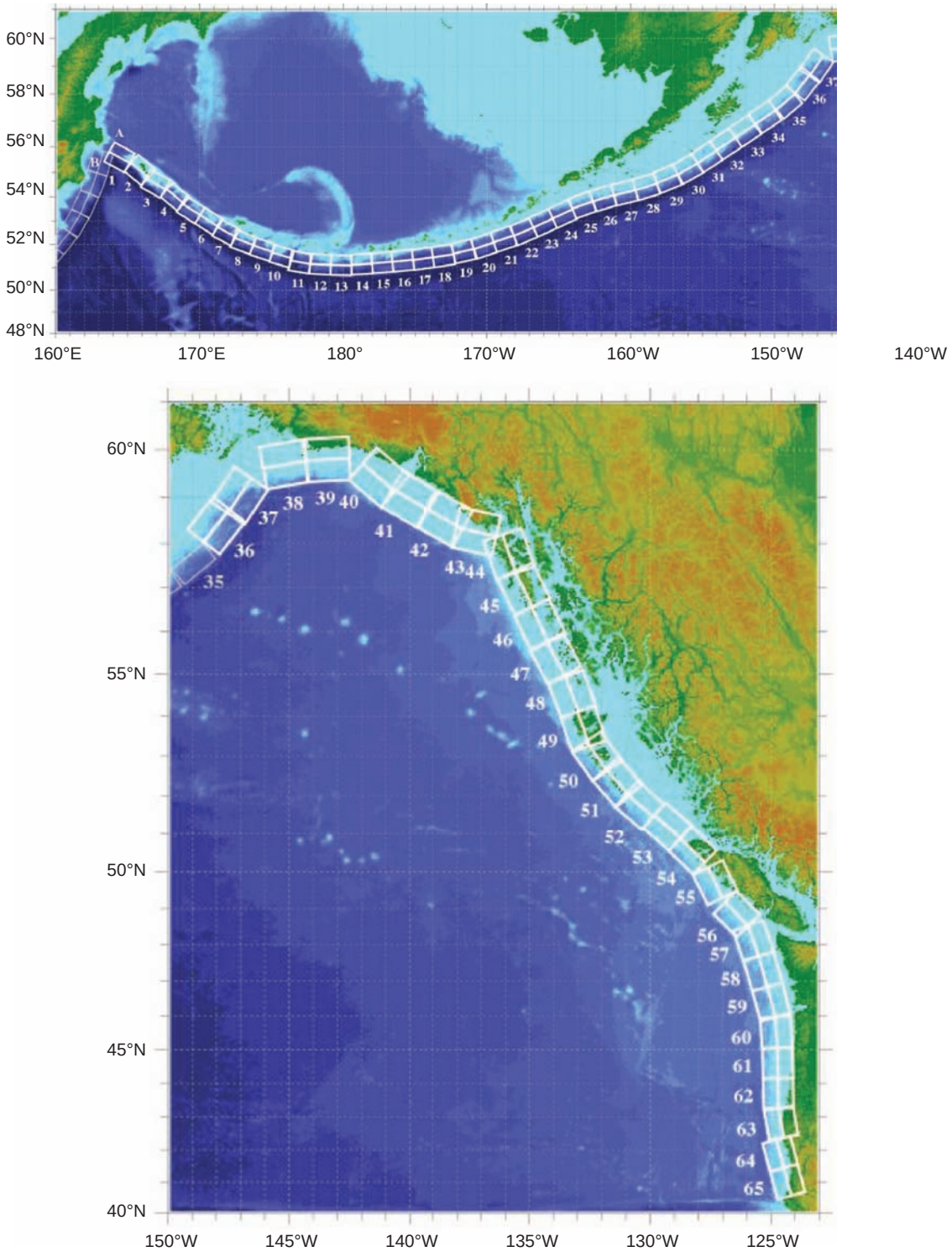

Figure B1: Aleutians-Alaska-Canada Subduction Zones unit sources.

Table B1: Aleutians-Alaska-Canada Subduction Zones unit sources parameters.

Locator	Longitude	Latitude	Strike Angle	Dip Angle	Depth (km)
acsza1	164.7994	55.9606	299.00	17.00	17.94
acszb1	164.4310	55.5849	299.00	17.00	5.00
acsza2	166.3418	55.4016	310.17	17.00	17.94
acszb2	165.8578	55.0734	310.17	17.00	5.00
acsza3	167.2939	54.8919	300.22	23.36	17.94
acszb3	166.9362	54.5356	300.22	23.36	5.00
acsza4	168.7131	54.2852	310.21	38.51	17.94
acszb4	168.3269	54.0168	310.21	24.00	5.00
acsza5	169.7447	53.7808	302.77	37.02	17.94
acszb5	169.4185	53.4793	302.77	21.77	5.00
acsza6	171.0144	53.3054	303.16	35.31	17.94
acszb6	170.6813	52.9986	303.16	21.00	5.00
acsza7	172.1500	52.8528	298.16	35.56	17.94
acszb7	171.8665	52.5307	298.16	17.65	5.00
acsza8	173.2726	52.4579	290.75	37.92	17.94
acszb8	173.0681	52.1266	290.75	17.88	5.00
acsza9	174.5866	52.1434	289.03	39.09	17.94
acszb9	174.4027	51.8138	289.03	18.73	5.00
acsza10	175.8784	51.8526	286.07	40.51	17.94
acszb10	175.7265	51.5245	286.07	18.51	5.00
acsza11	177.1140	51.6488	280.00	15.00	17.94
acszb11	176.9937	51.2215	280.00	15.00	5.00
acszb12	178.4130	51.1200	273.00	15.00	5.00
acsza13	179.8550	51.5340	271.00	15.00	17.94
acszb13	179.8420	51.0850	271.00	15.00	5.00
acsza14	181.2340	51.5780	267.00	15.00	17.94
acszb14	181.2720	51.1290	267.00	15.00	5.00
acsza15	182.6380	51.6470	265.00	15.00	17.94
acszb15	182.7000	51.2000	265.00	15.00	5.00
acsza16	184.0550	51.7250	264.00	15.00	17.94
acszb16	184.1280	51.2780	264.00	15.00	5.00
acsza17	185.4560	51.8170	262.00	15.00	17.94
acszb17	185.5560	51.3720	262.00	15.00	5.00
acsza18	186.8680	51.9410	261.00	15.00	17.94
acszb18	186.9810	51.4970	261.00	15.00	5.00
acsza19	188.2430	52.1280	257.00	15.00	17.94
acszb19	188.4060	51.6900	257.00	15.00	5.00
acsza20	189.5810	52.3550	251.00	15.00	17.94
acszb20	189.8180	51.9300	251.00	15.00	5.00
acsza21	190.9570	52.6470	251.00	15.00	17.94
acszb21	191.1960	52.2220	251.00	15.00	5.00
acsza22	192.2940	52.9430	247.00	15.00	17.94
acszb22	192.5820	52.5300	247.00	15.00	5.00
acsza23	193.6270	53.3070	245.00	15.00	17.94
acszb23	193.9410	52.9000	245.00	15.00	5.00
acsza24	194.9740	53.6870	245.00	15.00	17.94
acszb24	195.2910	53.2800	245.00	15.00	5.00
acsza25	196.4340	54.0760	250.00	15.00	17.94
acszb25	196.6930	53.6543	250.00	15.00	5.00
acsza26	197.8970	54.3600	253.00	15.00	17.94
acszb26	198.1200	53.9300	253.00	15.00	5.00
acsza27	199.4340	54.5960	256.00	15.00	17.94
acszb27	199.6200	54.1600	256.00	15.00	5.00
acsza28	200.8820	54.8300	253.00	15.00	17.94
acszb28	201.1080	54.4000	253.00	15.00	5.00

Table B1: (continued)

Locator	Longitude	Latitude	Strike Angle	Dip Angle	Depth (km)
acsza29	202.2610	55.1330	247.00	15.00	17.94
acszb29	202.5650	54.7200	247.00	15.00	5.00
acsza30	203.6040	55.5090	240.00	15.00	17.94
acszb30	203.9970	55.1200	240.00	15.00	5.00
acsza31	204.8950	55.9700	236.00	15.00	17.94
acszb31	205.3400	55.5980	236.00	15.00	5.00
acsza32	206.2080	56.4730	236.00	15.00	17.94
acszb32	206.6580	56.1000	236.00	15.00	5.00
acsza33	207.5370	56.9750	236.00	15.00	17.94
acszb33	207.9930	56.6030	236.00	15.00	5.00
acsza34	208.9371	57.5124	236.00	15.00	17.94
acszb34	209.4000	57.1400	236.00	15.00	5.00
acsza35	210.2597	58.0441	230.00	15.00	17.94
acszb35	210.8000	57.7000	230.00	15.00	5.00
acsza36	211.3249	58.6565	218.00	15.00	17.94
acszb36	212.0000	58.3800	218.00	15.00	5.00
acsza37	212.2505	59.2720	213.71	15.00	17.94
acszb37	212.9519	59.0312	213.71	15.00	5.00
acsza38	214.6555	60.1351	260.08	0.00	15.00
acszb38	214.8088	59.6927	260.08	0.00	15.00
acsza39	216.5607	60.2480	267.04	0.00	15.00
acszb39	216.6068	59.7994	267.04	0.00	15.00
acsza40	219.3069	59.7574	310.91	0.00	15.00
acszb40	218.7288	59.4180	310.91	0.00	15.00
acsza41	220.4832	59.3390	300.73	0.00	15.00
acszb41	220.0382	58.9529	300.73	0.00	15.00
acsza42	221.8835	58.9310	298.94	0.00	15.00
acszb42	221.4671	58.5379	298.94	0.00	15.00
acsza43	222.9711	58.6934	282.34	0.00	15.00
acszb43	222.7887	58.2546	282.34	0.00	15.00
acsza44	224.9379	57.9054	340.91	12.00	11.09
acszb44	224.1596	57.7617	340.91	7.00	5.00
acsza45	225.4994	57.1634	334.15	12.00	11.09
acszb45	224.7740	56.9718	334.15	7.00	5.00
acsza46	226.1459	56.3552	334.15	12.00	11.09
acszb46	225.4358	56.1636	334.15	7.00	5.00
acsza47	226.7731	55.5830	332.26	12.00	11.09
acszb47	226.0887	55.3785	332.26	7.00	5.00
acsza48	227.4799	54.6763	339.40	12.00	11.09
acszb48	226.7713	54.5217	339.40	7.00	5.00
acsza49	227.9482	53.8155	341.17	12.00	11.09
acszb49	227.2462	53.6737	341.17	7.00	5.00
acsza50	228.3970	53.2509	324.51	12.00	11.09
acszb50	227.8027	52.9958	324.51	7.00	5.00
acsza51	229.1844	52.6297	318.36	12.00	11.09
acszb51	228.6470	52.3378	318.36	7.00	5.00
acsza52	230.0306	52.0768	310.85	12.00	11.09
acszb52	229.5665	51.7445	310.85	7.00	5.00
acsza53	231.1735	51.5258	310.85	12.00	11.09
acszb53	230.7150	51.1935	310.85	7.00	5.00
acsza54	232.2453	50.8809	314.11	12.00	11.09
acszb54	231.7639	50.5655	314.11	7.00	5.00
acsza55	233.3066	49.9032	333.71	12.00	11.09
acszb55	232.6975	49.7086	333.71	7.00	5.00

Table B1: (continued)

Locator	Longitude	Latitude	Strike Angle	Dip Angle	Depth (km)
acsza56	234.0588	49.1702	315.00	11.00	12.82
acszb56	233.5849	48.8584	315.00	9.00	5.00
acsza57	234.9041	48.2596	341.00	11.00	12.82
acszb57	234.2797	48.1161	341.00	9.00	5.00
acsza58	235.3021	47.3812	344.00	11.00	12.82
acszb58	234.6776	47.2597	344.00	9.00	5.00
acsza59	235.6432	46.5082	345.00	11.00	12.82
acszb59	235.0257	46.3941	345.00	9.00	5.00
acsza60	235.8640	45.5429	356.00	11.00	12.82
acszb60	235.2363	45.5122	356.00	9.00	5.00
acsza61	235.9106	44.6227	359.00	11.00	12.82
acszb61	235.2913	44.6150	359.00	9.00	5.00
acsza62	235.9229	43.7245	359.00	11.00	12.82
acszb62	235.3130	43.7168	359.00	9.00	5.00
acsza63	236.0220	42.9020	350.00	11.00	12.82
acszb63	235.4300	42.8254	350.00	9.00	5.00
acsza64	235.9638	41.9818	345.00	11.00	12.82
acszb64	235.3919	41.8677	345.00	9.00	5.00
acsza65	236.2643	41.1141	345.00	11.00	12.82
acszb65	235.7000	41.0000	345.00	9.00	5.00

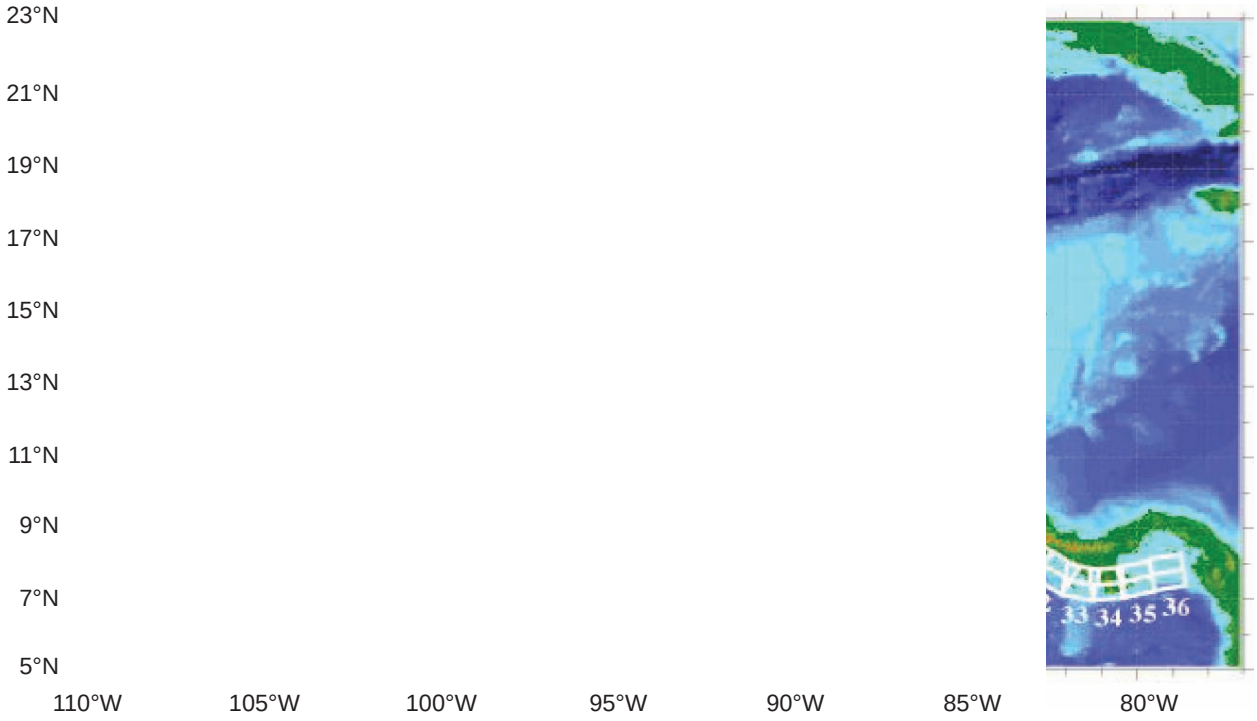

Figure B2: Central America Subduction Zone unit sources.

Table B2: Central America Subduction Zone unit sources parameters.

Locator	Longitude	Latitude	Strike Angle	Dip Angle	Depth (km)
casza1	254.2924	21.7738	329.18	19.00	15.40
caszb1	253.9003	21.5562	329.18	12.00	5.00
casza2	254.6885	20.5300	0.00	19.00	15.40
caszb2	254.2350	20.5300	0.00	12.00	5.00
casza3	254.7875	20.1947	325.00	20.00	20.45
caszb3	254.4152	19.9497	325.00	18.00	5.00
casza4	255.3452	19.6221	310.00	19.00	19.62
caszb4	255.0527	19.2930	310.00	17.00	5.00
casza5	256.0677	19.0770	307.00	19.00	19.62
caszb5	255.7948	18.7340	307.00	17.00	5.00
casza6	256.8119	18.6025	301.00	18.00	18.78
caszb6	256.5778	18.2324	301.00	16.00	5.00
casza7	257.6014	18.2025	295.00	18.00	18.78
caszb7	257.4098	17.8112	295.00	16.00	5.00
casza8	258.4391	17.8655	291.00	17.00	17.94
caszb8	258.2761	17.4604	291.00	15.00	5.00
casza9	259.3164	17.5435	291.00	17.00	17.94
caszb9	259.1537	17.1385	291.00	15.00	5.00
casza10	260.1922	17.2216	291.00	17.00	17.94
caszb10	260.0298	16.8166	291.00	15.00	5.00
casza11	261.0665	16.8997	291.00	17.00	17.94
caszb11	260.9044	16.4946	291.00	15.00	5.00
casza12	261.9310	16.5995	289.00	16.00	17.10
caszb12	261.7833	16.1875	289.00	14.00	5.00
casza13	262.7821	16.3648	283.00	16.00	17.10
caszb13	262.6801	15.9402	283.00	14.00	5.00
casza14	263.6395	16.2342	275.00	16.00	17.10
caszb14	263.6000	15.8000	275.00	14.00	5.00
casza15	264.8679	15.9189	300.41	12.00	15.40
caszb15	264.6371	15.5400	300.41	12.00	5.00
casza16	265.6918	15.3784	304.32	16.00	16.67
caszb16	265.4398	15.0218	304.22	13.50	5.00
casza17	266.4103	14.9517	298.39	20.00	17.94
caszb17	266.2029	14.5804	298.39	15.00	5.00
casza18	267.2204	14.5206	298.11	21.50	17.94
caszb18	267.0173	14.1520	298.11	15.00	5.00
casza19	268.0216	14.1474	292.94	23.00	17.94
caszb19	267.8557	13.7666	292.94	15.00	5.00
casza20	268.8880	13.7068	301.62	24.00	17.94
caszb20	268.6669	13.3574	301.62	15.00	5.00
casza21	269.4925	13.4678	284.19	25.00	17.94
caszb21	269.3900	13.0731	284.19	15.00	5.00
casza22	270.4537	13.1669	290.89	25.00	17.94
caszb22	270.3049	12.7866	290.89	15.00	5.00
casza23	271.3520	12.8001	294.43	25.00	17.94
caszb23	271.1796	12.4295	294.43	15.00	5.00
casza24	272.2762	12.3131	302.97	25.00	17.94
caszb24	272.0498	11.9716	302.97	15.00	5.00
casza25	273.0854	11.6524	311.16	25.00	17.94
caszb25	272.8122	11.3459	311.16	15.00	5.00
casza26	273.7765	11.0012	316.02	25.00	17.94
caszb26	273.4784	10.7185	316.02	15.00	5.00
casza27	274.3685	10.3111	317.14	25.00	17.94
caszb27	274.0655	10.0342	317.14	15.00	5.00

Table B2: (continued)

Locator	Longitude	Latitude	Strike Angle	Dip Angle	Depth (km)
casza28	274.8612	9.9268	299.64	22.00	14.54
caszb28	274.6523	9.5648	299.64	11.00	5.00
casza29	275.6107	9.5204	295.19	19.00	11.09
caszb29	275.4276	9.1361	295.19	7.00	5.00
casza30	276.4399	9.0563	301.06	19.00	9.36
caszb30	276.2183	8.6925	301.06	5.00	5.00
casza31	277.2476	8.5804	304.54	19.00	7.62
caszb31	277.0043	8.2306	304.54	3.00	5.00
casza32	277.9907	8.1118	302.07	4.00	8.49
caszb32	277.7506	7.7321	302.07	4.00	5.00
casza33	278.5039	7.9087	281.40	6.00	10.23
caszb33	278.4149	7.4708	281.40	6.00	5.00
casza34	279.1266	7.8594	265.12	15.00	17.94
caszb34	279.1638	7.4271	265.12	15.00	5.00
casza35	279.8976	7.9941	257.82	11.00	14.54
caszb35	279.9915	7.5631	257.82	11.00	5.00
casza36	280.8001	8.1967	260.47	7.00	11.09
caszb36	280.8746	7.7570	260.47	7.00	5.00

This page is intentionally left blank.

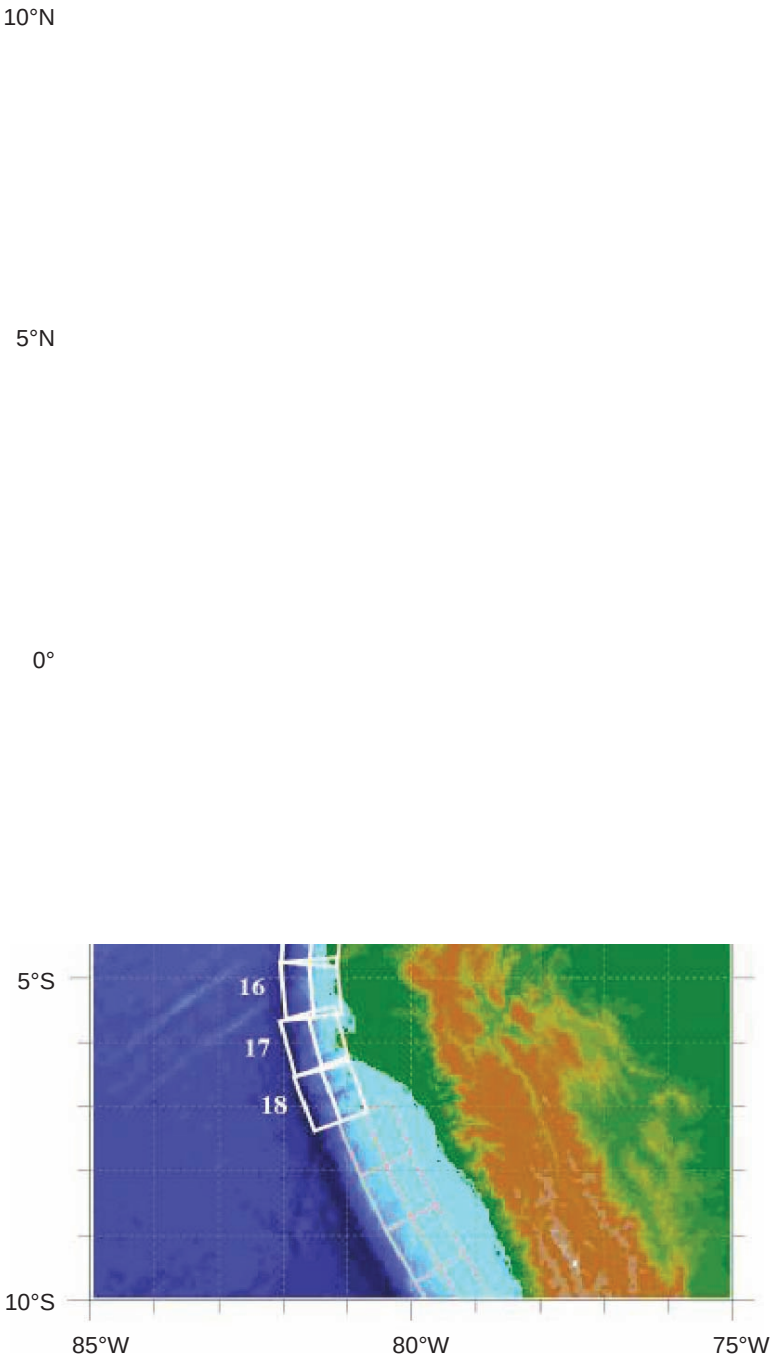

Figure B3: Ecuador-Columbia Subduction Zone unit sources.

Table B3: Ecuador-Columbia Subduction Zone unit sources parameters.

Locator	Longitude	Latitude	Strike Angle	Dip Angle	Depth (km)
ecsza1	281.7997	7.7216	303.79	17.00	10.23
ecszb1	281.5588	7.3646	303.79	6.00	5.00
ecsza2	282.6814	6.6244	340.00	17.00	10.23
ecszb2	282.2752	6.4775	340.00	6.00	5.00
ecsza3	282.8648	5.3941	3.56	17.00	10.23
ecszb3	282.4342	5.4208	3.56	6.00	5.00
ecsza4	282.6403	4.2231	19.02	17.00	10.23
ecszb4	282.2330	4.3631	19.02	6.00	5.00
ecsza5	282.2712	3.3116	24.41	17.00	10.23
ecszb5	281.8794	3.4891	24.41	6.00	5.00
ecsza6	281.6385	2.3767	39.72	17.00	10.23
ecszb6	281.3078	2.6512	39.72	6.00	5.00
ecsza7	281.0255	1.6737	41.91	17.00	10.23
ecszb7	280.7057	1.9606	41.91	6.00	5.00
ecsza8	280.4619	1.0784	36.91	17.00	10.23
ecszb8	280.1184	1.3364	36.91	6.00	5.00
ecsza9	280.1088	0.4294	26.25	10.00	8.49
ecszb9	279.7121	0.6250	26.25	4.00	5.00
ecsza10	279.7140	−0.3756	26.04	10.00	8.49
ecszb10	279.3166	−0.1814	26.04	4.00	5.00
ecsza11	279.5110	−1.0408	13.33	10.00	8.49
ecszb11	279.0805	−0.9388	13.33	4.00	5.00
ecsza12	279.4411	−1.8540	5.00	10.00	8.49
ecszb12	279.0002	−1.8154	5.00	4.00	5.00
ecsza13	279.3179	−2.6971	5.44	10.00	8.49
ecszb13	278.8771	−2.6552	5.44	4.00	5.00
ecsza14	279.0309	−3.8540	26.38	14.00	17.10
ecszb14	278.6397	−3.6604	26.38	14.00	5.00
ecsza15	278.8817	−4.3865	5.25	14.00	17.10
ecszb15	278.4464	−4.3466	5.25	14.00	5.00
ecsza16	278.8726	−5.1251	354.53	14.00	17.10
ecszb16	278.4370	−5.1666	354.53	14.00	5.00
ecsza17	278.9174	−5.8727	344.56	14.00	17.10
ecszb17	278.4950	−5.9887	344.56	14.00	5.00
ecsza18	279.1506	−6.6608	339.49	14.00	17.10
ecszb18	278.7395	−6.8135	339.49	14.00	5.00

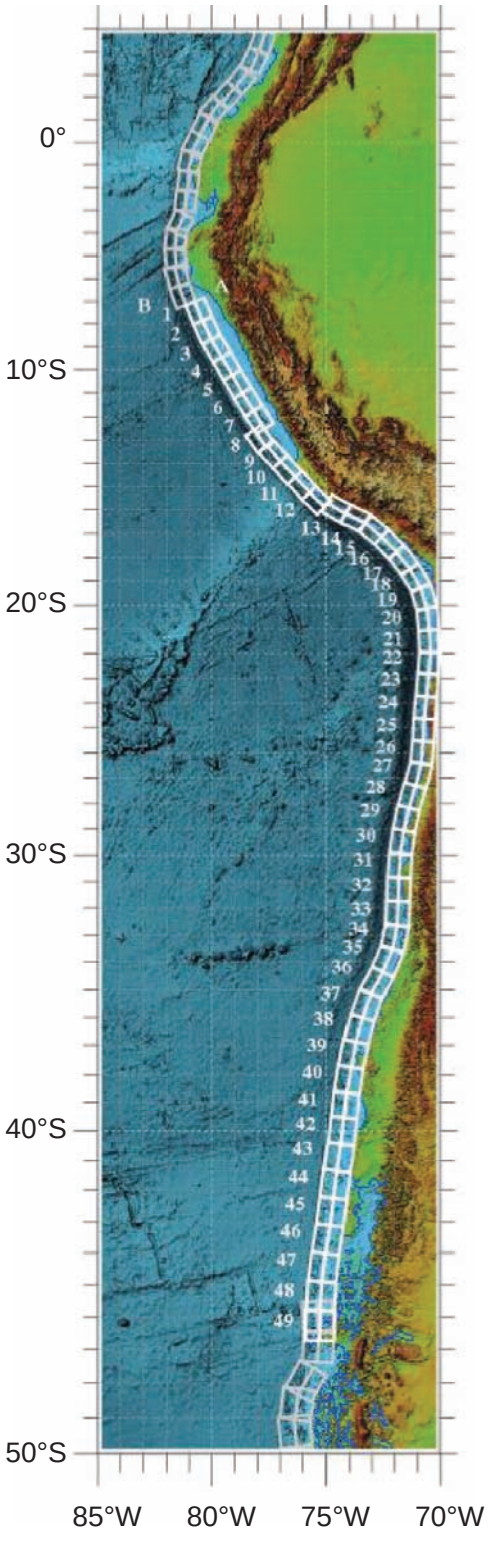

Figure B4: South America Subduction Zone unit sources.

Table B4: South America Subduction Zone unit sources parameters.

Locator	Longitude	Latitude	Strike Angle	Dip Angle	Depth (km)
sasza1	279.8455	−7.3307	338.00	14.00	17.10
saszb1	279.4379	−7.4940	338.00	14.00	5.00
sasza2	280.1990	−8.1333	335.00	14.00	17.10
saszb2	279.7998	−8.3175	335.00	14.00	5.00
sasza3	280.6018	−8.8956	330.00	14.00	17.10
saszb3	280.2195	−9.1136	330.00	14.00	5.00
sasza4	281.0585	−9.6736	330.00	14.00	17.10
saszb4	280.6754	−9.8915	330.00	14.00	5.00
sasza5	281.5164	−10.4516	330.00	14.00	17.10
saszb5	281.1324	−10.6695	330.00	14.00	5.00
sasza6	281.9814	−11.2084	328.00	14.00	17.10
saszb6	281.6043	−11.4394	328.00	14.00	5.00
sasza7	282.4695	−11.9702	328.00	14.00	17.10
saszb7	282.0914	−12.2012	328.00	14.00	5.00
sasza8	282.4500	−12.7861	324.89	33.00	13.68
saszb8	282.1337	−13.0028	324.89	10.00	5.00
sasza9	283.0044	−13.3839	318.33	33.00	13.68
saszb9	282.7148	−13.6343	318.33	10.00	5.00
sasza10	283.6329	−14.0541	318.19	33.00	13.68
saszb10	283.3431	−14.3052	318.19	10.00	5.00
sasza11	284.2751	−14.7214	317.98	33.00	13.68
saszb11	283.9854	−14.9736	317.98	10.00	5.00
sasza12	284.8854	−15.3469	314.64	33.00	13.68
saszb12	284.6106	−15.6149	314.64	10.00	5.00
sasza13	285.6695	−15.6125	300.00	19.00	20.45
saszb13	285.4486	−15.9803	300.00	18.00	5.00
sasza14	286.4690	−16.0200	296.00	19.00	20.45
saszb14	286.2749	−16.4017	296.00	18.00	5.00
sasza15	287.3417	−16.5620	310.00	19.00	20.45
saszb15	287.0564	−16.8874	310.00	18.00	5.00
sasza16	288.0626	−17.2060	316.00	20.00	21.28
saszb16	287.7443	−17.4992	316.00	19.00	5.00
sasza17	288.7138	−17.9163	322.00	20.00	21.28
saszb17	288.3637	−18.1762	322.00	19.00	5.00
sasza18	289.2798	−18.7081	330.00	20.00	21.28
saszb18	288.8934	−18.9191	330.00	19.00	5.00
sasza19	289.6917	−19.6243	−16.00	21.00	22.10
saszb19	289.2635	−19.7399	−16.00	20.00	5.00
sasza20	289.8914	−20.5745	−6.00	21.00	22.10
saszb20	289.4459	−20.6183	−6.00	20.00	5.00
sasza21	289.9717	−21.4916	−3.00	21.00	22.10
saszb21	289.5216	−21.5135	−3.00	20.00	5.00
sasza22	289.9565	−22.4461	5.00	21.00	22.10
saszb22	289.5047	−22.4095	5.00	20.00	5.00
sasza23	289.8742	−23.3410	5.00	21.00	22.10
saszb23	289.4194	−23.3044	5.00	20.00	5.00
sasza24	289.7916	−24.2359	5.00	21.00	21.28
saszb24	289.3336	−24.1993	5.00	19.00	5.00
sasza25	289.7268	−25.1172	3.00	20.00	21.28
saszb25	289.2644	−25.0953	3.00	19.00	5.00
sasza26	289.6625	−26.0281	5.00	20.00	20.45
saszb26	289.1947	−25.9913	5.00	18.00	5.00
sasza27	289.4910	−26.9773	14.00	19.00	19.62
saszb27	289.0290	−26.8745	14.00	17.00	5.00

Table B4: (continued)

Locator	Longitude	Latitude	Strike Angle	Dip Angle	Depth (km)
sasza28	289.2104	−27.8551	16.00	19.00	19.62
saszb28	288.7492	−27.7381	16.00	17.00	5.00
sasza29	288.9778	−28.6980	12.00	18.00	18.78
saszb29	288.5018	−28.6092	12.00	16.00	5.00
sasza30	288.8087	−29.5527	8.00	18.00	18.78
saszb30	288.3227	−29.4933	8.00	16.00	5.00
sasza31	288.7079	−30.4159	4.00	18.00	18.78
saszb31	288.2139	−30.3861	4.00	16.00	5.00
sasza32	288.6584	−31.2980	2.00	18.00	18.78
saszb32	288.1589	−31.2831	2.00	16.00	5.00
sasza33	288.6263	−32.1957	2.00	18.00	18.78
sasza38	286.9635	−36.5253	15.00	18.00	18.78
saszb38	286.4508	−36.4148	15.00	16.00	5.00
sasza39	286.7297	−37.3719	11.00	16.00	17.10
saszb39	286.1970	−37.2895	11.00	14.00	5.00
sasza40	286.5410	−38.2416	9.00	16.00	17.10
saszb40	285.9986	−38.1741	9.00	14.00	5.00
sasza41	286.4007	−39.1095	6.00	16.00	17.10
saszb41	285.8477	−39.0644	6.00	14.00	5.00
sasza42	286.2854	−40.0029	6.00	16.00	17.10
saszb42	285.7252	−39.9578	6.00	14.00	5.00
sasza43	286.1339	−40.9156	9.00	16.00	17.10
saszb43	285.5702	−40.8481	9.00	14.00	5.00
sasza44	285.9770	−41.7902	7.00	16.00	17.10
saszb44	285.4027	−41.7375	7.00	14.00	5.00
sasza45	285.8364	−42.6818	7.00	16.00	17.10
saszb45	285.2539	−42.6292	7.00	14.00	5.00
sasza46	285.6696	−43.5861	9.00	16.00	17.10
saszb46	285.0815	−43.5186	9.00	14.00	5.00
sasza47	285.5064	−44.4606	7.00	16.00	17.10
saszb47	284.9065	−44.4080	7.00	14.00	5.00
sasza48	285.4083	−45.3250	3.00	16.00	17.10
saszb48	284.7953	−45.3024	3.00	14.00	5.00
sasza49	285.3796	−46.2076	1.00	16.00	17.10
saszb49	284.7500	−46.2000	1.00	14.00	5.00
saszb33	288.1219	−32.1808	2.00	16.00	5.00
sasza34	288.5013	−33.1521	11.00	18.00	18.78
saszb34	288.0009	−33.0706	11.00	16.00	5.00
sasza35	288.1600	−34.0919	23.00	18.00	18.78
saszb35	287.6861	−33.9249	23.00	16.00	5.00
sasza36	287.6749	−34.9355	28.00	18.00	18.78
saszb36	287.2159	−34.7350	28.00	16.00	5.00
sasza37	287.2735	−35.6953	19.00	18.00	18.78
saszb37	286.7770	−35.5562	19.00	16.00	5.00

This page is intentionally left blank.

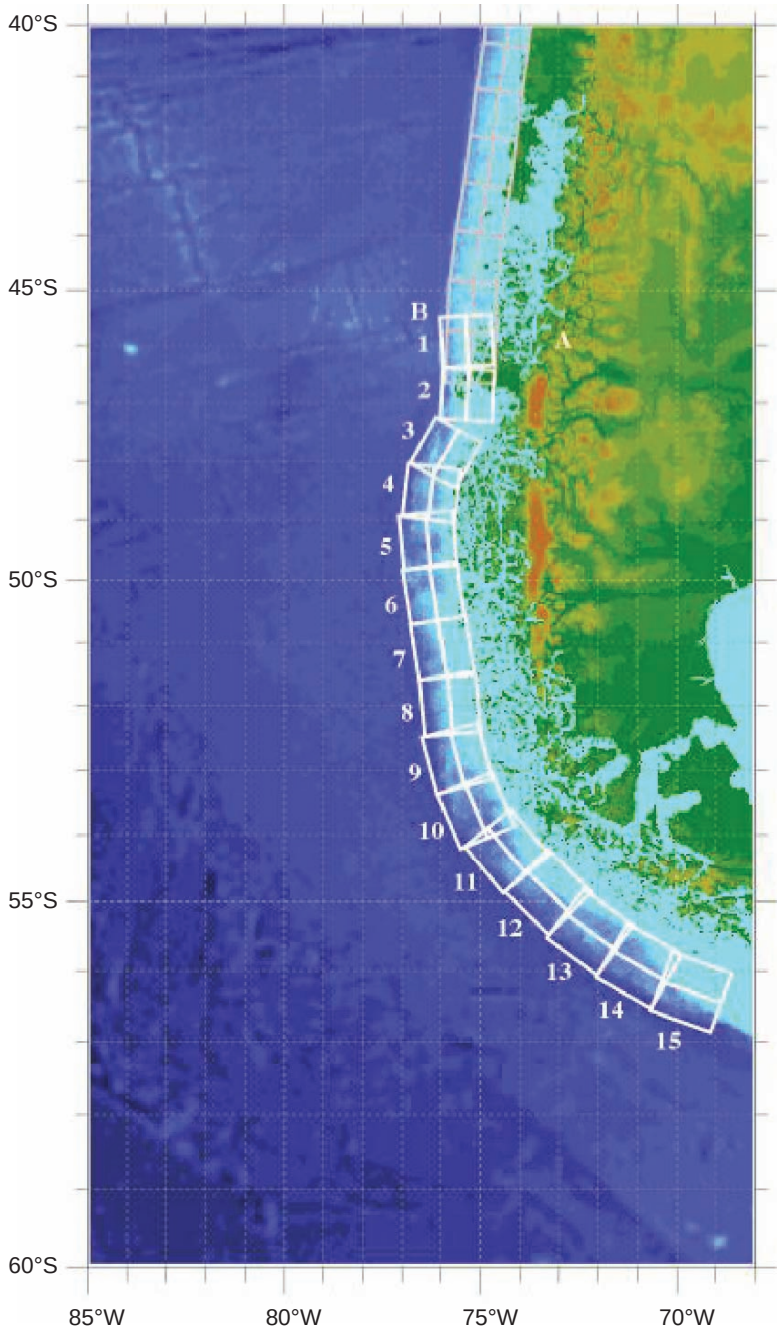

Figure B5: South Chile Subduction Zone unit sources.

Table B5: South Chile Subduction Zone unit sources parameters.

Locator	Longitude	Latitude	Strike Angle	Dip Angle	Depth (km)
scsza1	285.2954	−45.8804	356.78	5.00	9.36
scszb1	284.6534	−45.9055	356.78	5.00	5.00
scsza2	285.3181	−46.8766	3.00	7.50	11.53
scszb2	284.6678	−46.8533	3.00	7.50	5.00
scsza3	284.6876	−48.0785	29.18	10.00	13.68
Scszb3	284.1120	−47.8628	29.18	10.00	5.00
scsza4	284.4109	−48.5920	6.74	9.67	13.40
scszb4	283.7468	−48.5400	6.74	9.67	5.00
scsza5	284.3401	−49.2924	354.42	9.33	13.11
scszb5	283.6632	−49.3355	354.42	9.33	5.00
scsza6	284.4917	−50.1293	350.72	9.00	12.82
scszb6	283.8077	−50.2008	350.72	9.00	5.00
scsza7	284.7277	−51.0212	350.96	8.67	12.54
scszb7	284.0295	−51.0910	350.96	8.67	5.00
scsza8	284.9514	−51.9652	354.52	8.33	12.24
scszb8	284.2327	−52.0076	354.52	8.33	5.00
scsza9	285.1193	−52.7112	344.89	8.00	11.96
scszb9	284.4086	−52.8271	344.89	8.00	5.00
ssza10	285.5820	−53.4555	337.04	8.00	11.96
scszb10	284.8914	−53.6290	337.04	8.00	5.00
scsza11	286.2580	−53.9562	320.24	8.00	11.96
scszb11	285.6729	−54.2407	320.24	8.00	5.00
scsza12	287.2692	−54.5370	314.69	8.00	11.96
scszb12	286.7258	−54.8532	314.69	8.00	5.00
scsza13	288.2564	−55.0798	306.21	8.00	11.96
scszb13	287.7932	−55.4387	306.21	8.00	5.00
scsza14	289.4365	−55.5443	299.87	8.00	11.96
scszb14	289.0411	−55.9300	299.87	8.00	5.00
scsza15	290.6457	−55.8855	289.99	8.00	11.96
scszb15	290.3716	−56.3035	289.99	8.00	5.00

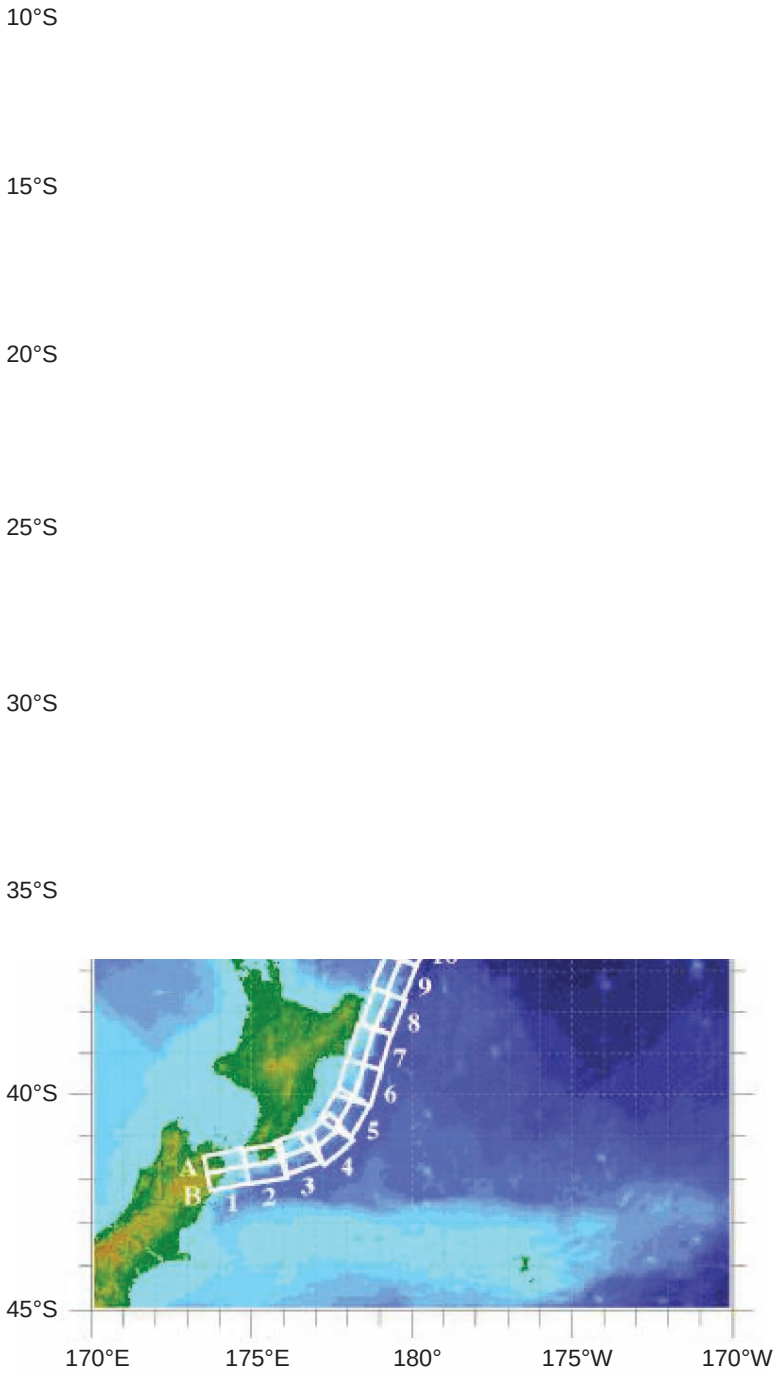

Figure B6: New Zealand-Kermadec-Tonga Subduction Zone unit sources.

Table B6: New Zealand-Kermadec-Tonga Subduction Zone unit sources parameters.

Locator	Longitude	Latitude	Strike Angle	Dip Angle	Depth (km)
ntsza1	174.0985	−41.3951	258.57	24.00	25.34
ntszb1	174.2076	−41.7973	258.57	24.00	5.00
ntsza2	175.3289	−41.2592	260.63	29.38	23.17
ntszb2	175.4142	−41.6454	260.63	21.31	5.00
ntsza3	176.2855	−40.9950	250.65	29.54	21.74
ntszb3	176.4580	−41.3637	250.65	19.56	5.00
ntsza4	177.0023	−40.7679	229.42	24.43	18.87
ntszb4	177.3552	−41.0785	229.42	16.10	5.00
ntsza5	177.4114	−40.2396	210.04	18.80	19.29
ntszb5	177.8951	−40.4525	210.04	16.61	5.00
ntsza6	177.8036	−39.6085	196.68	18.17	15.80
ntszb6	178.3352	−39.7310	196.68	12.48	5.00
ntsza7	178.1676	−38.7480	197.03	28.10	17.85
ntszb7	178.6541	−38.8640	197.03	14.89	5.00
ntsza8	178.6263	−37.8501	201.41	31.47	18.78
ntszb8	179.0788	−37.9899	201.41	16.00	5.00
ntsza9	178.9833	−36.9770	202.19	29.58	20.02
ntszb9	179.4369	−37.1245	202.19	17.48	5.00
ntsza10	179.5534	−36.0655	210.62	32.10	20.72
ntszb10	179.9595	−36.2593	210.62	18.32	5.00
ntsza11	179.9267	−35.3538	201.65	25.00	16.09
ntszb11	180.3915	−35.5040	201.65	12.81	5.00
ntsza12	180.4433	−34.5759	201.18	25.00	15.46
ntszb12	180.9051	−34.7230	201.18	12.08	5.00
ntsza13	180.7990	−33.7707	199.75	25.87	19.06
ntszb13	181.2573	−33.9073	199.75	16.33	5.00
ntsza14	181.2828	−32.9288	202.41	31.28	22.73
ntszb14	181.7063	−33.0751	202.41	20.77	5.00
ntsza15	181.4918	−32.0035	205.43	32.33	22.64
ntszb15	181.8967	−32.1665	205.43	20.66	5.00
ntsza16	181.9781	−31.2535	205.48	34.29	23.59
ntszb16	182.3706	−31.4131	205.48	21.83	5.00
ntsza17	182.4819	−30.3859	210.31	37.60	25.58
ntszb17	182.8387	−30.5655	210.31	24.30	5.00
ntsza18	182.8176	−29.6545	201.63	37.65	26.13
ntszb18	183.1985	−29.7856	201.63	25.00	5.00
ntsza19	183.0622	−28.8739	195.70	34.41	26.13
ntszb19	183.4700	−28.9742	195.70	25.00	5.00
ntsza20	183.2724	−28.0967	188.80	38.00	26.13
ntszb20	183.6691	−28.1508	188.80	25.00	5.00
ntsza21	183.5747	−27.1402	197.10	32.29	24.83
ntszb21	183.9829	−27.2518	197.10	23.37	5.00
ntsza22	183.6608	−26.4975	180.00	29.56	18.63
ntszb22	184.0974	−26.4975	180.00	15.82	5.00
ntsza23	183.7599	−25.5371	185.77	32.42	20.56
ntszb23	184.1781	−25.5752	185.77	18.13	5.00
ntsza24	183.9139	−24.6201	188.17	33.31	23.73
ntszb24	184.3228	−24.6734	188.17	22.00	5.00
ntsza25	184.1266	−23.5922	198.48	29.34	19.64
ntszb25	184.5322	−23.7163	198.48	17.03	5.00
ntsza26	184.6613	−22.6460	211.67	30.26	19.43
ntszb26	185.0196	−22.8497	211.67	16.78	5.00
ntsza27	185.0879	−21.9139	207.93	31.73	20.67
ntszb27	185.4522	−22.0928	207.93	18.27	5.00

Table B6: (continued)

Locator	Longitude	Latitude	Strike Angle	Dip Angle	Depth (km)
ntsza28	185.4037	−21.1758	200.48	32.44	21.76
ntszb28	185.7849	−21.3084	200.48	19.58	5.00
ntsza29	185.8087	−20.2629	206.37	32.47	20.40
ntszb29	186.1710	−20.4312	206.37	17.94	5.00
ntsza30	186.1499	−19.5087	200.91	32.98	22.46
ntszb30	186.5236	−19.6432	200.91	20.44	5.00
ntsza31	186.3538	−18.7332	193.88	34.41	21.19
ntszb31	186.7339	−18.8221	193.88	18.89	5.00
ntsza32	186.5949	−17.8587	194.12	30.00	19.12
ntszb32	186.9914	−17.9536	194.12	16.40	5.00
ntsza33	186.8172	−17.0581	190.04	33.15	23.34
ntszb33	187.2047	−17.1237	190.04	21.52	5.00
ntsza34	186.7814	−16.2598	182.13	15.00	13.41
ntszb34	187.2330	−16.2759	182.13	9.68	5.00
ntsza35	186.8000	−15.8563	149.85	15.00	12.17
ntszb35	187.1896	−15.6384	149.85	8.24	5.00
ntsza36	186.5406	−15.3862	123.91	40.44	36.72
ntszb36	186.7381	−15.1025	123.91	39.38	5.00
ntsza37	185.9883	−14.9861	101.95	68.94	30.99
ntszb37	186.0229	−14.8282	101.95	31.32	5.00
ntsza38	185.2067	−14.8259	88.40	80.00	26.13
ntszb38	185.2044	−14.7479	88.40	25.00	5.00
ntsza39	184.3412	−14.9409	82.55	80.00	26.13
ntszb39	184.3307	−14.8636	82.55	25.00	5.00

This page is intentionally left blank.

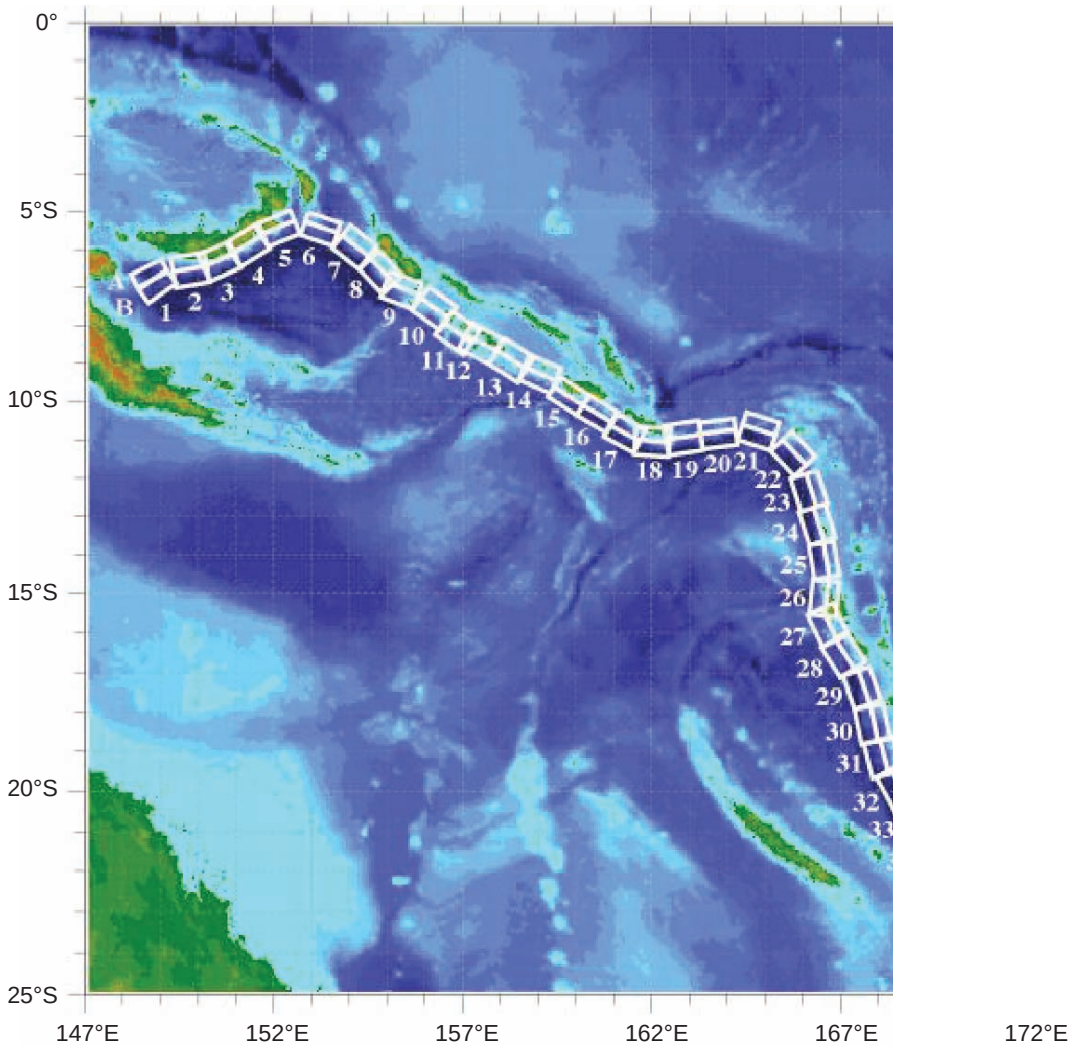

Figure B7: New Britain-Solomons-Vanuatu Subduction Zone unit sources.

Table B7: New Britain-Solomons-Vanuatu Subduction Zone unit sources parameters.

Locator	Longitude	Latitude	Strike Angle	Dip Angle	Depth (km)
nvsza1	148.6217	−6.4616	243.15	32.34	15.69
nvszb1	148.7943	−6.8002	234.15	12.34	5.00
nvsza2	149.7218	−6.1459	260.06	35.10	16.36
nvszb2	149.7856	−6.5079	260.06	13.13	5.00
nvsza3	150.4075	−5.9659	245.69	42.35	18.59
nvszb3	150.5450	−6.2684	245.69	15.77	5.00
nvsza4	151.1095	−5.5820	238.22	42.41	23.63
nvszb4	151.2851	−5.8639	238.22	21.88	5.00
nvsza5	152.0205	−5.1305	247.73	49.22	32.39
nvszb5	152.1322	−5.4020	247.73	33.22	5.00
nvsza6	153.3450	−5.1558	288.58	53.53	33.59
nvszb6	153.2595	−5.4089	288.58	34.87	5.00
nvsza7	154.3814	−5.6308	308.27	39.72	19.18
nvszb7	154.1658	−5.9017	308.27	16.48	5.00
nvsza8	155.1097	−6.3511	317.22	45.33	22.92
nvszb8	154.8764	−6.5656	317.22	21.00	5.00
nvsza9	155.5027	−6.7430	290.51	48.75	22.92
nvszb9	155.3981	−7.0204	290.51	21.00	5.00
nsza10	156.4742	−7.2515	305.85	36.88	27.62
nvszb10	156.2619	−7.5427	305.85	26.90	5.00
nvsza11	157.0830	−7.8830	305.36	32.97	29.72
nvszb11	156.8627	−8.1903	305.36	29.63	5.00
nvsza12	157.6537	−8.1483	297.94	37.53	28.57
nvszb12	157.4850	−8.4630	297.94	28.13	5.00
nvsza13	158.5089	−8.5953	302.73	33.62	23.02
nvszb13	158.3042	−8.9099	302.73	21.12	5.00
nvsza14	159.1872	−8.9516	293.32	38.44	34.06
nvszb14	159.0461	−9.2747	293.32	35.54	5.00
nvsza15	159.9736	−9.5993	302.76	46.69	41.38
nvszb15	159.8044	−9.8584	302.76	46.69	5.00
nvsza16	160.7343	−10.0574	300.99	46.05	41.00
nvszb16	160.5712	−10.3246	300.99	46.05	5.00
nvsza17	161.4562	−10.5241	298.37	40.12	37.22
nvszb17	161.2900	−10.8263	298.37	40.12	5.00
nvsza18	162.0467	−10.6823	274.07	40.33	29.03
nvszb18	162.0219	−11.0238	274.07	28.72	5.00
nvsza19	162.7818	−10.5645	261.27	34.25	24.14
nvszb19	162.8392	−10.9315	261.27	22.51	5.00
nvsza20	163.7222	−10.5014	262.93	50.35	26.30
nvszb20	163.7581	−10.7858	262.93	25.22	5.00
nvsza21	164.9445	−10.4183	287.89	40.31	23.30
nvszb21	164.8374	−10.7442	287.89	21.47	5.00
nvsza22	166.0261	−11.1069	317.08	42.39	20.78
nvszb22	165.7783	−11.3328	317.08	18.40	5.00
nvsza23	166.5179	−12.2260	342.37	47.95	22.43
nvszb23	166.2244	−12.3171	342.37	20.40	5.00
nvsza24	166.7236	−13.1065	342.60	47.13	28.52
nvszb24	166.4241	−13.1979	342.60	28.06	5.00
nvsza25	166.8914	−14.0785	350.28	54.10	31.16
nvszb25	166.6237	−14.1230	350.28	31.55	5.00
nvsza26	166.9200	−15.1450	365.62	50.46	29.05
nvszb26	166.6252	−15.1170	365.62	28.75	5.00
nvsza27	167.0053	−15.6308	334.23	44.74	25.46
nvszb27	166.7068	−15.7695	334.23	24.15	5.00

Table B7: (continued)

Locator	Longitude	Latitude	Strike Angle	Dip Angle	Depth (km)
nvsza28	167.4074	−16.3455	327.46	41.53	22.44
nvszb28	167.1117	−16.5264	327.46	20.42	5.00
nvsza29	167.9145	−17.2807	341.16	49.10	24.12
nvszb29	167.6229	−17.3757	341.16	22.48	5.00
nvsza30	168.2220	−18.2353	348.58	44.19	23.99
nvszb30	167.8895	−18.2991	348.58	22.32	5.00
nvsza31	168.5022	−19.0510	345.59	42.20	22.26
nvszb31	168.1611	−19.1338	345.59	20.20	5.00
nvsza32	168.8775	−19.6724	331.06	42.03	21.68
nvszb32	168.5671	−19.8338	331.06	19.49	5.00
nvsza33	169.3422	−20.4892	332.91	40.25	22.40
nvszb33	169.0161	−20.6453	332.91	20.37	5.00
nvsza34	169.8304	−21.2121	329.15	39.00	22.73
nvszb34	169.5086	−21.3911	329.15	20.77	5.00
nvsza35	170.3119	−21.6945	311.89	39.00	22.13
nvszb35	170.0606	−21.9543	311.89	20.03	5.00
nvsza36	170.9487	−22.1585	300.43	39.42	23.50
nvszb36	170.7585	−22.4577	300.43	21.71	5.00
nvsza37	171.6335	−22.3087	281.26	30.00	22.10
nvszb37	171.5512	−22.6902	281.26	20.00	5.00

This page is intentionally left blank.

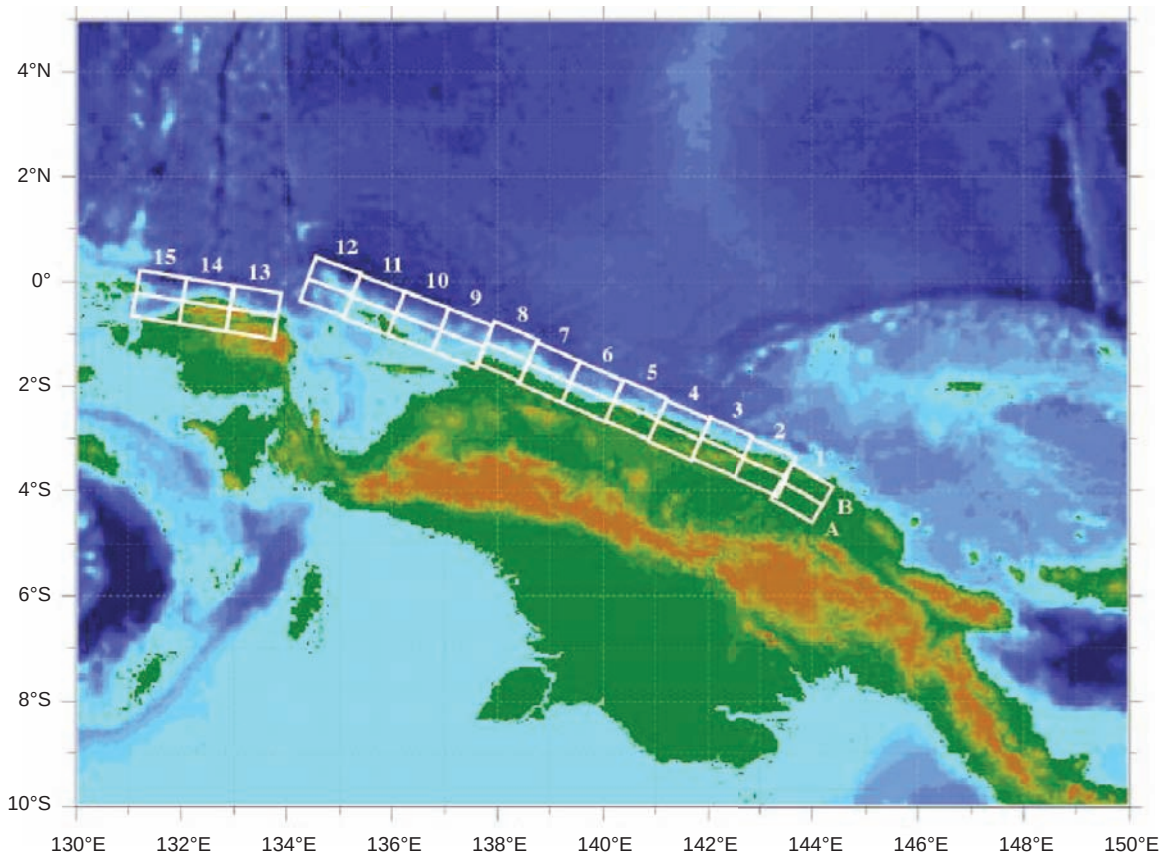

Figure B8: North New Guinea Subduction Zone unit sources.

Table B8: North New Guinea Subduction Zone unit sources parameters.

Locator	Longitude	Latitude	Strike Angle	Dip Angle	Depth (km)
ngsza1	143.6063	−4.3804	120.00	29.00	25.64
ngszb1	143.8032	−4.0402	120.00	29.00	1.40
ngsza2	142.9310	−3.9263	114.00	27.63	24.79
ngszb2	143.0932	−3.5628	114.00	21.72	1.60
ngsza3	142.1076	−3.5632	114.00	20.06	22.15
ngszb3	142.2795	−3.1778	114.00	15.94	5.00
ngsza4	141.2681	−3.2376	114.00	21.00	22.92
ngszb4	141.4389	−2.8545	114.00	14.79	5.00
ngsza5	140.4592	−2.8429	114.00	21.26	23.13
ngszb5	140.6296	−2.4605	114.00	12.87	5.00
ngsza6	139.6288	−2.4960	114.00	22.72	24.31
ngszb6	139.7974	−2.1175	114.00	12.00	5.00
ngsza7	138.8074	−2.1312	114.00	21.39	23.24
ngszb7	138.9776	−1.7491	114.00	12.00	5.00
ngsza8	138.0185	−1.7353	113.09	18.79	21.11
ngszb8	138.1853	−1.3441	113.09	11.70	5.00
ngsza9	137.1805	−1.5037	111.00	15.24	18.14
ngszb9	137.3358	−1.0991	111.00	9.47	5.00
ngsza10	136.3418	−1.1774	111.00	13.51	16.68
ngszb10	136.4983	−0.7697	111.00	7.00	5.00
ngsza11	135.4984	−0.8641	111.00	11.38	14.87
ngszb11	135.6562	−0.4530	111.00	8.62	5.00
ngsza12	134.6759	−0.5216	110.48	10.00	13.68
ngszb12	134.8307	−0.1072	110.48	10.00	5.00
ngsza13	133.3065	−1.0298	99.50	10.00	13.68
ngszb13	133.3795	−0.5935	99.50	10.00	5.00
ngsza14	132.4048	−0.8816	99.50	10.00	13.68
ngszb14	132.4778	−0.4453	99.50	10.00	5.00
ngsza15	131.5141	−0.7353	99.50	10.00	13.68
ngszb15	131.5871	−0.2990	99.50	10.00	5.00

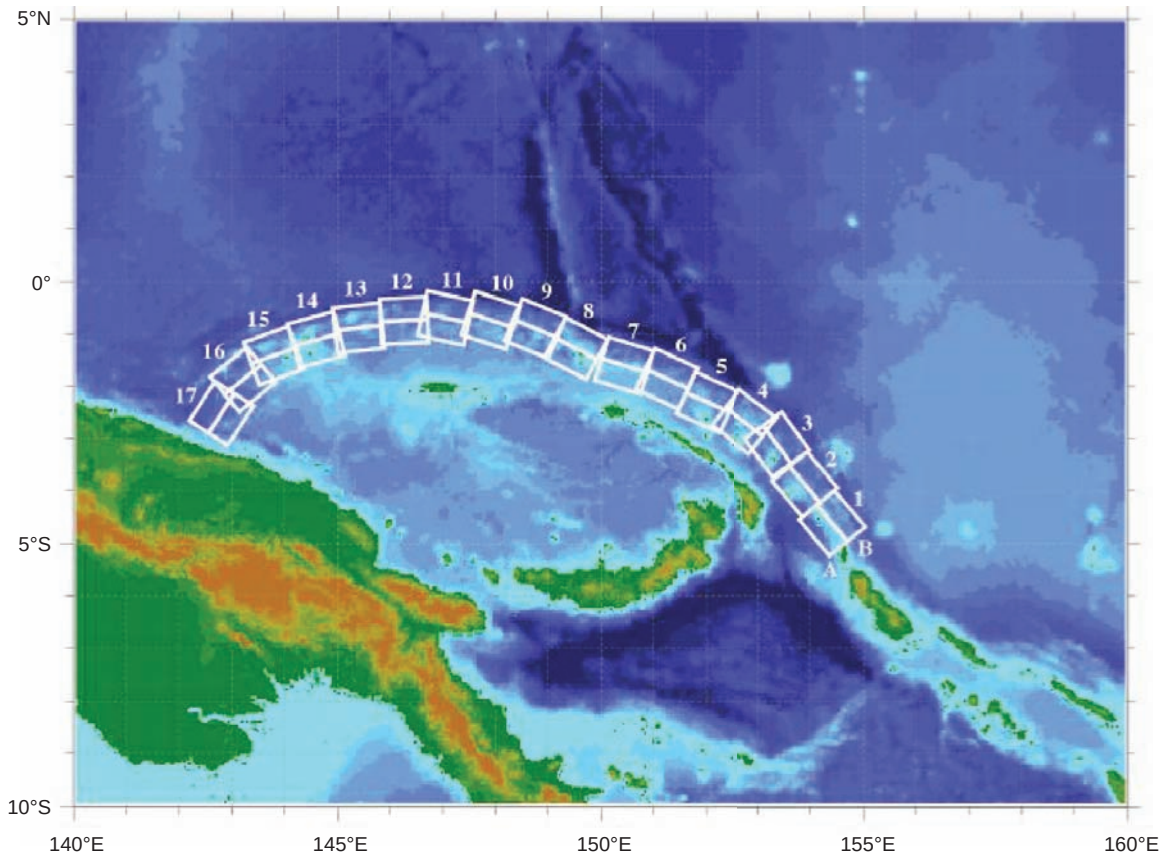

Figure B9: Manus Ocean Convergence Boundary unit sources.

Table B9: Manus Ocean Convergence Boundary unit sources parameters.

Locator	Longitude	Latitude	Strike Angle	Dip Angle	Depth (km)
mosza1	154.0737	−4.8960	140.23	15.00	15.88
moszb1	154.4082	−4.6185	140.23	15.00	2.94
mosza2	153.5589	−4.1575	140.23	15.00	15.91
moszb2	153.8931	−3.8800	140.23	15.00	2.97
mosza3	153.0151	−3.3716	143.91	15.00	16.64
moszb3	153.3662	−3.1160	143.91	15.00	3.70
mosza4	152.4667	−3.0241	127.66	15.00	17.32
moszb4	152.7321	−2.6806	127.66	15.00	4.38
mosza5	151.8447	−2.7066	114.32	15.00	17.57
moszb5	152.0235	−2.3112	114.32	15.00	4.63
mosza6	151.0679	−2.2550	114.99	15.00	17.66
moszb6	151.2513	−1.8618	114.99	15.00	4.72
mosza7	150.3210	−2.0236	107.20	15.00	17.73
moszb7	150.4493	−1.6092	107.20	15.00	4.79
mosza8	149.3226	−1.6666	117.82	15.00	17.83
moszb8	149.5251	−1.2829	117.82	15.00	4.89
mosza9	148.5865	−1.3017	112.71	15.00	17.84
moszb9	148.7540	−0.9015	112.71	15.00	4.90
mosza10	147.7760	−1.1560	108.01	15.00	17.78
moszb10	147.9102	−0.7434	108.01	15.00	4.84
mosza11	146.9596	−1.1226	102.45	15.00	17.54
moszb11	147.0531	−0.6990	102.45	15.00	4.60
mosza12	146.2858	−1.1820	87.48	15.00	17.29
moszb12	146.2667	−0.7486	87.48	15.00	4.35
mosza13	145.4540	−1.3214	83.75	15.00	17.34
moszb13	145.4068	−0.8901	83.75	15.00	4.40
mosza14	144.7151	−1.5346	75.09	15.00	17.21
moszb14	144.6035	−1.1154	75.09	15.00	4.27
mosza15	143.9394	−1.8278	70.43	15.00	16.52
moszb15	143.7940	−1.4190	70.43	15.00	3.58
mosza16	143.4850	−2.2118	50.79	15.00	15.86
moszb16	143.2106	−1.8756	50.79	15.00	2.92
mosza17	143.1655	−2.7580	33.00	15.00	16.64
moszb17	142.8013	−2.5217	33.00	15.00	3.70

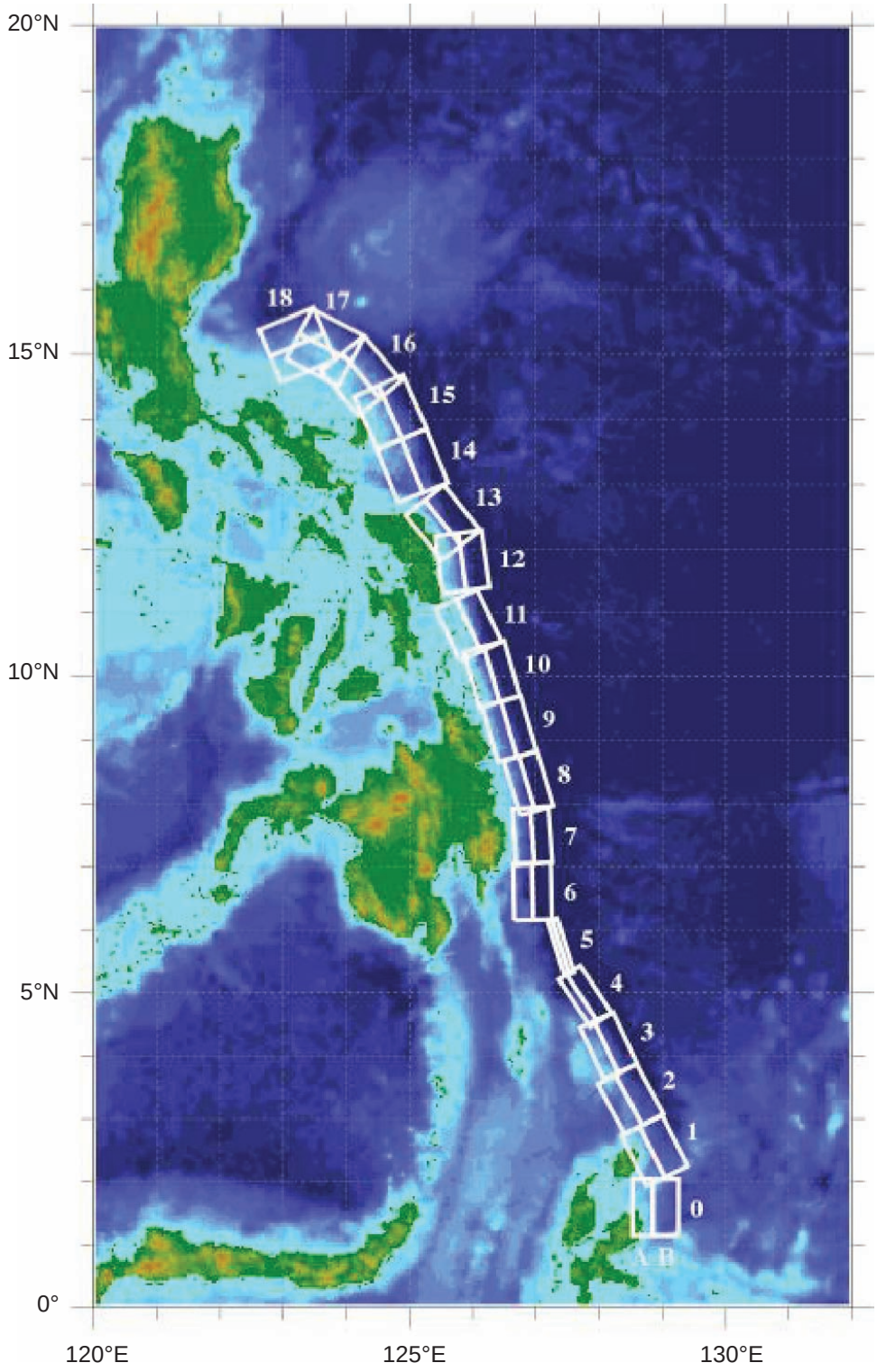

Figure B10: East Philippines Subduction Zone unit sources.

Table B10: East Philippines Subduction Zone unit sources parameters.

Locator	Longitude	Latitude	Strike Angle	Dip Angle	Depth (km)
epsza0	128.5264	1.5930	180.00	44.00	26.92
epszb0	128.8496	1.5930	180.00	26.00	5.00
epsza1	128.5521	2.3289	153.61	44.20	27.62
epszb1	128.8408	2.4720	153.61	26.90	5.00
epsza2	128.1943	3.1508	151.93	45.90	32.44
epszb2	128.4706	3.2979	151.93	32.80	5.35
epsza3	127.8899	4.0428	155.22	57.30	40.22
epszb3	128.1108	4.1445	155.22	42.70	6.31
epsza4	127.6120	4.8371	146.84	71.40	48.25
epszb4	127.7324	4.9155	146.84	54.80	7.39
epsza5	127.3173	5.7040	162.87	79.90	57.40
epszb5	127.3930	5.7272	162.87	79.40	8.25
epsza6	126.6488	6.6027	178.89	48.60	45.09
epszb6	126.9478	6.6085	178.89	48.60	7.58
epsza7	126.6578	7.4711	175.76	50.70	45.52
epszb7	126.9439	7.4921	175.76	50.70	6.83
epsza8	126.6227	8.2456	163.31	56.70	45.60
epszb8	126.8614	8.3164	163.31	48.90	7.92
epsza9	126.2751	9.0961	164.09	47.00	43.59
epszb9	126.5735	9.1801	164.09	44.90	8.30
epsza10	125.9798	9.9559	164.46	43.10	42.25
epszb10	126.3007	10.0438	164.46	43.10	8.09
epsza11	125.6079	10.6557	154.97	37.80	38.29
epszb11	125.9353	10.8059	154.97	37.80	7.64
epsza12	125.4697	11.7452	172.14	36.00	37.01
epszb12	125.8374	11.7949	172.14	36.00	7.62
epsza13	125.2238	12.1670	141.53	32.40	33.87
epszb13	125.5278	12.4029	141.53	32.40	7.08
epsza14	124.6476	13.1365	158.23	23.00	25.92
epszb14	125.0421	13.2898	158.23	23.00	6.38
epsza15	124.3107	13.9453	156.12	24.10	26.51
epszb15	124.6973	14.1113	156.12	24.10	6.09
epsza16	123.8998	14.4025	140.32	19.50	21.69
epszb16	124.2366	14.6728	140.32	19.50	5.00
epsza17	123.4604	14.7222	117.58	15.30	18.19
epszb17	123.6682	15.1062	117.58	15.30	5.00
epsza18	123.3946	14.7462	67.40	15.00	17.94
epszb18	123.2219	15.1467	67.40	15.00	5.00

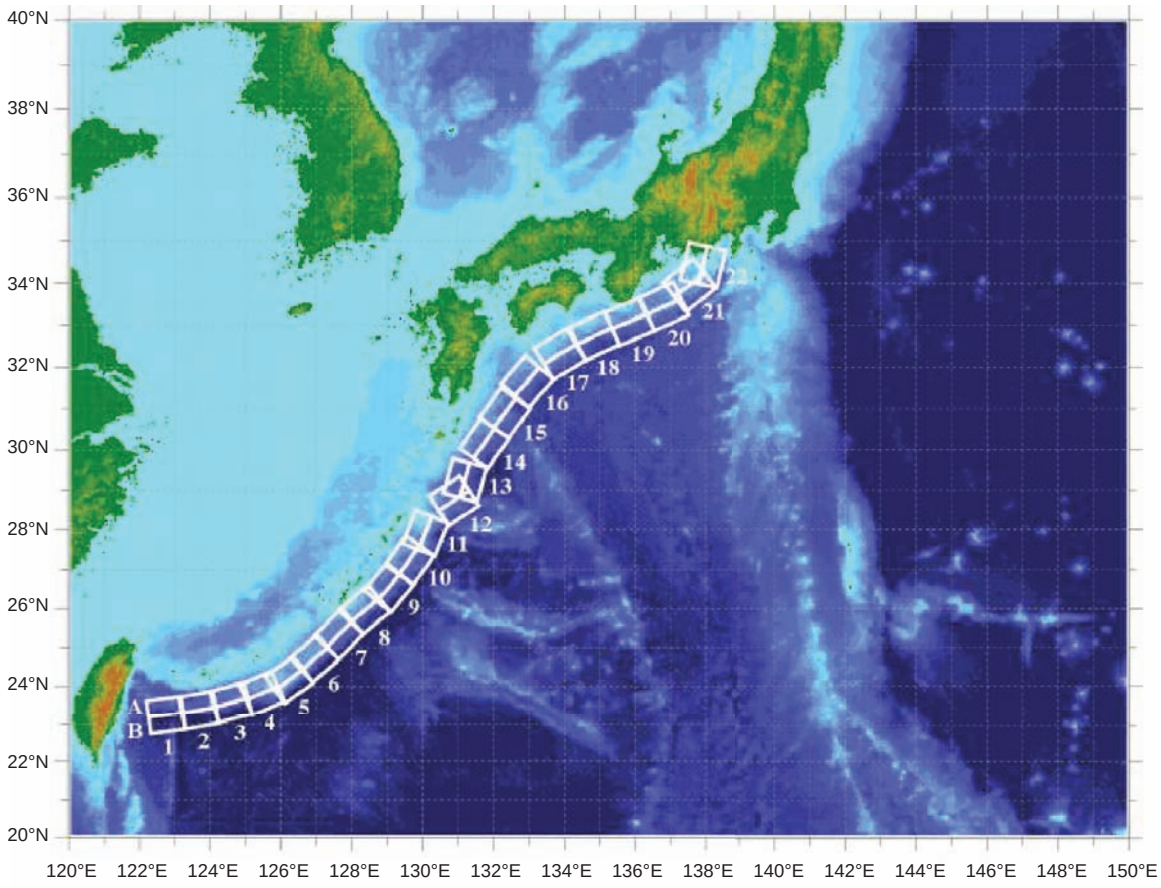

Figure B11: Ryukyus-Kyushu-Nankai Subduction Zone unit sources.

Table B11: Ryukyus-Kyushu-Nankai Subduction Zone unit sources parameters.

Locator	Longitude	Latitude	Strike Angle	Dip Angle	Depth (km)
rnsza1	122.6672	23.6696	262.00	14.00	11.88
rnszb1	122.7332	23.2380	262.00	10.00	3.20
rnsza2	123.5939	23.7929	259.95	18.11	12.28
rnszb2	123.6751	23.3725	259.95	10.00	3.60
rnsza3	124.4604	23.9777	254.63	19.27	14.65
rnszb3	124.5830	23.5689	254.63	12.18	4.10
rnsza4	125.2720	24.2102	246.75	18.00	20.38
rnszb4	125.4563	23.8177	246.75	16.00	6.60
rnsza5	125.9465	24.5085	233.64	18.00	20.21
rnszb5	126.2241	24.1645	233.64	16.00	6.43
rnsza6	126.6349	25.0402	228.73	17.16	19.55
rnszb6	126.9465	24.7176	228.73	15.16	6.47
rnsza7	127.2867	25.6343	224.04	15.85	17.98
rnszb7	127.6303	25.3339	224.04	13.56	6.26
rnsza8	128.0725	26.3146	229.69	14.55	14.31
rnszb8	128.3854	25.9831	229.69	9.64	5.94
rnsza9	128.6642	26.8177	219.24	15.40	12.62
rnszb9	129.0391	26.5438	219.24	8.00	5.66
rsza10	129.2286	27.4879	215.21	17.00	12.55
rnszb10	129.6233	27.2402	215.21	8.16	5.45
rnsza11	129.6169	28.0741	201.30	17.00	12.91
rnszb11	130.0698	27.9181	201.30	8.80	5.26
rnsza12	130.6175	29.0900	236.69	16.42	13.05
rnszb12	130.8873	28.7299	236.69	9.57	4.74
rnsza13	130.7223	29.3465	195.18	20.25	15.89
rnszb13	131.1884	29.2362	195.18	12.98	4.66
rnsza14	131.3467	30.3899	215.11	22.16	19.73
rnszb14	131.7402	30.1507	215.11	17.48	4.71
rnsza15	131.9149	31.1450	216.04	15.11	16.12
rnszb15	132.3235	30.8899	216.04	13.46	4.48
rnsza16	132.5628	31.9468	220.90	10.81	10.88
rnszb16	132.9546	31.6579	220.90	7.19	4.62
rnsza17	133.6125	32.6956	238.96	10.14	12.01
rnszb17	133.8823	32.3168	238.96	8.41	4.70
rnsza18	134.6416	33.1488	244.70	10.99	14.21
rnszb18	134.8656	32.7502	244.47	10.97	4.70
rnsza19	135.6450	33.5008	246.46	14.49	14.72
rnszb19	135.8523	33.1021	246.46	11.87	4.44
rnsza20	136.5962	33.8506	244.77	15.00	14.38
rnszb20	136.8179	33.4581	244.77	12.00	3.98
rnsza21	137.2252	34.3094	231.90	15.00	15.40
rnszb21	137.5480	33.9680	231.90	12.00	5.00
rnsza22	137.4161	34.5249	192.27	15.00	15.40
rnszb22	137.9301	34.4327	192.27	12.00	5.00

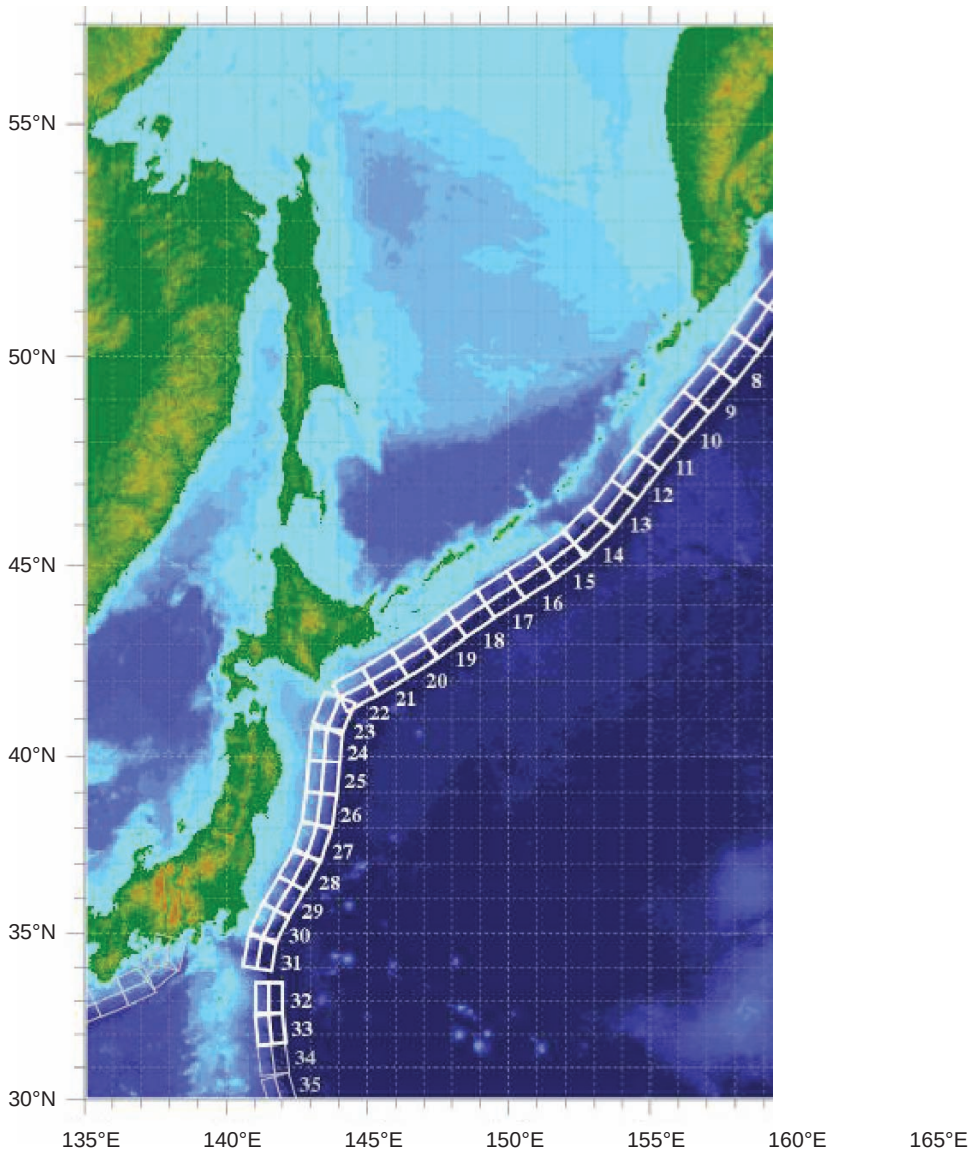

Figure B12a: Kamchatka-Yap-Mariana-Izu-Bonin unit sources, part 1.

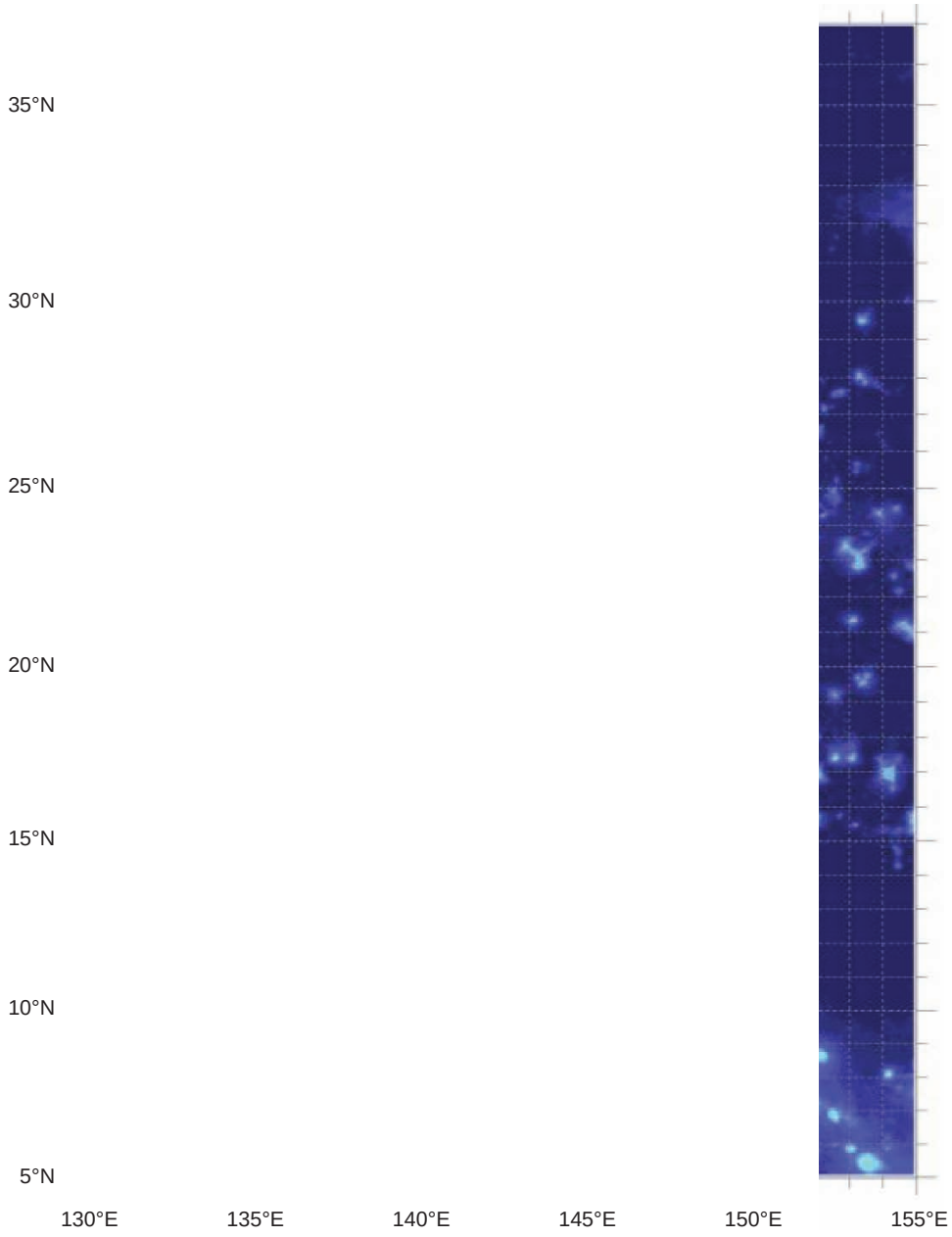

Figure B12b: Kamchatka-Yap-Mariana-Izu-Bonin unit sources, part 2.

Table B12: Kamchatka-Yap-Mariana-Izu-Bonin unit sources parameters.

Locator	Longitude	Latitude	Strike Angle	Dip Angle	Depth (km)
kisza1	162.4318	55.5017	195.00	29.00	26.13
kiszb1	163.1000	55.4000	195.00	25.00	5.00
kisza2	161.9883	54.6784	200.00	29.00	26.13
kiszb2	162.6247	54.5440	200.00	25.00	5.00
kisza3	161.4385	53.8714	204.00	29.00	26.13
kiszb3	162.0449	53.7116	204.00	25.00	5.00
kisza4	160.7926	53.1087	210.00	29.00	26.13
kiszb4	161.3568	52.9123	210.00	25.00	5.00
kisza5	160.0211	52.4113	218.00	29.00	26.13
kiszb5	160.5258	52.1694	218.00	25.00	5.00
kisza6	159.1272	51.7034	218.00	29.00	26.13
kiszb6	159.6241	51.4615	218.00	25.00	5.00
kisza7	158.2625	50.9549	214.00	29.00	26.13
kiszb7	158.7771	50.7352	214.00	25.00	5.00
kisza8	157.4712	50.2459	218.00	31.00	27.70
kiszb8	157.9433	50.0089	218.00	27.00	5.00
kisza9	156.6114	49.5584	220.00	31.00	27.70
kiszb9	157.0638	49.3109	220.00	27.00	5.00
kisza10	155.7294	48.8804	221.00	31.00	27.70
kiszb10	156.1690	48.6278	221.00	27.00	5.00
kisza11	154.8489	48.1821	219.00	31.00	27.70
kiszb11	155.2955	47.9398	219.00	27.00	5.00
kisza12	153.9994	47.4729	217.00	31.00	27.70
kiszb12	154.4701	47.2320	217.00	27.00	5.00
kisza13	153.2239	46.7564	218.00	31.00	27.70
kiszb13	153.6648	46.5194	218.00	27.00	5.00
kisza14	152.3657	46.1515	225.00	23.00	24.54
kiszb14	152.7855	45.8591	225.00	23.00	5.00
kisza15	151.4663	45.5963	233.00	25.00	23.73
kiszb15	151.8144	45.2712	233.00	22.00	5.00
kisza16	150.4572	45.0977	237.00	25.00	23.73
kiszb16	150.7694	44.7563	237.00	22.00	5.00
kisza17	149.3989	44.6084	237.00	25.00	23.73
kiszb17	149.7085	44.2670	237.00	22.00	5.00
kisza18	148.3454	44.0982	235.00	25.00	23.73
kiszb18	148.6687	43.7647	235.00	22.00	5.00
kisza19	147.3262	43.5619	233.00	25.00	23.73
kiszb19	147.6625	43.2368	233.00	22.00	5.00
kisza20	146.3513	43.0633	237.00	25.00	23.73
kiszb20	146.6531	42.7219	237.00	22.00	5.00
kisza21	145.3331	42.5948	239.00	25.00	23.73
kiszb21	145.6163	42.2459	239.00	22.00	5.00
kisza22	144.3041	42.1631	242.00	25.00	23.73
kiszb22	144.5605	41.8037	242.00	22.00	5.00
kisza23	143.2863	41.3335	202.00	21.00	21.28
kiszb23	143.8028	41.1764	202.00	19.00	5.00
kisza24	142.9795	40.3490	185.00	21.00	21.28
kiszb24	143.5273	40.3125	185.00	19.00	5.00
kisza25	142.8839	39.4541	185.00	21.00	21.28
kiszb25	143.4246	39.4176	185.00	19.00	5.00
kisza26	142.7622	38.5837	188.00	21.00	21.28
kiszb26	143.2930	38.5254	188.00	19.00	5.00
kisza27	142.5320	37.7830	198.00	21.00	21.28
kiszb27	143.0357	37.6534	198.00	19.00	5.00
kisza28	142.1315	37.0265	208.00	21.00	21.28
kiszb28	142.5941	36.8297	208.00	19.00	5.00

Table B12: (continued)

Locator	Longitude	Latitude	Strike Angle	Dip Angle	Depth (km)
kisza29	141.5970	36.2640	211.00	21.00	21.28
kiszb29	142.0416	36.0481	211.00	19.00	5.00
kisza30	141.0553	35.4332	205.00	21.00	21.28
kiszb30	141.5207	35.2560	205.00	19.00	5.00
kisza31	140.6956	34.4789	190.00	22.00	22.10
kiszb31	141.1927	34.4066	190.00	20.00	5.00
kisza32	141.0551	33.0921	180.00	32.00	23.48
kiszb32	141.5098	33.0921	180.00	21.69	5.00
kisza33	141.0924	32.1047	173.85	27.65	20.67
kiszb33	141.5596	32.1473	173.85	18.27	5.00
kisza34	141.1869	31.1851	172.14	25.00	18.26
kiszb34	141.6585	31.2408	172.14	15.38	5.00
kisza35	141.4154	30.1707	162.98	25.00	17.12
kiszb35	141.8662	30.2899	162.98	14.03	5.00
kisza36	141.6261	29.2740	161.68	25.73	18.71
kiszb36	142.0670	29.4012	161.68	15.91	5.00
kisza37	142.0120	28.3322	154.72	20.00	14.54
kiszb37	142.4463	28.5124	154.72	11.00	5.00
kisza38	142.2254	27.6946	170.27	20.00	14.54
kiszb38	142.6955	27.7659	170.27	11.00	5.00
kisza39	142.3085	26.9127	177.23	24.23	17.42
kiszb39	142.7674	26.9325	177.23	14.38	5.00
kisza40	142.2673	26.1923	189.44	26.49	22.26
kiszb40	142.7090	26.1264	189.44	20.20	5.00
kisza41	142.1595	25.0729	173.72	22.07	19.08
kiszb41	142.6165	25.1184	173.72	16.36	5.00
kisza42	142.7641	23.8947	143.50	21.54	18.40
kiszb42	143.1321	24.1432	143.50	15.54	5.00
kisza43	143.5281	23.0423	129.21	23.02	18.77
kiszb43	143.8128	23.3626	129.21	15.99	5.00
kisza44	144.2230	22.5240	134.63	28.24	18.56
kiszb44	144.5246	22.8056	134.63	15.74	5.00
kisza45	145.0895	21.8866	125.83	36.73	22.79
kiszb45	145.3171	22.1785	125.83	20.84	5.00
kisza46	145.6972	21.3783	135.90	30.75	20.63
kiszb46	145.9954	21.6469	135.90	18.22	5.00
kisza47	146.0406	20.9341	160.07	29.87	19.62
kiszb47	146.4330	21.0669	160.07	17.00	5.00
kisza48	146.3836	20.0690	157.96	32.75	19.68
kiszb48	146.7567	20.2108	157.96	17.07	5.00
kisza49	146.6689	19.3123	164.48	25.07	21.41
kiszb49	147.0846	19.4212	164.48	19.16	5.00
kisza50	146.9297	18.5663	172.07	22.00	22.10
kiszb50	147.3650	18.6238	172.07	20.00	5.00
kisza51	146.9495	17.7148	175.11	22.06	22.04
kiszb51	147.3850	17.7503	175.11	19.93	5.00
kisza52	146.9447	16.8869	180.00	25.51	18.61
kiszb52	147.3683	16.8869	180.00	15.79	5.00
kisza53	146.8626	16.0669	185.18	27.39	18.41
kiszb53	147.2758	16.0309	185.18	15.56	5.00
kisza54	146.7068	15.3883	199.05	28.12	20.91
kiszb54	147.0949	15.2590	199.05	18.56	5.00
kisza55	146.4717	14.6025	204.35	29.60	26.23
kiszb55	146.8391	14.4415	204.35	25.18	5.00
kisza56	146.1678	13.9485	217.45	32.04	26.79
kiszb56	146.4789	13.7170	217.45	25.84	5.00

Table B12: (continued)

Locator	Longitude	Latitude	Strike Angle	Dip Angle	Depth (km)
kisza57	145.6515	13.5576	235.81	37.00	24.54
kiszb57	145.8586	13.2609	235.81	23.00	5.00
kisza58	144.9648	12.9990	237.80	37.72	24.54
kiszb58	145.1589	12.6984	237.80	23.00	5.00
kisza59	144.1799	12.6914	242.87	34.33	22.31
kiszb59	144.3531	12.3613	242.87	20.25	5.00
kisza60	143.3687	12.3280	244.95	30.90	20.62
kiszb60	143.5355	11.9788	244.95	18.20	5.00
kisza61	142.7051	12.1507	261.84	35.41	25.41
kiszb61	142.7582	11.7883	261.84	24.22	5.00
kisza62	141.6301	11.8447	245.69	39.86	34.35
kiszb62	141.7750	11.5305	245.69	35.94	5.00
kisza63	140.8923	11.5740	256.20	42.00	38.46
kiszb63	140.9735	11.2498	256.20	42.00	5.00
kisza64	140.1387	11.6028	269.61	42.48	38.77
kiszb64	140.1410	11.2716	269.61	42.48	5.00
kisza65	139.4595	11.5883	288.71	44.16	39.83
kiszb65	139.3541	11.2831	288.71	44.16	5.00
kisza66	138.1823	11.2648	193.08	45.00	40.36
kiszb66	138.4977	11.1929	193.08	45.00	5.00
kisza67	137.9923	10.3398	189.83	45.00	40.36
kiszb67	138.3104	10.2856	189.83	45.00	5.00
kisza68	137.7607	9.6136	201.68	45.00	40.36
kiszb68	138.0599	9.4963	201.68	45.00	5.00
kisza69	137.4537	8.8996	213.54	45.00	40.36
kiszb69	137.7215	8.7241	213.54	45.00	5.00
kisza70	137.0191	8.2872	226.47	45.00	40.36
kiszb70	137.2400	8.0569	226.47	45.00	5.00

This page is intentionally left blank.

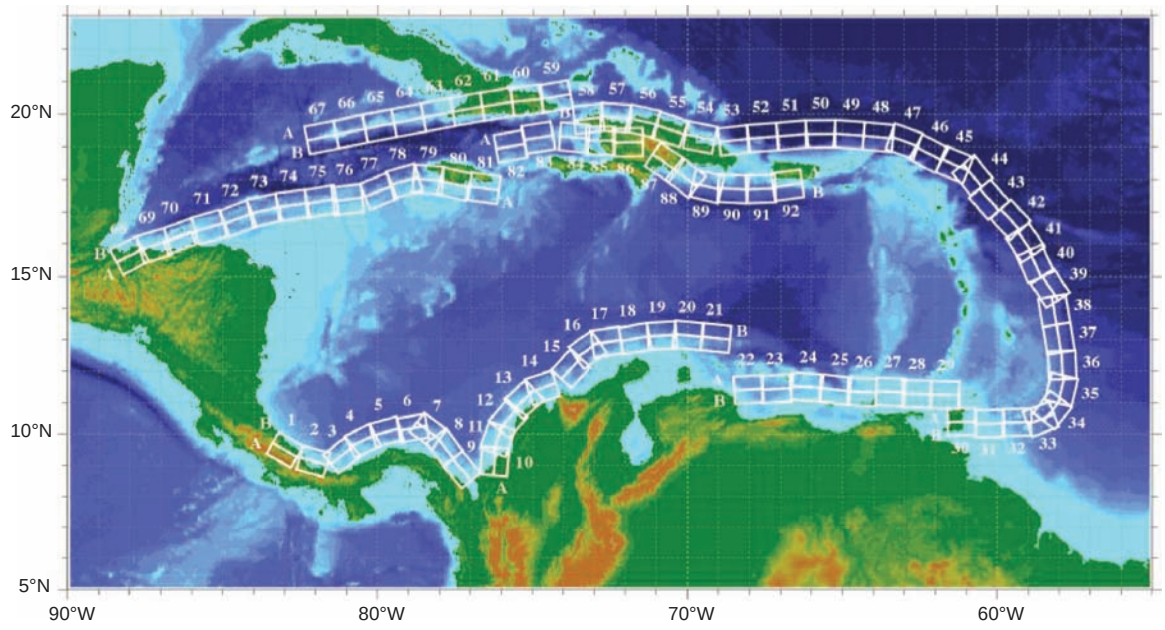

Figure B13: Atlantic Subduction Zone unit sources.

Table B13: Atlantic Subduction Zone unit sources parameters.

Locator	Longitude	Latitude	Strike Angle	Dip Angle	Depth (km)
atsza1	−83.2020	9.1449	120.00	27.50	28.09
atszb1	−83.0000	9.4899	120.00	27.50	5.00
atsza2	−82.1932	8.7408	105.11	27.50	28.09
atszb2	−82.0880	9.1254	105.11	27.50	5.00
atsza3	−80.9172	9.0103	51.31	30.00	30.00
atszb3	−81.1636	9.3139	51.31	30.00	5.00
atsza4	−80.3265	9.4308	63.49	30.00	30.00
atszb4	−80.5027	9.7789	63.49	30.00	5.00
atsza5	−79.6247	9.6961	74.44	30.00	30.00
atszb5	−79.7307	10.0708	74.44	30.00	5.00
atsza6	−78.8069	9.8083	79.71	30.00	30.00
atszb6	−78.8775	10.1910	79.71	30.00	5.00
atsza7	−78.6237	9.7963	127.25	30.00	30.00
atszb7	−78.3845	10.1059	127.25	30.00	5.00
atsza8	−78.1693	9.3544	143.76	30.00	30.00
atszb8	−77.8511	9.5844	143.76	30.00	5.00
atsza9	−77.5913	8.5989	139.93	30.00	30.00
atszb9	−77.2900	8.8493	139.93	30.00	5.00
atsza10	−75.8109	9.0881	4.67	17.00	19.62
atszb10	−76.2445	9.1231	4.67	17.00	5.00
atsza11	−75.7406	9.6929	19.67	17.00	19.62
atszb11	−76.1511	9.8375	19.67	17.00	5.00
atsza12	−75.4763	10.2042	40.40	17.00	19.62
atszb12	−75.8089	10.4826	40.40	17.00	5.00
atsza13	−74.9914	10.7914	47.17	17.00	19.62
atszb13	−75.2890	11.1064	47.17	17.00	5.00
atsza14	−74.5666	11.0708	71.68	17.00	19.62
atszb14	−74.7043	11.4786	71.68	17.00	5.00
atsza15	−73.4576	11.8012	42.69	17.00	19.62
atszb15	−73.7805	12.0924	42.69	17.00	5.00
atsza16	−72.9788	12.3365	54.75	17.00	19.62
atszb16	−73.2329	12.6873	54.75	17.00	5.00
atsza17	−72.5454	12.5061	81.96	17.00	19.62
atszb17	−72.6071	12.9314	81.96	17.00	5.00
atsza18	−71.6045	12.6174	79.63	17.00	19.62
atszb18	−71.6839	13.0399	79.63	17.00	5.00
atsza19	−70.7970	12.7078	86.32	17.00	19.62
atszb19	−70.8253	13.1364	86.32	17.00	5.00
atsza20	−70.0246	12.7185	95.94	17.00	19.62
atszb20	−69.9789	13.1457	95.94	17.00	5.00
atsza21	−69.1244	12.6320	95.94	17.00	19.62
atszb21	−69.0788	13.0592	95.94	17.00	5.00
atsza22	−68.0338	11.4286	86.94	15.00	17.94
atszb22	−68.0102	10.9954	86.94	15.00	5.00
atsza23	−67.1246	11.4487	86.94	15.00	17.94
atszb23	−67.1010	11.0155	86.94	15.00	5.00
atsza24	−66.1656	11.5055	93.30	15.00	17.94
atszb24	−66.1911	11.0724	93.30	15.00	5.00
atsza25	−65.2126	11.4246	96.36	15.00	17.94
atszb25	−65.2616	10.9934	96.36	15.00	5.00
atsza26	−64.3641	11.3516	92.87	15.00	17.94
atszb26	−64.3862	10.9183	92.87	15.00	5.00
atsza27	−63.4472	11.3516	92.93	15.00	17.94
atszb27	−63.4698	10.9183	92.93	15.00	5.00
atsza28	−62.6104	11.2831	91.11	15.00	17.94
atszb28	−62.6189	10.8493	91.11	15.00	5.00

Table B13: (continued)

Locator	Longitude	Latitude	Strike Angle	Dip Angle	Depth (km)
atsza29	−61.6826	11.2518	91.57	15.00	17.94
atszb29	−61.6947	10.8181	91.57	15.00	5.00
atsza30	−61.1569	10.8303	269.01	15.00	17.94
atszb30	−61.1493	10.3965	269.01	15.00	5.00
atsza31	−60.2529	10.7739	269.01	15.00	17.94
atszb31	−60.2453	10.3401	269.01	15.00	5.00
atsza32	−59.3510	10.8123	269.01	15.00	17.94
atszb32	−59.3734	10.3785	269.01	15.00	5.00
atsza33	−58.7592	10.8785	248.62	15.00	17.94
atszb33	−58.5984	10.4745	248.62	15.00	5.00
atsza34	−58.5699	11.0330	217.15	15.00	17.94
atszb34	−58.2179	10.7710	217.15	15.00	5.00
atsza35	−58.3549	11.5300	193.68	15.00	17.94
atszb35	−57.9248	11.4274	193.68	15.00	5.00
atsza36	−58.3432	12.1858	177.65	15.00	17.94
atszb36	−57.8997	12.2036	177.65	15.00	5.00
atsza37	−58.4490	12.9725	170.73	15.00	17.94
atszb37	−58.0095	13.0424	170.73	15.00	5.00
atsza38	−58.6079	13.8503	170.22	15.00	17.94
atszb38	−58.1674	13.9240	170.22	15.00	5.00
atsza39	−58.6667	14.3915	146.85	15.00	17.94
atszb39	−58.2913	14.6287	146.85	15.00	5.00
atsza40	−59.1899	15.2143	156.23	15.00	17.94
atszb40	−58.7781	15.3892	156.23	15.00	5.00
atsza41	−59.4723	15.7987	146.33	15.00	17.94
atszb41	−59.0966	16.0392	146.33	15.00	5.00
atsza42	−59.9029	16.4535	136.99	15.00	17.94
atszb42	−59.5716	16.7494	136.99	15.00	5.00
atsza43	−60.5996	17.0903	138.71	15.00	17.94
atszb43	−60.2580	17.3766	138.71	15.00	5.00
atsza44	−61.1559	17.8560	141.07	15.00	17.94
atszb44	−60.8008	18.1286	141.07	15.00	5.00
atsza45	−61.5491	18.0566	112.84	15.00	17.94
atszb45	−61.3716	18.4564	112.84	15.00	5.00
atsza46	−62.4217	18.4149	117.86	15.00	17.94
atszb46	−62.2075	18.7985	117.86	15.00	5.00
atsza47	−63.1649	18.7844	110.46	20.00	22.10
atszb47	−63.0087	19.1798	110.46	20.00	5.00
atsza48	−63.8800	18.8870	95.37	20.00	22.10
atszb48	−63.8382	19.3072	95.37	20.00	5.00
atsza49	−64.8153	18.9650	94.34	20.00	22.10
atszb49	−64.7814	19.3859	94.34	20.00	5.00
atsza50	−65.6921	18.9848	89.59	20.00	22.10
atszb50	−65.6953	19.4069	89.59	20.00	5.00
atsza51	−66.5742	18.9484	84.98	20.00	22.10
atszb51	−66.6133	19.3688	84.98	20.00	5.00
atsza52	−67.5412	18.8738	85.87	20.00	22.10
atszb52	−67.5734	19.2948	85.87	20.00	5.00
atsza53	−68.4547	18.7853	83.64	20.00	22.10
atszb53	−68.5042	19.2048	83.64	20.00	5.00
atsza54	−69.6740	18.8841	101.54	20.00	22.10
atszb54	−69.5846	19.2976	101.54	20.00	5.00
atsza55	−70.7045	19.1376	108.19	20.00	22.10
atszb55	−70.5647	19.5386	108.19	20.00	5.00
atsza56	−71.5368	19.3853	102.64	20.00	22.10
atszb56	−71.4386	19.7971	102.64	20.00	5.00

Table B13: (continued)

Locator	Longitude	Latitude	Strike Angle	Dip Angle	Depth (km)
atsza57	−72.3535	19.4838	94.20	20.00	22.10
atszb57	−72.3206	19.9047	94.20	20.00	5.00
atsza58	−73.1580	19.4498	84.34	20.00	22.10
atszb58	−73.2022	19.8698	84.34	20.00	5.00
atsza59	−74.3567	20.9620	259.74	20.00	22.10
atszb59	−74.2764	20.5467	259.74	20.00	5.00
atsza60	−75.2386	20.8622	264.18	15.00	17.94
atszb60	−75.1917	20.4306	264.18	15.00	5.00
atsza61	−76.2383	20.7425	260.70	15.00	17.94
atszb61	−76.1635	20.3144	260.70	15.00	5.00
atsza62	−77.2021	20.5910	259.95	15.00	17.94
atszb62	−77.1214	20.1638	259.95	15.00	5.00
atsza63	−78.1540	20.4189	259.03	15.00	17.94
atszb63	−78.0661	19.9930	259.03	15.00	5.00
atsza64	−79.0959	20.2498	259.24	15.00	17.94
atszb64	−79.0098	19.8236	259.24	15.00	5.00
atsza65	−80.0393	20.0773	258.85	15.00	17.94
atszb65	−79.9502	19.6516	258.85	15.00	5.00
atsza66	−80.9675	19.8993	258.60	15.00	17.94
atszb66	−80.8766	19.4740	258.60	15.00	5.00
atsza67	−81.9065	19.7214	258.51	15.00	17.94
atszb67	−81.8149	19.2962	258.51	15.00	5.00
atsza68	−87.8003	15.2509	62.69	15.00	17.94
atszb68	−88.0070	15.6364	62.69	15.00	5.00
atsza69	−87.0824	15.5331	72.73	15.00	17.94
atszb69	−87.2163	15.9474	72.73	15.00	5.00
atsza70	−86.3120	15.8274	70.64	15.00	17.94
atszb70	−86.3120	16.2367	70.64	15.00	5.00
atsza71	−85.3117	16.1052	73.70	15.00	17.94
atszb71	−85.4387	16.5216	73.70	15.00	5.00
atsza72	−84.3470	16.3820	69.66	15.00	17.94
atszb72	−84.5045	16.7888	69.66	15.00	5.00
atsza73	−83.5657	16.6196	77.36	15.00	17.94
atszb73	−83.6650	17.0429	77.36	15.00	5.00
atsza74	−82.7104	16.7695	82.35	15.00	17.94
atszb74	−82.7709	17.1995	82.35	15.00	5.00
atsza75	−81.7297	16.9003	79.86	15.00	17.94
atszb75	−81.8097	17.3274	79.86	15.00	5.00
atsza76	−80.9196	16.9495	82.95	15.00	17.94
atszb76	−80.9754	17.3801	82.95	15.00	5.00
atsza77	−79.8086	17.2357	67.95	15.00	17.94
atszb77	−79.9795	17.6378	67.95	15.00	5.00
atsza78	−79.0245	17.5415	73.61	15.00	17.94
atszb78	−79.1532	17.9577	73.61	15.00	5.00
atsza79	−78.4122	17.5689	94.07	15.00	17.94
atszb79	−78.3798	18.0017	94.07	15.00	5.00
atsza80	−77.6403	17.4391	103.33	15.00	17.94
atszb80	−77.5352	17.8613	103.33	15.00	5.00
atsza81	−76.6376	17.2984	98.21	15.00	17.94
atszb81	−76.5726	17.7278	98.21	15.00	5.00
atsza82	−75.7299	19.0217	80.15	15.00	17.94
atszb82	−75.6516	18.5942	80.15	15.00	5.00
atsza83	−74.8351	19.2911	80.83	15.00	17.94
atszb83	−74.7621	18.8628	80.83	15.00	5.00
atsza84	−73.6639	19.2991	94.84	15.00	17.94
atszb84	−73.7026	18.8668	94.84	15.00	5.00

Table B13: (continued)

Locator	Longitude	Latitude	Strike Angle	Dip Angle	Depth (km)
atsza85	−72.8198	19.2019	90.60	15.00	17.94
atszb85	−72.8246	18.7681	90.60	15.00	5.00
atsza86	−71.9143	19.1477	89.06	15.00	17.94
atszb86	−71.9068	18.7139	89.06	15.00	5.00
atsza87	−70.4738	18.8821	304.49	15.00	17.94
atszb87	−70.7329	18.5245	304.49	15.00	5.00
atsza88	−69.7710	18.3902	308.94	15.00	17.94
atszb88	−70.0547	18.0504	308.44	15.00	5.00
atsza89	−69.2635	18.2099	283.88	15.00	17.94
atszb89	−69.3728	17.7887	283.88	15.00	5.00
atsza90	−68.5059	18.1443	272.93	15.00	17.94
atszb90	−68.5284	17.7110	272.93	15.00	5.00
atsza91	−67.6428	18.1438	267.84	15.00	17.94
atszb91	−67.6256	17.7103	267.84	15.00	5.00
atsza92	−66.8261	18.2536	262.00	15.00	17.94
atszb92	−66.7627	17.8240	262.00	15.00	5.00

This page is intentionally left blank.

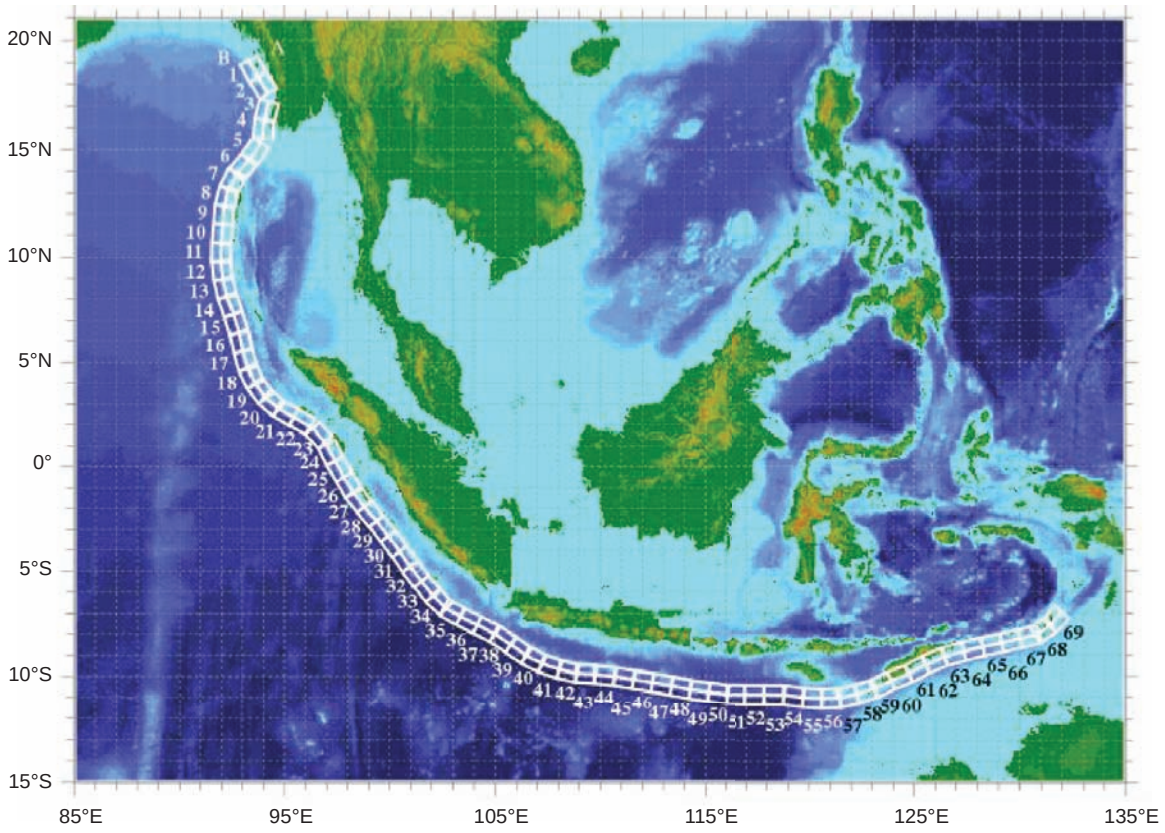

Figure B14: Indian Ocean Subduction Zone unit sources.

Table B14: Indian Ocean Subduction Zone unit sources parameters.

Locator	Longitude	Latitude	Strike Angle	Dip Angle	Depth (km)
iosza1	93.9315	18.9075	332.17	8.00	11.96
ioszb1	93.5161	18.6999	332.17	8.00	5.00
iosza2	94.3652	18.1830	328.15	8.00	11.96
ioszb2	93.9678	17.9483	328.15	8.00	5.00
iosza3	94.5975	16.6699	14.85	8.00	11.96
ioszb3	94.1486	16.7840	14.85	8.00	5.00
iosza4	94.4593	15.9374	5.10	8.00	11.96
ioszb4	93.9984	15.9769	5.10	8.00	5.00
iosza5	94.0010	14.7002	33.95	8.00	11.96
ioszb5	93.6183	14.9486	33.95	8.00	5.00
iosza6	93.3511	13.8912	40.04	8.00	11.96
ioszb6	92.9992	14.1773	40.04	8.00	5.00
iosza7	92.9475	13.3087	27.46	8.00	11.96
ioszb7	92.5409	13.5138	27.46	8.00	5.00
iosza8	92.6808	12.6519	15.22	8.00	11.96
ioszb8	92.2400	12.7687	15.22	8.00	5.00
iosza9	92.5543	11.9414	4.06	8.00	11.96
ioszb9	92.0999	11.9729	4.06	8.00	5.00
iosza10	92.4759	11.0297	5.21	8.00	11.96
ioszb10	92.0239	11.0701	5.21	8.00	5.00
iosza11	92.4305	10.2061	0.63	8.00	11.96
ioszb11	91.9778	10.2110	0.63	8.00	5.00
iosza12	92.4690	9.4219	353.51	8.00	11.96
ioszb12	92.0204	9.3716	353.51	8.00	5.00
iosza13	92.6051	8.6389	346.99	7.00	11.09
ioszb13	92.1653	8.5385	346.99	7.00	5.00
iosza14	92.8288	7.8793	340.24	7.00	11.09
ioszb14	92.4049	7.7286	340.24	7.00	5.00
iosza15	93.1255	6.9844	343.16	7.00	11.09
ioszb15	92.6953	6.8552	343.16	7.00	5.00
iosza16	93.3667	6.0395	348.16	7.00	11.09
ioszb16	92.9277	5.9480	348.16	7.00	5.00
iosza17	93.5657	5.2172	344.58	7.00	11.09
ioszb17	93.1339	5.0987	344.58	7.00	5.00
iosza18	93.8250	4.5314	333.99	7.00	11.09
ioszb18	93.4228	4.3359	333.99	7.00	5.00
iosza19	94.2068	3.9031	323.48	7.00	11.09
ioszb19	93.8475	3.6378	323.48	7.00	5.00
iosza20	94.6815	3.3907	310.83	7.00	11.09
ioszb20	94.3895	3.0534	310.83	7.00	5.00
iosza21	95.2701	2.9719	300.01	7.00	11.09
ioszb21	95.0467	2.5859	300.01	7.00	5.00
iosza22	96.0351	2.5381	299.13	7.00	11.09
ioszb22	95.8177	2.1487	299.13	7.00	5.00
iosza23	96.9564	1.8021	318.04	7.00	11.09
ioszb23	96.6247	1.5040	318.04	7.00	5.00
iosza24	97.5929	0.8677	333.47	7.00	11.09
ioszb24	97.1940	0.6686	333.47	7.00	5.00
iosza25	97.9937	0.1158	330.40	7.00	11.09
ioszb25	97.6061	−0.1044	330.40	7.00	5.00
iosza26	98.4375	−0.6495	329.40	7.00	11.09
ioszb26	98.0538	−0.8764	329.40	7.00	5.00
iosza27	98.8807	−1.3120	323.09	7.00	11.09
ioszb27	98.5242	−1.5797	323.09	7.00	5.00

Table B14: (continued)

Locator	Longitude	Latitude	Strike Angle	Dip Angle	Depth (km)
iosza28	99.4058	−1.9694	319.70	7.00	11.09
ioszb28	99.0658	−2.2577	319.70	7.00	5.00
iosza29	99.9949	−2.6957	322.32	7.00	11.09
ioszb29	99.6419	−2.9682	322.32	7.00	5.00
iosza30	100.5471	−3.4209	323.25	7.00	11.09
ioszb30	100.1895	−3.6876	323.25	7.00	5.00
iosza31	101.0916	−4.1852	326.05	7.00	11.09
ioszb31	100.7210	−4.4342	326.05	7.00	5.00
iosza32	101.5837	−4.8643	322.38	7.00	11.09
ioszb32	101.2296	−5.1364	322.38	7.00	5.00
iosza33	102.1320	−5.5548	321.09	7.00	11.09
ioszb33	101.7837	−5.8348	321.09	7.00	5.00
iosza34	102.6731	−6.1513	314.92	7.00	11.09
ioszb34	102.3568	−6.4670	314.92	7.00	5.00
iosza35	103.1950	−6.5654	300.22	12.00	15.40
ioszb35	102.9728	−6.9450	300.22	12.00	5.00
iosza36	103.9372	−6.9608	296.31	12.00	15.40
ioszb36	103.7414	−7.3546	296.31	12.00	5.00
iosza37	104.7589	−7.3735	297.50	12.00	15.40
ioszb37	104.5548	−7.7632	297.50	12.00	5.00
iosza38	105.6233	−7.8839	304.18	12.00	15.40
ioszb38	105.3744	−8.2474	304.18	12.00	5.00
iosza39	106.3845	−8.4061	305.40	12.00	15.40
ioszb39	106.1276	−8.7642	305.40	12.00	5.00
iosza40	107.0467	−8.8006	296.87	12.00	15.40
ioszb40	106.8462	−9.1925	296.87	12.00	5.00
iosza41	107.7745	−9.1062	289.34	12.00	15.40
ioszb41	107.6276	−9.5207	289.34	12.00	5.00
iosza42	108.5585	−9.3316	283.23	12.00	15.40
ioszb42	108.4570	−9.7593	283.23	12.00	5.00
iosza43	109.3121	−9.4422	273.71	12.00	15.40
ioszb43	109.2840	−9.8806	273.71	12.00	5.00
iosza44	110.2556	−9.5200	275.87	12.00	15.40
ioszb44	110.2107	−9.9570	275.87	12.00	5.00
iosza45	111.2195	−9.6494	279.69	12.00	15.40
ioszb45	111.1451	−10.0825	279.69	12.00	5.00
iosza46	112.1080	−9.7925	278.93	12.00	15.40
ioszb46	112.0394	−10.2265	278.93	12.00	5.00
iosza47	113.0246	−9.9427	280.01	12.00	15.40
ioszb47	112.9476	−10.3754	280.01	12.00	5.00
iosza48	113.9418	−10.1133	281.45	12.00	15.40
ioszb48	113.8538	−10.5439	281.45	12.00	5.00
iosza49	114.7788	−10.2517	277.68	12.00	15.40
ioszb49	114.7197	−10.6871	277.68	12.00	5.00
iosza50	115.6826	−10.3732	277.93	12.00	15.40
ioszb50	115.6217	−10.8083	277.93	12.00	5.00
iosza51	116.4873	−10.4381	271.48	12.00	15.40
ioszb51	116.4764	−10.8773	271.48	12.00	5.00
iosza52	117.3800	−10.4494	270.00	12.00	15.40
ioszb52	117.3800	−10.8887	270.00	12.00	5.00
iosza53	118.3078	−10.4539	270.57	12.00	15.40
ioszb53	118.3043	−10.8932	270.57	12.00	5.00
iosza54	119.3339	−10.5288	278.00	12.00	15.40
ioszb54	119.2724	−10.9639	278.00	12.00	5.00
iosza55	120.1649	−10.6064	272.92	12.00	15.40
ioszb55	120.1429	−11.0452	272.92	12.00	5.00

Table B14: (continued)

Locator	Longitude	Latitude	Strike Angle	Dip Angle	Depth (km)
iosza56	121.0062	−10.6148	268.20	12.00	15.40
ioszb56	121.0213	−11.0539	268.20	12.00	5.00
iosza57	121.7443	−10.5229	257.41	12.00	15.40
ioszb57	121.8425	−10.9517	257.41	12.00	5.00
iosza58	122.5657	−10.3119	253.18	12.00	15.40
ioszb58	122.6957	−10.7324	253.18	12.00	5.00
iosza59	123.2606	−10.0387	243.13	12.00	15.40
ioszb59	123.4631	−10.4306	243.13	12.00	5.00
iosza60	124.1591	−9.6372	247.92	12.00	15.40
ioszb60	124.3274	−10.0443	247.92	12.00	5.00
iosza61	124.9051	−9.2940	241.93	12.00	15.40
ioszb61	125.1153	−9.6817	241.93	12.00	5.00
iosza62	125.7970	−8.8712	246.67	12.00	15.40
ioszb62	125.9738	−9.2746	246.67	12.00	5.00
iosza63	126.7658	−8.5307	254.10	12.00	15.40
ioszb63	126.8882	−8.9532	254.10	12.00	5.00
iosza64	127.6800	−8.2901	256.03	12.00	15.40
ioszb64	127.7878	−8.7164	256.03	12.00	5.00
iosza65	128.6032	−8.0817	258.23	12.00	15.40
ioszb65	128.6944	−8.5118	258.23	12.00	5.00
iosza66	129.4805	−7.8944	257.38	12.00	15.40
ioszb66	129.5780	−8.3231	257.38	12.00	5.00
iosza67	130.3466	−7.6928	256.11	12.00	15.40
ioszb67	130.4535	−8.1193	256.11	12.00	5.00
iosza68	130.8673	−7.4586	235.11	12.00	15.40
ioszb68	131.1214	−7.8190	235.11	12.00	5.00
iosza69	131.3863	−7.0023	221.51	12.00	15.40
ioszb69	131.7184	−7.2935	221.51	12.00	5.00

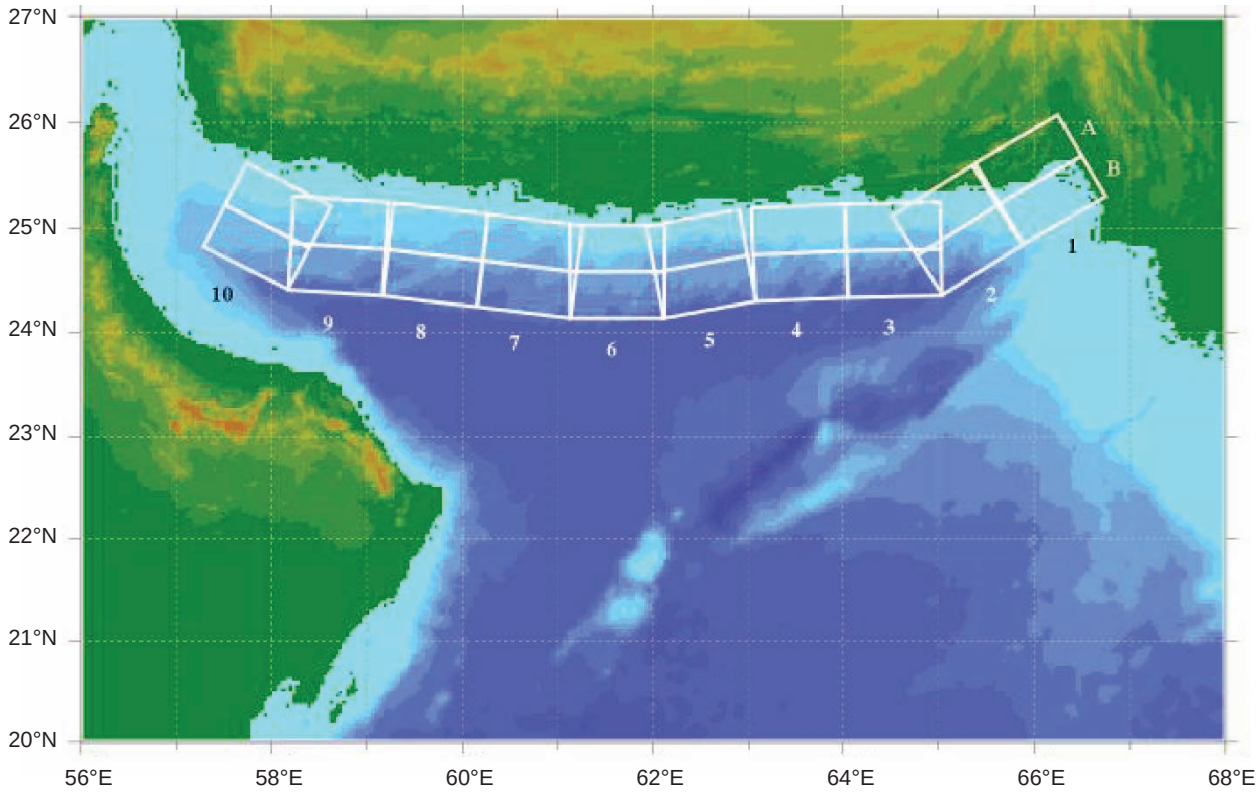

Figure B15: Makran Subduction Zone unit sources.

Table B15: Makran Subduction Zone unit sources parameters.

Locator	Longitude	Latitude	Strike Angle	Dip Angle	Depth (km)
mksza1	65.8163	25.8503	239.612	3.00	7.62
mkszb1	66.0688	25.4637	239.612	3.00	5.00
mksza2	64.9317	25.3606	237.752	3.00	7.62
mkszb2	65.1970	24.9817	237.752	3.00	5.00
mksza3	64.5214	25.2436	268.831	3.00	7.62
mkszb3	64.5315	24.7952	268.831	3.00	5.00
mksza4	63.5221	25.2159	267.657	3.00	7.62
mkszb4	63.5424	24.7677	267.657	3.00	5.00
mksza5	62.4110	25.1007	259.360	3.00	7.62
mkszb5	62.5027	24.6599	259.360	3.00	5.00
mksza6	61.6246	25.0339	270.000	3.00	7.62
mkszb6	61.6246	24.5854	270.000	3.00	5.00
mksza7	60.7661	25.0821	276.990	3.00	7.62
mkszb7	60.7057	24.6369	276.990	3.00	5.00
mksza8	59.7748	25.1917	276.858	3.00	7.62
mkszb8	59.7155	24.7465	276.858	3.00	5.00
mksza9	58.7285	25.2787	273.517	3.00	7.62
mkszb9	58.6980	24.8310	273.517	3.00	5.00
mksza10	58.1818	25.4182	297.188	3.00	7.62
mkszb10	57.9545	25.0196	297.188	3.00	5.00